Wayne State University Dissertations

1-1-2016

Mechanisms Of Pancreatic Beta Cell Dysfunction In Diabetes

Vaibhav Sidarala
Wayne State University,

MECHANISMS OF PANCREATIC BETA CELL DYSFUNCTION IN DIABETES

by

VAIBHAV SIDARALA

DISSERTATION

Submitted to the Graduate School

of Wayne State University,

Detroit, Michigan

in partial fulfillment of the requirements

for the degree of

DOCTOR OF PHILOSOPHY

2016

MAJOR: PHARMACEUTICAL SCIENCES

Approved By:

_____

Advisor   Date

_____

_____

_____

DEDICATION

This work is dedicated to my parents, Dr. Narasimha Rao Sidarala and

Dr. Meera Bai Sidarala; and my brother, Vasishth Sidarala.

ACKNOWLEDGEMENTS

Firstly, I would like to express my sincere gratitude to my academic advisor, Dr. Anjaneyulu Kowluru, who has been a constant source of inspiration, for guiding me during my graduate studies. His teachings have had a huge positive impact on my attitude, and will continue to motivate me, as I move forward in my career. I am truly grateful for being a part of Dr. Kowluru's laboratory, and for the opportunity to be trained under his guidance.

I am also grateful for being so fortunate to have worked with previous and present members of Dr. Kowluru's research laboratory, Dr. Rajakrishnan Veluthakal, Dr. Khadija Syeda, Dr. Abiy Mussa Mohammed, Dr. Daleep Arora, Dr. Anil Chekuri and Dr. Anil Poudel. I am thankful for their support during my PhD, and for reminding me that "Teamwork makes the dream work".

I am thankful to Dr. Fei Chen, Dr. Randall Commissaris and Dr. Timothy Hadden, for making time and being on my dissertation committee. Our discussions have aided me in critically analyzing scientific data and develop the skills needed for effectively presenting my research findings. I am also very thankful to the Department of Pharmaceutical Sciences at Wayne State University. A special thanks to Dr. George Corcoran, for his ever so encouraging support.

I also thank my friends and family for their immense support, without which I would not have made it this far. I am truly grateful to my parents for constantly reminding me that every milestone we reach, marks the beginning of a new endeavor. My sincere gratitude to everyone who has been a part of this incredible and enlightening journey.

TABLE OF CONTENTS

LIST OF TABLES

LIST OF FIGURES

viii

LIST OF ABBREVIATIONS

2-BP - 2-bromopalmitate

ATM kinase – Ataxia telangiectasia mutated kinase

Cdc42 – Cell division control protein 42

DCFDA – 2',-7'-dichlorofluorescein diacetate

ECL – Electrochemiluminescence

ERK 1/2 – Extracellular regulated kinase 1/2

FPP – Farnesyl pyrophosphate

Ftase – Farnesyl transferase

GDP – Guanosine diphosphate

GEF – Guanine nucleotide exchange factor

GGPP – Geranygeranyl pyrophosphate

GGTI – Geranylgeranyl transferase inhibitor

GSIS – Glucose-stimulated insulin secretion

GGtase – Geranylgeranyl transferase

GTP – Guanosine triphosphate

HG – High glucose

JNK1/2 – c-jun N-terminal kinase 1/2

LG – Low glucose

LG-LS – Low glucose-low serum

T1DM – Type 1 diabetes mellitus

T2DM – Type 2 diabetes mellitus

Nox2 – NADPH oxidase 2

p38MAPK – p38 mitogen-activated protein kinase

Rac1 – Ras-related C3 botulinum toxin substrate 1

RhoA – Ras homolog gene family, member A

ROS – Reactive oxygen species

SAPK/MAPK – Stress activated protein kinase/mitogen activated protein kinase

Tiam1 – T-lymphoma invasion and metastasis 1

ZDF – Zucker Diabetic fatty rat

ZLC – Zucker lean control rat

x

CHAPTER 1: INTRODUCTION

The human body is composed of millions of cells which utilize glucose as their primary source of energy. Depending on the energy demand and expenditure, glucose levels in the bloodstream are regulated by several mechanisms including glycolysis, glycogenolysis and gluconeogenesis. Glucose is metabolized via glycolysis and the TCA cycle, resulting in the generation of ATP, available to the cell for its energy requirements. However, during fasting when the blood glucose levels are low, glucose homeostasis is maintained by glycogen synthesis and gluconeogenesis, occurring in various tissues of the body including skeletal muscle, fat tissue, kidney, liver and brain. These metabolic processes are tightly regulated to maintain a normal fasting blood glucose levels.

Islet of Langerhans constitute the endocrine part of the pancreas and are embedded in the surrounding exocrine tissue. These clusters of cells are composed mainly of α-, β-, δ- and ε-cells. α-cells constitute about ~20% of the total cell composition and secrete the endocrine hormone, glucagon. β-cells, which constitute the majority of the cell population, secrete the hormone insulin. Other hormones such as somatostatin and polypeptide are also secreted from the pancreatic islet. The human pancreas are composed of nearly 3 million islets, with a distinct morphology where the different endocrine cell types are scattered throughout islet **(1)**. In contrast, rodent islets are composed of insulin expressing β-cells clustered in the islet core, surrounded by α- and δ-cells **(2).**
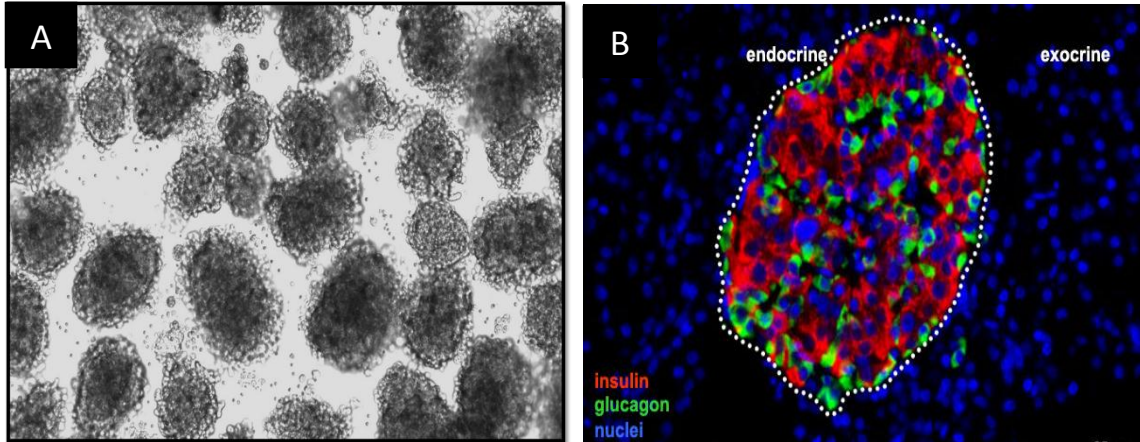
Figure 1-1: The pancreatic islet: Panel A: Rodent pancreatic islets isolated from 8 weeks old normal Sprague Dawley rats [representative of islet preparations used for our experiments]. **Panel B:** Section of an adult human pancreas stained for glucagon (green) and insulin (red). [Modified from Scharfmann et al., ref. **(3)**]

Insulin: Structure, Receptor and Functions:

Insulin, secreted by the pancreatic β-cells, is involved in several metabolic processes and regulates nutrient uptake and utilization in the peripheral tissues. It is a 51-amino acid peptide comprised of chains A and B, which are connected by disulphide bonds. The insulin gene product preproinsulin mRNA is first translated and processed in the rough endoplasmic reticulum to produce proinsulin. Proinsulin, which consists of the C-peptide connecting the A and B chains is converted to mature insulin by converting enzymes which cleave the C-peptide in the Golgi. The mature insulin and C-peptide are then packaged into secretory granules in the Golgi complex **(4)**.

The insulin receptor is a tyrosine kinase receptor composed of two extracellular alpha and two transmembrane beta subunits linked by disulfide bonds **(5).** The interaction of insulin with the alpha sub-units of the insulin receptor induces a conformation change in the beta sub-units, activating their intrinsic tyrosine activity leading to auto-phosphorylation of the receptor. This results in the phosphorylation of insulin receptor substrate (IRS) proteins. IRS1 and IRS2, which are the major isoforms present in the muscle cell, further activate phosphoinositide-3-kinase

(PI3K) and protein kinase B/Akt. Subsequent intracellular events lead to the translocation of GLUT-4 transporter from intracellular storage pools towards the plasma membrane, thereby mediating uptake of glucose from the circulating bloodstream **(6, 7)**. Additionally, storage of excess glucose by glycogen synthesis catalyzed by glycogen synthase is promoted by insulin. In the adipose tissue, insulin also stimulates lipogenesis by increasing glucose and free fatty acid uptake, where they are converted and stored as triglycerides.
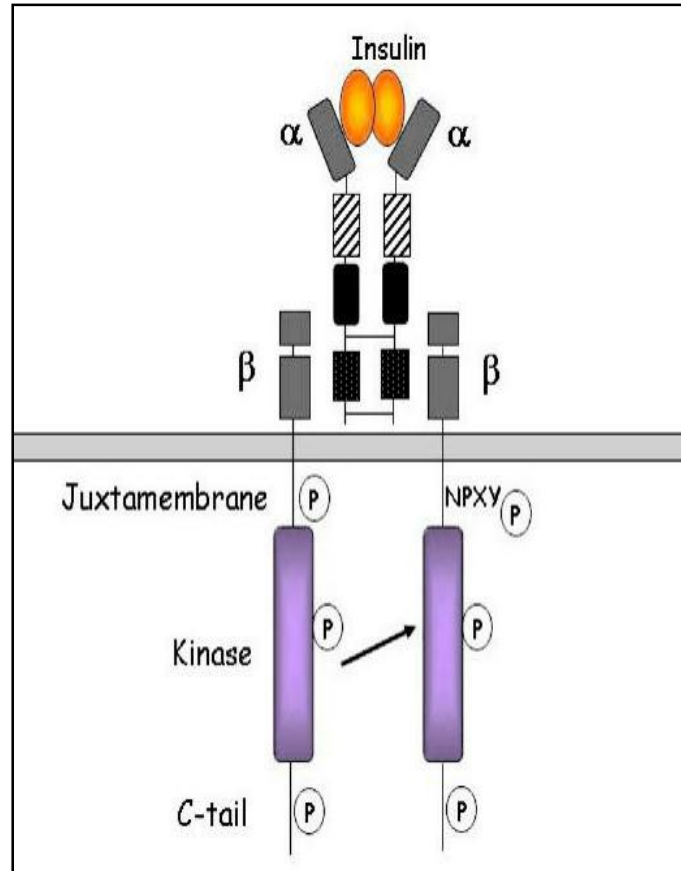
Figure 1-2: The Insulin receptor [Chang L et al. ref **(5)**]

Glucose-stimulated insulin secretion (GSIS) from the pancreatic β-cell:

The primary function of the pancreatic β-cell is insulin secretion coupled with glucose stimulation. Circulating glucose enters the β-cell through GLUT-2 receptors and is then metabolized via the glycolytic pathway and TCA cycle resulting in the generation of ATP. The resulting decrease in ATP/ADP ratio results in closure of ATP-sensitive K^+ channels, causing the plasma membrane to depolarize. This results in the opening of voltage-gated Ca^{+2} channels causing an influx of Ca^{+2} ions and an increase in intracellular Ca^{+2} levels. This mobilization of Ca^{+2} within the β-cells mediates the translocation of insulin granules towards the membrane for fusion and release. This involves cytoskeletal remodeling which enables migration of insulin granules from intracellular sites towards the membrane. Although the precise mechanisms involved in cytoskeletal reorganization are yet to be fully understood, several investigations have delineated

the roles of small GTP-binding proteins in mediating F-actin reorganization and insulin granule transport **(8)**. The docking and fusion of insulin granules at membrane docking sites is also mediated by several SNARE proteins such as syntaxin and vesicle-associated membrane protein.
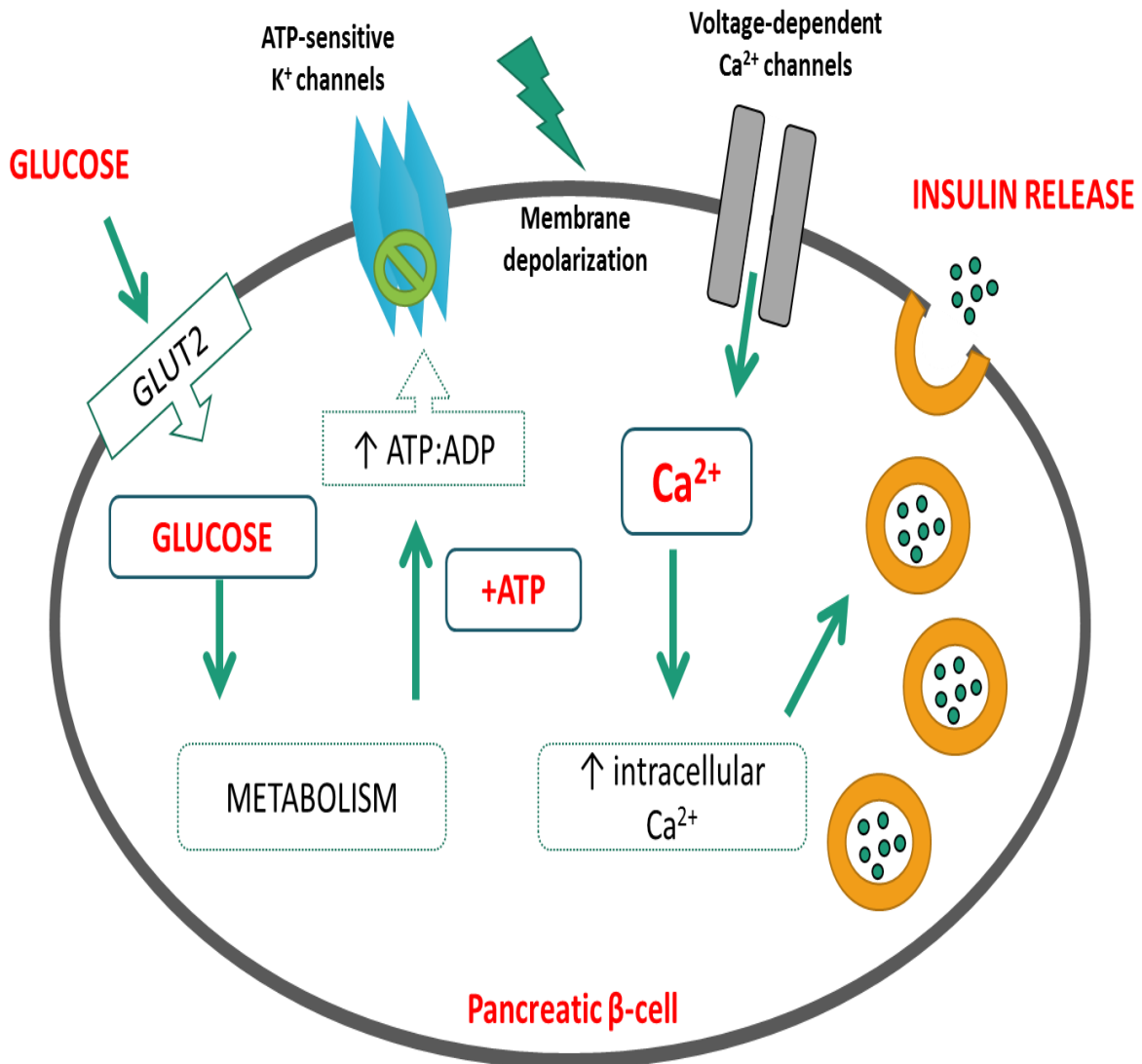
Figure 1-3: Glucose-stimulated insulin secretion (GSIS) [Modified from Wang Z et al. ref **(8)**]

Diabetes

Diabetes is a serious pathological condition characterized by decreased glucose disposal in the body, caused by insufficient insulin secretion from the pancreatic β-cell and decreased insulin sensitivity in the peripheral tissues. According to the 2015 International Diabetes Federation (IDF) atlas, approximately 415 million adults have been diagnosed with Diabetes worldwide, and it is estimated that the number of cases will rise up to 642 million by the year 2040. In addition, it is also reported that there are nearly 318 million adults with impaired glucose tolerance and increased risk of developing diabetes. Diabetes is mainly of two types: Type 1 Diabetes (T1DM), also known as insulin-dependent diabetes mellitus (IDDM), and Type 2 Diabetes (T2DM), also referred to as non-insulin dependent diabetes mellitus (NIDDM). T1D is characterized by insufficient insulin secretion caused by auto-immune destruction of the insulin-secretin pancreatic β-cells. This is mediated by cell death induced by inflammatory cytokines secreted by the immune cells, resulting in severe hyperglycemic conditions. Although the causes for T1D still remain less understood, it has been suggested that genetic and/or environmental risk factors contribute to disease development and progression **(9).** T2D, however, is characterized by insulin resistance and decreased glucose tolerance in the peripheral tissues, resulting from environmental and genetic risk factors. This results in prolonged exposure of pancreatic β-cells to elevated levels of hyperglycemia, eventually leading to defects in insulin secretory response and overt diabetic state. Elevated levels of circulating glucose can affect other tissues including retina, kidney and cardiomyocytes and lead to serious diabetes-related complications.
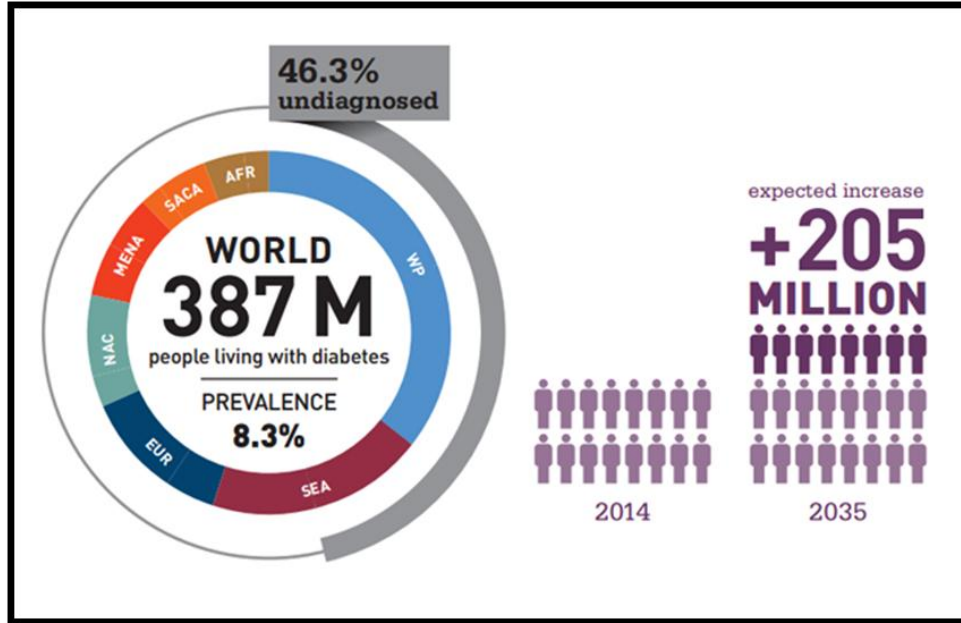
Figure 1-4: Prevalence of Diabetes worldwide and estimated increase in the number of patients according to the International Diabetes Federation [IDF Diabetes Atlas 2013]

Pancreatic β-cell dysfunction:

Exposure of pancreatic β-cells to glucose results in initiation of several intracellular metabolic pathways that mediate GSIS. As reviewed by Bensallem and associates, physiological glucose concentrations play a major role in regulating β-cell function **(10).** Acute exposure to stimulatory glucose concentrations has been shown to improve Ca+2 mobilization, protein synthesis and β-cell function **(11, 12)**. Furthermore, studies have indicated that prolonged exposure to physiological glucose concentrations improves gene expression and is crucial for maintaining optimal β-cell function and cell mass **(13)**. However, prolonged exposure to elevated levels of glucose exert toxic effects on the β-cell, causing decreased β-cell function and proliferation. This condition, termed as glucotoxicity, results in decreased insulin secretory response to the high metabolic demand and reduced β-cell mass **(14, 15).**
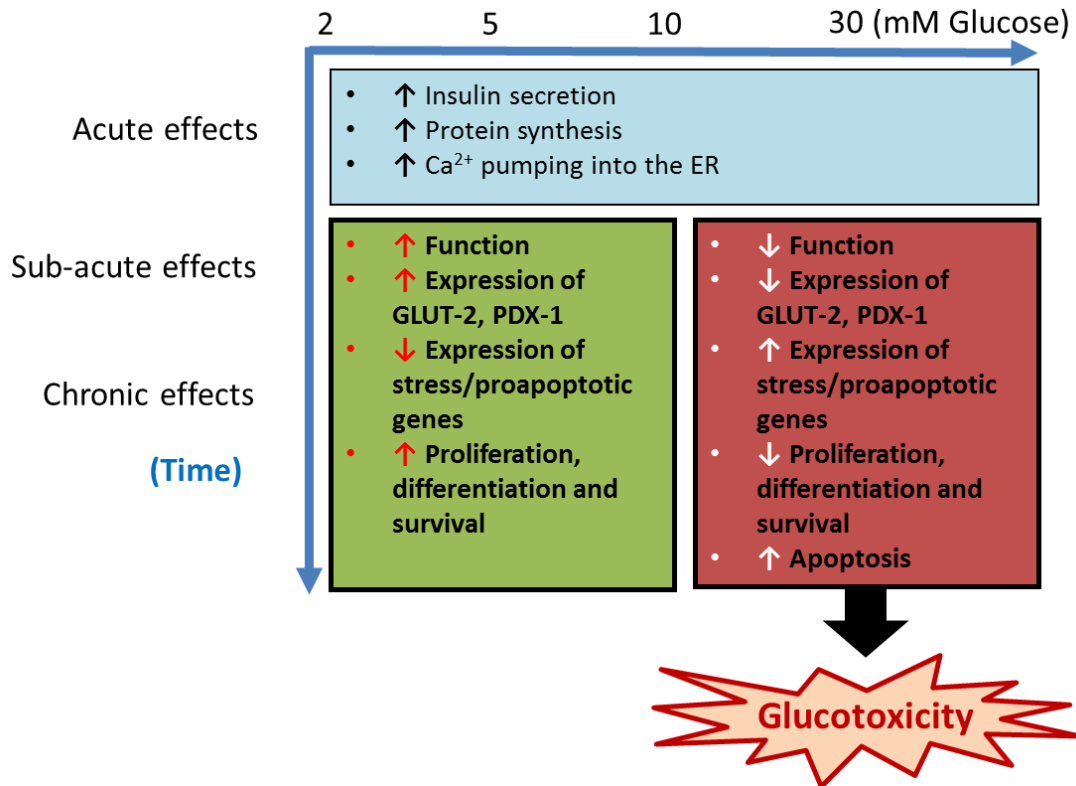
Figure 1-5: Effects of acute and chronic exposure to glucose concentrations on the pancreatic β-cell [Modified from Bensallem *et al.* ref **(10)**]

GTP-binding proteins

It is now well-established that changes in intracellular Ca concentrations and generation of several soluble second messenger molecules (cAMP) and hydrolytic products of phospholipases (PLases) A2, C and D are requisite for GSIS. Moreover, earlier studies have shown the requirement of GTP in the insulin secretory mechanism **(16, 17)**. This is further supported by evidence suggesting that activation of GTP-binding proteins is required for insulin secretion from the β-cell. These G-proteins are of three major classes: 1) The hetero-trimeric G-proteins, which are involved in membrane-receptor interactions and activation of their downstream effectors. 2) The small molecular weight G-proteins, which are mostly involved in cytoskeletal remodeling and membrane trafficking of secretory granules. 3) Elongation factors and Tau proteins, involved in protein synthesis.

Small G-proteins:

Small G-proteins are categorized into five subfamilies with varying degrees of homology. These include Ras, Rho, Rab, Arf and Ran GTPases which have been implicated in various cellular functions including gene expression, cytoskeletal remodeling, vesicle trafficking, nucleocytoplasmic transport [18]. In the context of β-cell function, G-proteins belonging to the Rho family including RhoA, Cdc42 and Rac1 have been implicated in cytoskeletal remodeling, vesicle fusion and GSIS [8]. Although the involvement of Rab sub-family GTPases that include Rap1, Rab3A and Rab27 are yet to be fully understood, it has been suggested that these G-proteins are involved in docking of insulin secretory granules at membrane docking sites [19]. These small G-proteins, which are inactive when bound to GDP, are activated by their interaction with GTP. This process is mediated by several regulatory factors which include: 1) guanine nucleotide exchange factors (GEFs), 2) GTPase-activating proteins (GAPs) and 3) GDP-dissociation inhibitors. Under basal conditions, G-proteins are inactive (GDP-bound) and are bound to GDI, which prevent their dissociation with GDP. However, upon stimulation, GDI dissociate from the G-protein, thereby releasing GDP. G-proteins can then be activated by interacting with GTP, which is mediated by GEFs. Similar to heterotrimeric G-proteins, small G-proteins also possess a small degree of intrinsic GTPase activity. Therefore, when activated, these GTPases shuttle back to their GDP-bound form by hydrolyzing GTP, and this is catalyzed by GAPs.
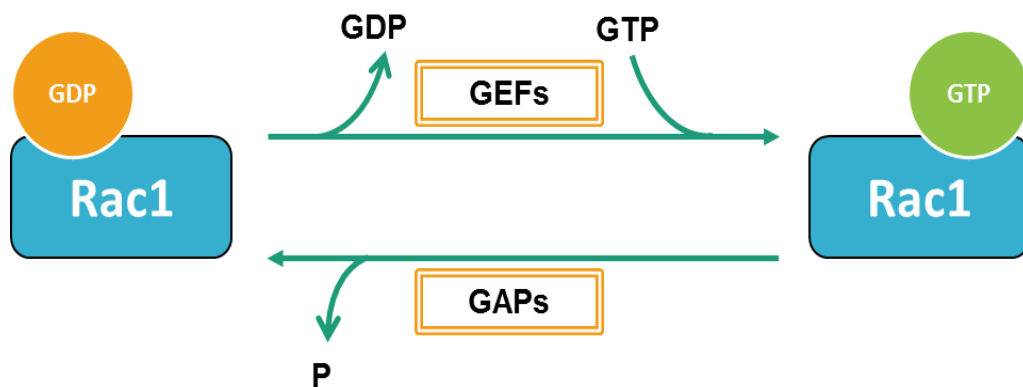
Figure 1-6: Rac1 activation cycle [Modified from Kowluru A, ref **(18)**]

9

Post-translational modifications:

In addition to the GTP/GDP activation cycle, small G-proteins also undergo a series of post-translational modifications at their C-terminal CAAX motifs (C-cysteine; A-amino acid; X-terminal amino acid). These include: 1) Prenylation, 2) Carboxymethylation and 3)Palmitoyaltion.

Prenylation involves the attachment of a prenyl moiety at the cysteine residue of the CAAX motif **(20, 21)**. The prenyl moiety are derivates of mevalonic acid synthesized via the cholesterol biosynthetic pathway, and include a 15-C farnesyl or a 20-C geranylgeranyl group. The attachment to the cysteine residue is catalyzed by prenyl tranferases namely, farnesyl transferase (FTase)-I and geranylgeranyl transferase (GGTase)-I and II. Following prenylation, the three amino acids (-AAX) adjacent to the prenylated cysteine are cleaved by Ras-converting enzyme, which exposes the carboxylate ion of the prenylated cysteine. This is followed by a carboxymethylation that involves methylation of the carboxylate group by isoprenylcysteine-O-carboxymethyl transferase (ICMT). Additionally, specific G-proteins also undergo palmitoylation at other cysteine residues. These modifications have been shown to increase hydrophobicity of the candidate G-proteins, that increases their localization in the membrane fraction of the cell required for optimal interaction with their respective effector proteins.

Role in glucose stimulated insulin secretion (GSIS):

Earlier studies in the β-cell have shown that depletion of intracellular GTP pools impairs physiological insulin secretion **(16, 17)**. Further investigations, focusing on Rho family GTPases including Rac1, have demonstrated that loss of function results in impairment in insulin secretory response to ambient glucose concentrations. Studies by Asahara and associates have utilized a β-cell specific Rac1 knockout model **(22).** They reported that these animals, when fed on a normal diet showed decreased GSIS. Furthermore, when these animals were fed on high-fat diet, signs of impaired glucose tolerance and GSIS were observed. Using pancreatic islets isolated from these animals and INS-1 cell line, they reported significant defects in GSIS and F-actin remodeling

upon loss of Rac1 function. Furthermore, studies in our own laboratory, have shown that siRNA-mediated depletion of Rac1 results in impaired GSIS **(23)**.

Rac1 is activated by dissociating with RhoGDI and its interaction with GTP. Several GEFs have been identified that regulated Rac1 function including Tiam1, Vav2, Trio **(18, 23)**. Rac1 is also known to undergo geranylgeranylation that increases its membrane association and substrate specificity. Previous investigations in our laboratory have utilized pharmacological agents to block Rac1 activity and demonstrated the role of Rac1 in physiological insulin secretion and cytoskeletal remodeling in the β-cell **(24, 25)**. The various pharmacological inhibitors used are depicted in Figure 1-7.
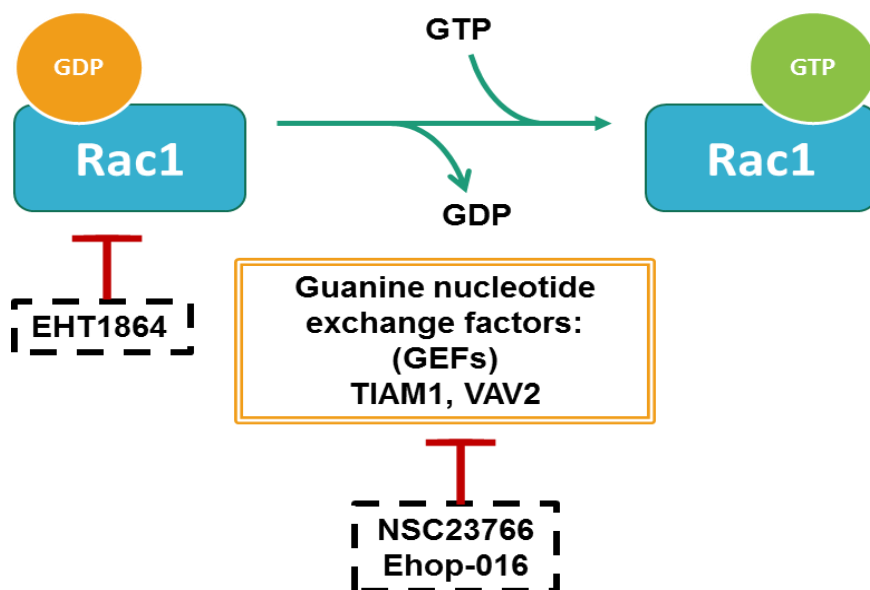
Figure 1-7: Pharmacological inhibitors of Rac1 [Modified from Nagase M et al. ref (33)]

NSC23766, synthesized by Gao and associates, blocks Tiam1-mediated Rac1 activation, and has been extensively used in multiple cell types to block Rac1 function **(26)**. Studies from our laboratory, have utilized this compound and reported a significant drop in insulin secretory response to stimulatory glucose **(24)**. Ehop-016, synthesized by Vlaar and associates, disrupts Vav2-mediated Rac1 activation. In a recent study from our laboratory, F-actin depolymerization was visualized using GFP-tagged LifeAct plasmid and live-cell imaging **(25)**. We reported that

glucose stimulation results in depolymerization of F-actin filaments, which is inhibited in presence of Ehop-016, thereby providing compelling evidence indicating the involvement of Rac1 in cytoskeletal remodeling and insulin secretion.

Besides NSC23766 and Ehop-016, which target GEF-mediated Rac1 activation, we utilized a novel inhibitor of Rac1, EHT1864, which blocks Rac1 function in a GEF-independent manner **(27)**. This compound, designed by Desire and associates, binds to Rac1 with a higher affinity than GTP/GDP, thereby retaining Rac1 in an inert, inactive state **(28)**. This compound has been used in multiple cell types to examine the role of Rac1 in normal cell physiology and pathology **(29-33).**

Additionally, previous published evidence have also shown that Rac1 geranylgeranylation is critical for GSIS, since presence of GGTI-2147, a specific inhibitor of geranylgeranyl transferase, blocked membrane association of Rac1 and insulin secretion in INS-1 832/13 cells **(34)**. Furthermore, when INS-1 832/13 cells were transfected with a dominant negative mutant of the alpha subunit of FTase and GGTase-I, insulin secretion was significantly blocked. These data have together confirmed the requisite role of prenylation of G-proteins including Rac1 in physiological insulin secretion from the β-cell.

Phagocyte-like NADPH oxidase (Nox2) and ROS generation:

The NADPH oxidase is a family of membrane-associated enzymes that catalyze oxidation of cytosolic NADPH and one electron reduction of molecular oxygen, resulting in the generation of superoxide. This family of enzymes includes seven members: Nox1, Nox2, Nox3 Nox4, Nox5, Duox1, Duox2 **(35, 36)**, which are composed of different membrane and cytosolic protein components. The phagocyte-like NADPH oxidase (Nox2) is composed of several membrane (gp91phox and p22phox) and cytosolic (p47phox, p67phox, p40phox and Rac1) components. Upon stimulation, the cytosolic components translocate to the membrane thereby, completing the holoenzyme assembly and activation of the holoenzyme. The superoxide generated from molecular oxygen is the major contributor of reactive oxygen species (ROS) and can be converted

to other ROS by superoxide dismutases. Pancreatic β-cells have known to be expressing Nox2 subunits, which represents a major source of extra-mitochondrial ROS **(36, 37)**. Recent studies have shown that a tonic increase in ROS in the pancreatic β-cell is required for GSIS. Although the mechanism is still poorly understood, evidence suggests that ROS act as second messengers and are known to regulate several downstream processes including mobilization of Ca and glucose metabolism **(38, 39)**. Interestingly, studies by Morgan et al. have demonstrated that inhibition of Nox2 using DPI or by downregulating expression of p47phox using an anti-sense oligonucleotide, resulted in impaired insulin secretion in rat pancreatic islets when perfused with stimulatory glucose concentrations **(40).** Studies in our own laboratory, have shown that inhibition of Nox2 (apocycin, DPI, siRNA p47phox) blocks glucose-induced ROS generation in insulin secreting INS-1 832/13 cells. Furthermore, we demonstrated that glucose stimulation results in increased Nox2 enzyme activity that is sensitive to apocynin. Additionally, studies using siRNA and pharmacological approaches demonstrated that prenylation is critical for GSIS. In this context, pharmacological inhibitors of prenylation (FTI-277 and GGTI-2147) blocked glucose-induced ROS generation, implicating the role of Nox2-ROS signaling in GSIS **(41)**.

Reactive oxygen species in pancreatic β-cell dysfunction:

Oxidative stress has been demonstrated to be a causal factor in the onset and development of various disorders including diabetes and its complications **(42-44)**. Earlier studies by Lenzen et al. have examined the expression of various antioxidant enzymes in pancreatic islets and compared with other tissues in albino mice **(45)**. Their studies revealed that expression levels of anti-oxidant enzymes such as glutathione peroxidase, Cu/Zn SOD and Mn SOD in the islet were significantly lower compared to other tissues. Studies in islets isolated from ob/ob mice, in which β-cells constitute about 90% of the total cell composition, have also shown low expression of antioxidant enzymes. The investigators concluded that pancreatic β-cells possess far lower levels of antioxidant compared to other endocrine and non-endocrine tissues. Several other studies have strongly suggested that pancreatic β-cells are highly susceptible to oxidative

damage and oxidative stress could be the causal mechanism leading to pancreatic β-cell death as seen in Type1 and Type2 diabetes **(46, 47)**.
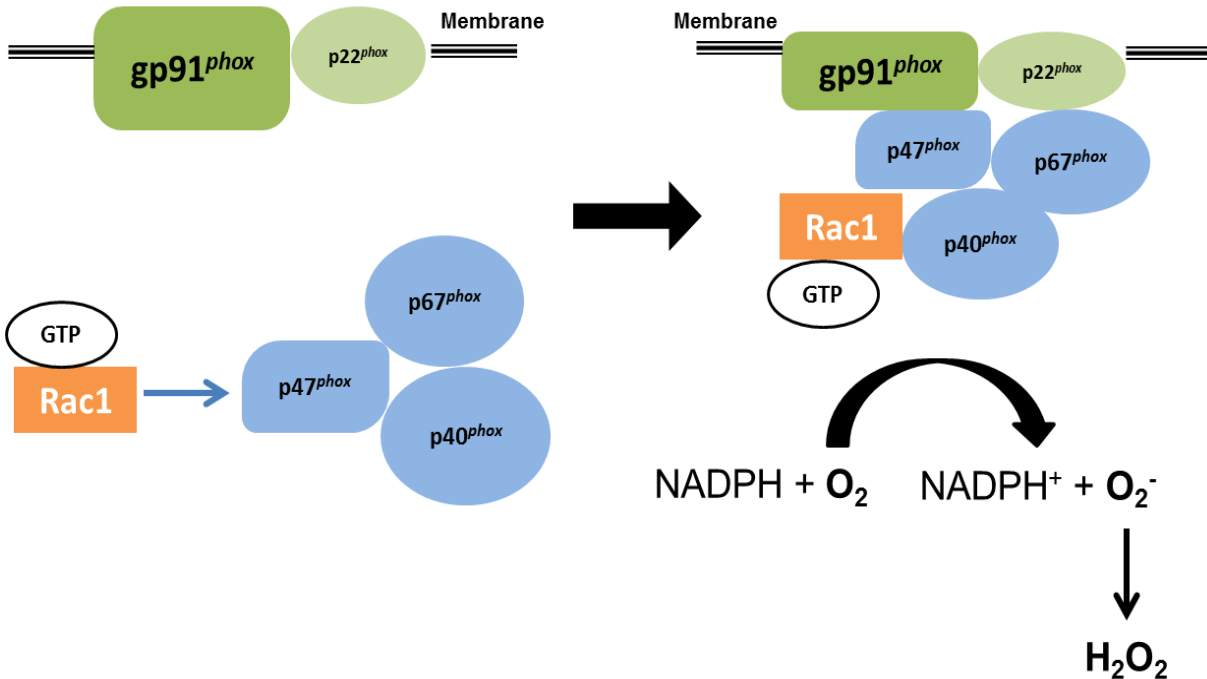
Figure 1-8: Functinal assembly and activation of NADPH oxidase 2 [Modified from Kowluru A, ref. **(18)**]

Although, low levels of ROS are requisite for GSIS and normal β-cell physiology, excess sustained activation of Rac1-Nox2 and associated oxidative stress can lead to β-cell demise under conditions of metabolic stress **(48-50)**. Studies by Yuan and associates have demonstrated that chronic exposure of clonal β-cells NIT-1 cells to high glucose and free-fatty acids results in increased Nox2-mediated ROS generation culminating in cell dysfunction and apoptosis, which is prevented in cells transfected with siRNA-Nox2 **(51)**. Along these lines, previous observations from our own laboratory have utilized inhibitors of Nox2 (DPI, Apocynin), Rac1 activation (NSC23766) and prenylation (GGTI-2147) and demonstrated the role of Rac1-Nox2 signaling in increased ROS generation in β-cells exposed to high glucose, palmitate and inflammatory cytokines **(50, 52)**. Furthermore, published evidence from our laboratory have demonstrated increased expression and activation of Rac1 and Nox2 subunits in islets derived from the Zucker

diabetic fatty (ZDF) rat, a model for type 2 diabetes, in normal human islets exposed to hyperglycemic conditions, and in islets from type2 diabetic human donors **(49)**. Further studies in INS-1 832/13 cells, ZDF islets and diabetic human islets have suggested significant increase in stress kinase JNK1/2 activation and caspase-3 activation. Together, these studies provide evidence suggesting that exposure of β-cells to diabetic conditions results in increased Rac1-Nox2 activity and the associated oxidative stress causes activation of downstream apoptotic stress kinase pathway, culminating in mitochondrial dysfunction and β-cell death.

Stress-activated protein kinases/Mitogen-activated protein kinases (SAPKs/MAPKs)

The mitogen-activated protein kinase family are serine-threonine protein kinases that regulate and integrate multiple intracellular signaling processes. These include 14 MAPKs known to be present in mammalian cells and are classifies into the conventional MAPKs and atypical MAPKs. The most widely studied group of MAPKs are the conventional the extra-cellular-regulate kinases (ERKs), c-jun NH2-terminal kinase (JNK) and p38MAPK isoforms. These conventional MAPKs are regulated by distinct MAPK signaling cascades composed of three components: 1. MAPK kinase kinase (MAPKKK); 2. MAPK kinase (MAPKK) and 3. MAPK.

In the presence of an extracellular stressor, MAPKKK are activated via interaction with a small G-protein including Rac1 **(53).** MAPKKK then phosphorylate and activate MAPKK, which in turn activate MAPKs. MAPKs are activated by phosphorylation on Threonine and Tyrosine residues located in the conserved activation loop of the kinase domain. Once activated MAPKs interact and phosphorylate several downstream kinases such as the MAPK-activated protein kinases (MAPKAPK) such as RSK1-4 and MSK1/2 and transcription factors such as Elk-1, c-jun, ATF3 and p53 **(54)**. The activation of downstream signaling cascades by MAPKs mediates the cellular responses to the stress stimuli including gene expression, mitosis, cell differentiation and apoptosis. In addition to their essential role in a wide range of cellular functions, emerging evidence implicates MAPK pathways in the pathogenesis of human diseases including diabetes, cancer and neurodegenerative diseases **(55)**.

Unlike the conventional MAPKs, the atypical MAPKs are not regulated by the three-tier kinase signaling cascade. The regulation and functions of these atypical MAPKs need to be further examined **(56).**
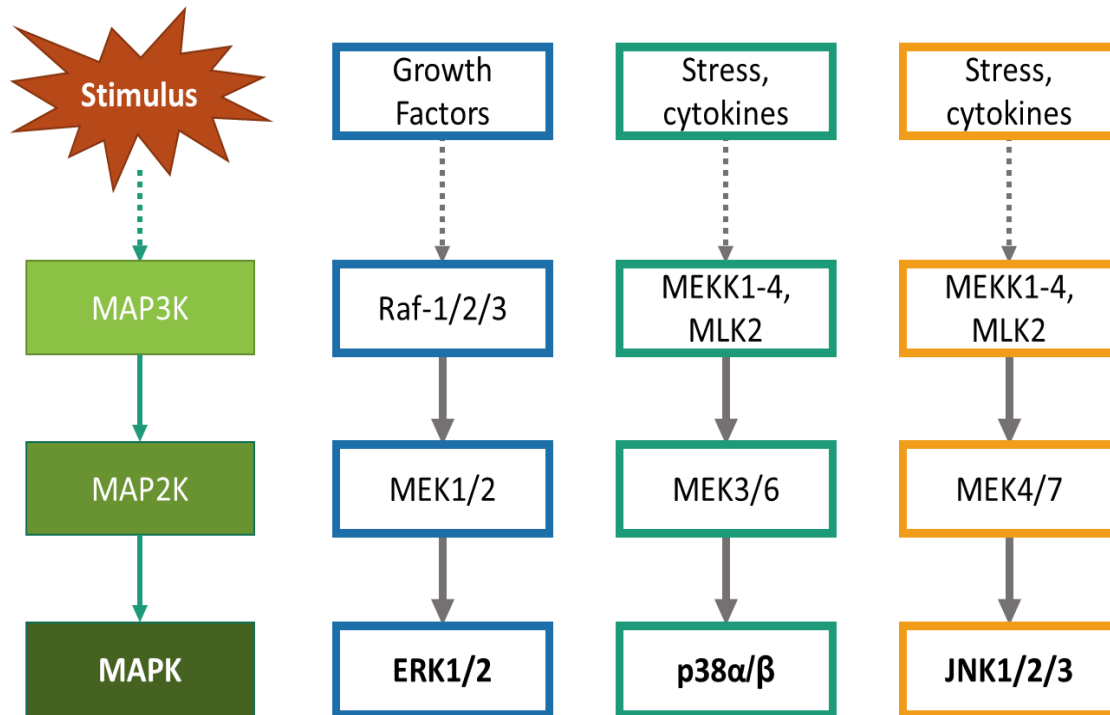
Figure 1-9: The conventional MAPK signaling pathways [Modified from Cargnello M et al. ref **(53)**]

Extracellular signal-regulated kinases (ERK1/2):

This group of MAPKs includes several isoforms including ERK1 to ERK8, among which the ERK1/2 module is the most extensively characterized. ERK1/2 exhibit ~83% homology and are phosphorylated on Tyr and Thr residues in response to extracellular stimuli. Several upstream regulators have been identified that are involved in the ERK MAPK pathway including the MAPKKK Raf, and MAPKK MEK1/2 **(54)**. The activation pathway is initiated by ligand binding to cell surface receptors such as tyrosine kinase receptors, which leads to dimerization of the receptor and autophosphorylation of the intracellular domain and binding with protein with Src-homology2- domain (e.g. Grb2) **(57).** The resulting signaling steps lead to the activation of Ras that interacts and activates Raf, which in turn activates ERK1/2 via MEK1/2. ERK1/2, once

activated, has been shown to localize and interact with several nuclear and cytosolic substrates. The major functions of this module include cell cycle progression, cell growth and proliferation. Several studies have implicated alterations in the ERK1/2 pathway in tumor development. For example, in certain cancer cells, constitutive activation of ERK signaling induced by overexpression of receptor tyrosine kinase or Ras/Raf mutations, has been associated with cancer development **(53, 57)**. Therefore, the ERK pathway is being extensively studied for drug discovery and pharmacological inhibitors of Ras, Raf and MEK are currently under development to prevent tumor progression.

c-jun NH2-terminal kinases (JNK):

The three isoforms of JNK identified in mammalian cells include JNK1/2/3, which share ~85% homology. While JNK1/2 are ubiquitously expressed in multiple cells, JNK3 seems to be expressed in neuronal tissues, testis and cardiomyocytes **(58).** These are activated in response to stress stimuli including inflammatory cytokines, oxidative stress, ionizing radiations and growth factor deprivation. Activation is initiated by upstream MAPKKK including MLK1-4, MEK1-4 and ASK1/2, which phosphorylate MAPKKs MKK4 and MKK7. MKK4/7 then activate JNKs by dual-phosphorylation on Thr and Tyr residues within the conserved Thr-Pro-Tyr motif in the activation loop. Once activated, JNK has been shown to phosphorylate and activate c-jun, promotes AP-1 complex formation and thereby mediates transcription of genes containing AP-1 binding sites **(59)**. It has also been reported that JNKs interact with other transcription factors including p53, ATF-2, c-Myc, STAT3 **(60).** Mice lacking JNK1/2/3-encoding genes showed significant defects in apoptosis and immune responses **(60).** In addition, inactivation of JNK1/2 has been associated with decreased response to DNA-damaging agents and UV radiation in cancer cells, implying the involvement of the JNK module in apoptosis **(61).** JNKs are also involved in cell metabolism, immune responses, cytokine production and actin reorganization **(62-64).** The JNK signaling pathway has been implicated in the pathologies of several neurological disorders including Alzheimer's and Parkinson's disease **(55).**

---

p38 MAPK:

This group of MAPK comprise of four splice variants including p38α, p38β, which are ubiquitously expressed in mammalian cells, p38ɣ and p38δ which are differentially expressed **(53).** These are activated by several extraneous stress stimuli including oxidative stress, UV radiation, inflammatory cytokines and hypoxia **(65).** Several upstream regulators including Rho family GTPases Rac1 and Cdc42, GPCRs and adaptors proteins are known to initiate the pathway, by recruiting MAPKKKs involved in p38MAPK activation. These MAPKKKs, which are common for JNK and p38, phosphorylate MKK3/6 which are involved in the activation of p38MAPK isoforms by dual phosphorylation at specific Thr-Gly-Tyr motifs in the activation loop. Activated p38MAPK then interacts with several cytoplasmic and nuclear substrates which mediate cellular responses including inflammation, cell cycle arrest, differentiation and apoptosis **(65).**

Functions of p38MAPK:

1. **p38MAPK in cell cycle regulation:** p38MAPK is activated in response to stress stimuli such as DNA damage , oxidative stress and osmotic stress. In response to DNA damage, p38MAPK has been shown to play a negative modulatory role in cell cycle progression at G2/M transition by several mechanisms **(66, 67).** This is initiated by detection of DNA damage by serine/threonine kinases that act as DNA damage sensors, including ATM and ATR kinases. These sensor DNA repair proteins are known to interact with Tau proteins that act as MAPKKK and activate MKK3/6, which in turn phosphorylate p38MAPK. p38MAPK is known to interact and phosphorylate p53 transcription factor, which induces the transcription of target genes namely p21 and Gadd45a, which are involved in cell cycle arrest at G2/M phase **(66).** In addition, p38MAPK can also induce G1/S cell cycle checkpoint in response to oxidative stress and hypoxia by several mechanisms including expression of regulatory proteins such as p16INK4a and p19ARF **(67).**

2. **p38MAPK in cell differentiation:** Several studies have implicated the positive and negative modulatory roles of p38MAPK in cellular differentiation. For example, it has been

suggested that p38MAPK induces cell cycle arrest in myoblasts which is followed by a gradual increase in expression of muscle-specific genes, thereby, inducing myocyte differentiation into myotubes **(68).** This is induced by increased activity of transcriptional factors and chromatin remodeling. In addition, p38MAPK has also been implicated in osteoclast differentiation initiated by RANKL signaling, by the activation of NFATc1 and NF-κB transcription factors **(69)**. Furthermore, studies in intestinal cells revealed that p38MAPK is activated in intestinal cells induced to differentiate and inhibition of p38MAPK blocks transcription of cell differentiation markers **(70)**. These effects were found to be coupled with the increased activity of CDX2/3 which are nuclear transcription factors, induced by their interaction with p38MAPK. Apart from studies indicating the role of p38MAPK in inducing cell differentiation, studies in adipocytes indicate inhibitory role of p38MAPK in adipocyte differentiation **(71, 72)**. Increased adipogenesis results in adipose tissue expansion and obesity. Studies by Aouadi and associates have revealed that both diet-induced and genetically obese mice exhibit decreased p38MAPK activity, resulting in increased adipogenesis **(71)**. Together, these observation suggest tissue-specific regulatory role of p38MAPK in cellular differentiation.

3. **p38MAPK in cell survival and apoptosis:** Evidence from multiple cell types indicate that p38MAPK exhibits cell-specific anti- and pro-apoptotic functions by interacting with its diverse substrate proteins **(53)**. Evidence from studies in certain cancer cells showed a pro-survival effect of p38MAPK activation. For example, treatment of Jurkat cells and T lymphocytes with p38MAPK inhibitor augmented the cytotoxic effect of 8-methoxypsoralen and UV-radiation treatment, thereby increasing the efficacy of this therapy **(73)**. Furthermore, studies by Gutiérrez-Uzquiza et al. have revealed a novel mechanism by which p38MAPK may play a role in cell survival in response to oxidative stress, by mediating the transcription of anti-oxidant genes including superoxide dismutases and catalase **(74)**. Although some observations indicate anti-apoptotic

function of p38MAPK, a majority of studies have demonstrated its pro-apoptotic role. Oxidative stress has been shown to be a major activator of p38MAPK in multiple cell types including pancreatic β-cells **(75)**, neurons **(76)** and cardiac myocytes **(77)**. Furthermore, treatment of cancer cell lines with All-trans-retinoic Acid activates p38MAPK in a Rac1-dependent manner, which in turn activates MAPKAPK2 and mediates apoptosis **(78)**. Studies by Bulavin et al. have demonstrated that p38MAPK is involved in the activation of p53 tumor suppressor pathway, where p38MAPK phosphorylates p53 at several residues at it N-terminus **(79)**. This causes p53 to dissociate from MDM2, a negative modulator of p53 function, protecting p53 from proteosomal degradation and allowing its function as a transcriptional factor. These events lead to the expression of pro-apoptotic target genes of p53, thereby inducing cell death.

p53 tumor suppressor

p53 tumor suppressor is a transcription factor belonging to a unique family of proteins which also includes p63 and p73 **(80, 81).** Encoded by the TP53 gene, p53 is commonly referred to as the "guardian of the genome" and is involved in inducing anti-proliferative cellular responses to DNA damage including cell cycle arrest, cellular senescence, DNA repair and apoptosis **(82)**. These functions are mediated by the binding of activated p53 to the DNA, thereby promoting the transcription of several target genes **(83)**. Evidence from mice lacking p53 demonstrated its critical role as a tumor suppressor, since p53 -/- mice spontaneously develop neoplastic tumors **(84)**. TP53 was initially identified as an oncogene, since p53 was found to be overexpressed in most tumor cells. However, later studies identified that these tumor cells expressed a missense mutant of p53 and the oncogenic nature resulted from loss of p53 function **(85, 86)**. Nearly 50 % of all human cancer types exhibit mutation or loss of p53 function, where it is inactivated either by mutation in TP53 gene, or mutations in genes encoding regulatory proteins that interact with p53 **(87)**. Several reports in multiple cell types have provided insights into the post-translational

modifications involved in the p53 signaling pathway and have identified the regulatory proteins involved in the modulation of p53 function **(88-91)**.

Structure of p53:

TP53 gene, located on the small arm of chromosome 17, encodes a nuclear phosphoprotein containing 393 amino acids composed of several structural and functional domains **(83, 89, 92)**. These are: 1) N-terminal transactivation domain (TAD) – divided into subdomains TAD1 (1-40 amino acid residues), TAD2 (40-61 amino acid residues) and a proline-rich region (61-94 amino acid residues); 2) Central DNA-binding domain (102-292 amino acid residues) and 3) C-terminal region – containing a tetramerization domain (324-355 amino acid residues), nuclear export and import signal sequences and a carboxyl-terminal regulatory domain (363-393). The N-terminal TAD is mostly involved in transcriptional activation and interacts with several regulatory factors including MDM2 and p300 **(90, 91)**. The central DNA-binding domain mediates site-specific binding of p53 to the DNA **(93)**. The C-terminal domain containing the tetramerization domain is required for the binding of p53 monomers to form tetramers that possess a greater affinity for DNA-binding sites **(94)**. Tetramerization also has been shown to promote nuclear localization as the nuclear export sequence is masked in p53 tetramers **(95)**. The carboxy-terminal has also been implicated in regulating DNA binding and tranactivation of p53 target genes **(96, 97)**. p53 also consists of nuclear localization (NLS) and nuclear exclusion sequences (NES) which regulate its nucleo-cytoplasmic shuttling **(98, 99).**
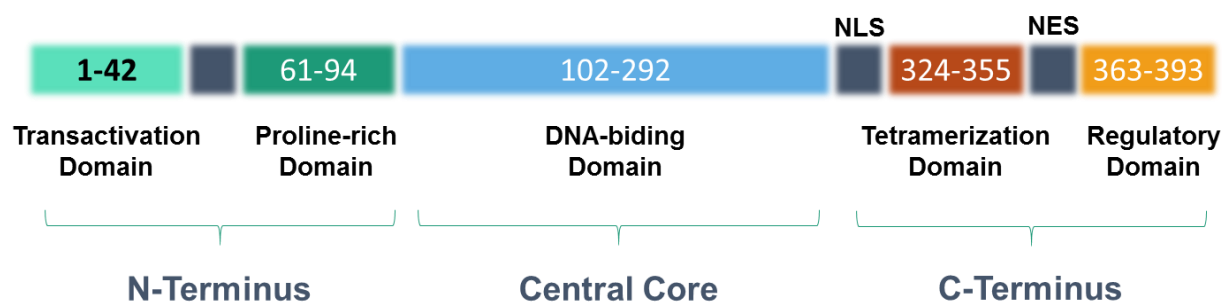
Figure 1-10: The structural and functional domains of the p53 tumor suppressor
[Modified from Joerger AC et al. ref **(92)**.

Regulation of p53 function

p53 expression levels and activity are maintained relatively low in the absence of a stress stimuli by several mechanisms **(100)**. Mice lacking p53 were found to be developmentally normal, suggesting that p53 function is not necessary for normal cell physiology and functioning **(84).** One of the mechanisms involved in down regulation of p53 function is mediated via its interaction with MDM2 **(101)**. MDM2 is an E3 ubiquitin ligase, encoded by a p53-inducible gene, and plays a critical role in suppressing p53 function in unstressed cells **(90, 101, 102)**. Studies in mice lacking MDM2 revealed that deletion of MDM2 gene results in embryonic lethality which is however, rescued by loss of p53 function **(103)**. MDM2 binds to p53 at the N-terminus TAD thereby suppressing activation of gene transcription. MDM2 also ubiquitinates p53, causing its degradation by the proteasomal system **(104)**. Ubiquitination also causes the nuclear exclusion of p53 into the cytoplasm, where it is more susceptible for proteasomal degradation **(105)**. This mechanism initiated by MDM2 expression induced by p53, represents an autoregulatory negative feedback loop that regulates the activity and levels of p53. However, in response to cellular stressors such as DNA damage, oxidative stress and hypoxia, p53 undergoes several post-translational modification that mediate its functional activation and stabilization **(88)**. These include phosphorylation, acetylation, ADP-ribosylation, sumoylation and ubiquitylation that occur at several amino acid residues present mostly in the N-terminal and C-terminal domains. Among these modifications, phosphorylation and acetylation have been implicated as the major contributors to functional activation and stabilization of p53 tetramers **(106, 107)**. The sites and importance of these modifications in the regulation of p53 function in various models of human disease are currently under investigation.
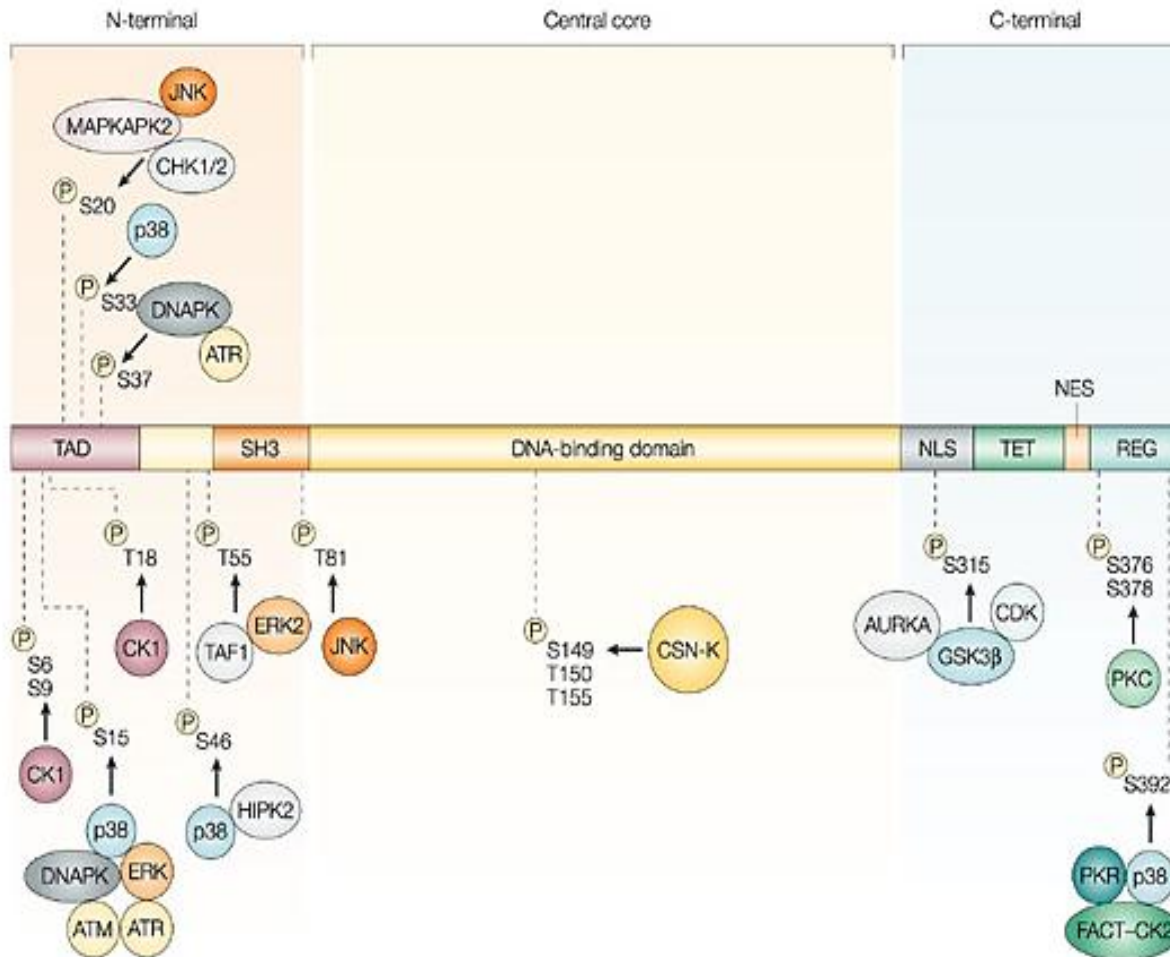
Figure 1-11: Several post-translational modifications induced by regulatory factors that modulate p53 function [Modified from Bode AM et al. ref **(89)**]

p53 in apoptosis

In the presence of stress stimuli, p53 undergoes post-translational modification that stabilize p53 tetramers and mediate their functional activation and nuclear localization. These p53 tetramers then are able to bind with specific DNA sequences and activate the transcription of several genes that mediate various cellular responses **(108, 109)**. This is mediated by the interaction with p53 response elements in the DNA that bind with p53 to activate transcription of target genes **(108)**. p53 is also known to interact with other transcriptional regulators such as p300 acetyl transferase **(91)**. This results in acetylation of p53 and histones surrounding the DNA binding sites, thereby increasing the DNA-binding activity. The gene transcription products

induced by p53 include p21, Gadd45, 14-3-3δ, Fas, Bax, PUMA and Noxa which are known to mediate cell cycle arrest and apoptosis, in response to stress stimuli **(110-114)**.

In the presence of stress stimuli, p53 is known to induce cell apoptosis by several mechanisms including the extrinsic and the intrinsic apoptotic pathway, and by inducing genes that suppress cell survival signaling **(83)**. The extrinsic pathway involves the binding of specific extracellular ligands (e.g., Fas ligand) to death receptors (e.g., Fas) which leads to the accumulation of FADD and initiator caspases causing apoptosis **(80)**. For example, the cytotoxic effects of bleomycin in hepatoma cells is mediated by increased nuclear accumulation of p53 and increased expression of Fas receptor **(115)**. It has also been suggested that p53 mediates membrane translocation of Fas receptor from the Golgi complex **(116)**. Additionally, p53 is also known to induce DR4 and DR5 death receptors which are involved in TNF-related apoptosis-inducing ligand (TRAIL) **(117, 118)**. Moreover, a majority of the p53-inducible genes are involved in the intrinsic apoptotic. p53 activates the transcription of pro-apoptotic proteins belonging to the Bcl2 family, which are modulators of mitochondrial membrane potential. Bcl2 family proteins can be classified intro three subfamilies: 1) Anti-apoptotic Bcl2; 2) Pro-apoptotic Bax; and 3) Pro-apoptotic BH3-only (Bcl2 homology-3) proteins. The pro-apoptotic Bax gene promoter region has been shown to possess p53 binding sites. Bax increases mitochondrial membrane permeability which releases cytochrome c into the cytoplasm and activates caspases and apoptosis. Similarly, an important target gene for p53 is the p53-upregulated modulator of apoptosis (PUMA), which is a BH3-only apoptotic protein. The PUMA gene, consisting of high affinity p53-binding sites, encodes for two isoforms which are known to upregulate Bax activity thereby activating apoptosis **(113)**. Another BH3-only protein regulated by p53 is Noxa, which also promotes Bax activity and apoptosis **(114).**
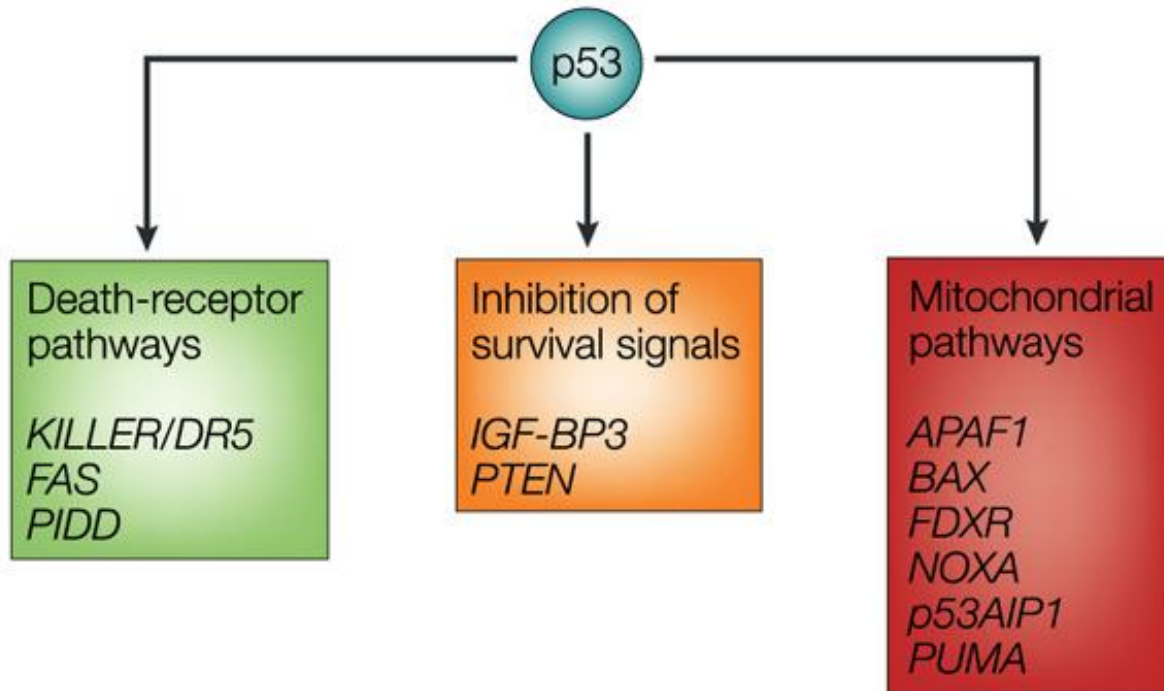
Figure 1-12: Mechanisms of p53-induced apoptosis [Vousden KH et al. ref **(83)**]

Hypothesis

Our preliminary data and above literature review indicate that excess generation of ROS by Rac1-Nox2 enzyme complex causes oxidative stress, which leads to the activation of downstream apoptotic stress kinases. Despite the above evidence suggesting the involvement of Rac1-Nox2 in β-cell dysfunction under diabetic conditions, the downstream signaling pathways need to be further elucidated. The central objective of my dissertation project is to examine the role of Rac1 and Nox2 in the generation of oxidative stress, leading to the activation of pro-apoptotic factors, resulting in pancreatic β-cell death under glucotoxic conditions. Using pharmacological approaches, we propose to examine the regulation of stress kinase p38MAPK and p53 pathways by Rac1-Nox2 enzyme complex in INS-1 832/13 cells, rodent and human pancreatic islets. Furthermore, we will extend these studies in *in vivo* models of obesity, insulin resistance and pancreatic β-cell dysfunction (Zucker diabetic fatty rat).

The proposed studies will test the hypothesis that (i) chronic exposure of pancreatic β-cells to glucotoxic conditions leads to sustained activation of Rac1-Nox2 holoenzyme and the resulting oxidative stress activate the p38MAPK and p53 signaling pathways, culminating in the activation of apoptotic pathways and β-cell death; and (ii) therapeutic intervention of Rac1-Nox2 signaling cascade prevents pancreatic β-cell death, induced by glucotoxic conditions, and onset of diabetes.

I will accomplish these goals by conducting studies under the following three specific aims:

Specific Aim 1: To determine if Rac1/Nox2 derived ROS leads to the activation of p38MAPK, under glucotoxic conditions

Specific Aim 2: To demonstrate the role of p53 phosphorylation in mediating the effects of Rac1/Nox2 under glucotoxic conditions

Specific Aim 3: To examine the Rac1-p38MAPK-p53 pathway in human pancreatic islets exposed to glucotoxic conditions and in whole animal models of pancreatic β-cell dysfunction
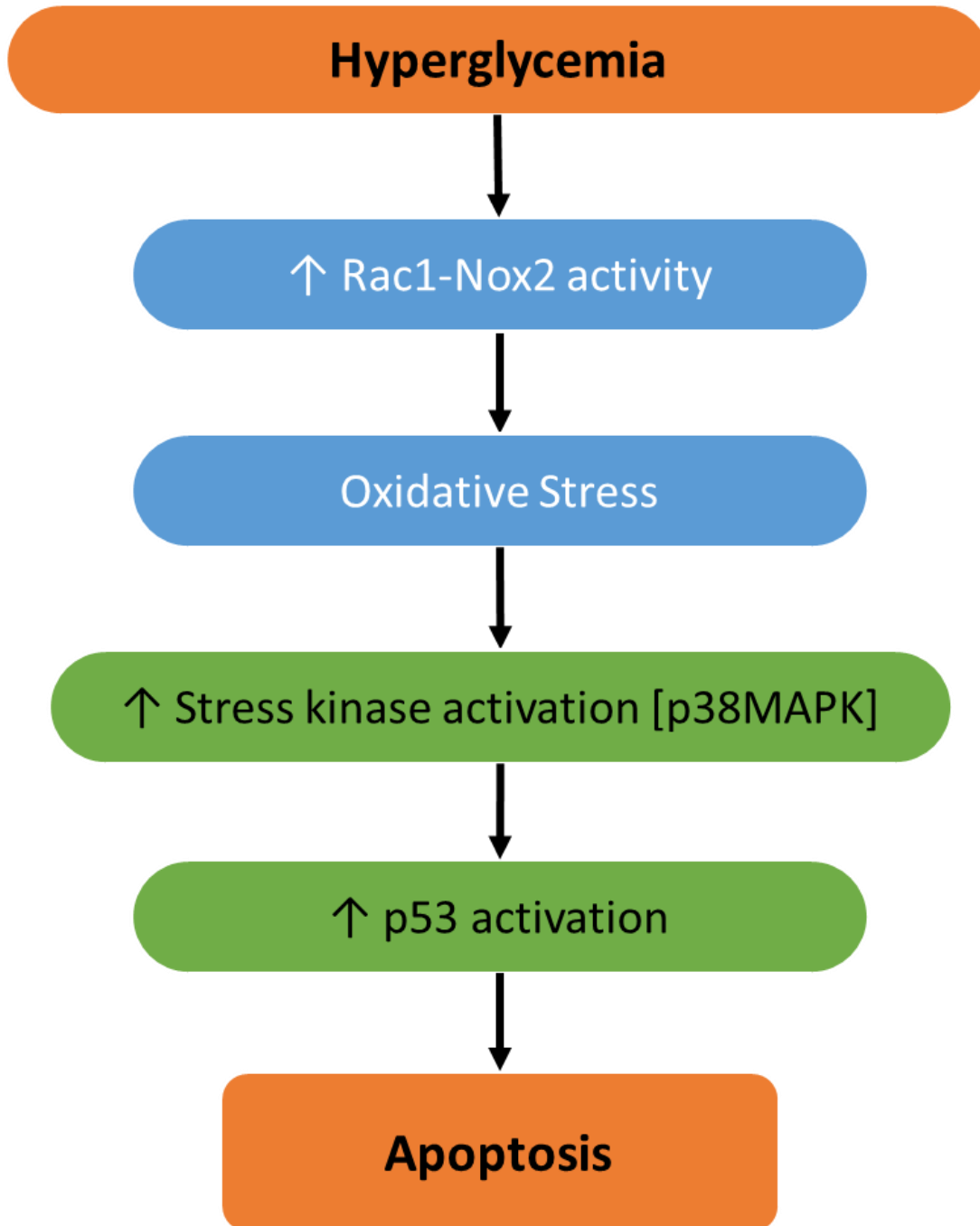
Figure 1-13: Proposed working model for Rac1-Nox2-induced oxidative stress and activation of p38MAPK-p53 signaling pathway in pancreatic β-cells under glucotoxic conditions: We propose that chronic exposure of β-cells to elevated glucose concentrations leads to sustained activation of Rac1-Nox2 holoenzyme and oxidative stress, which in turn activates p38MAPK and p53 tumor suppressor. This leads to activation of p53-target gene transcription, which ultimately induce β-cell apoptosis.

Pharmacological agent	Target	Mechanism of action	Functional Consequence
gp91-ds-tat	Nox2	Prevents association of p47phox with gp91phox	Inhibition of Nox2 holoenzyme assembly activation
NSC23766	Rac1	Blocks Tiam1-Rac1 interaction	Inhibition of Tiam1-mediated Rac1 activation
Ehop-016	Rac1	Blocks Vav2-Rac1 interaction	Inhibition of Vav2-mediated Rac1 activation
EHT1864	Rac1	Prevents GDP/GTP association of Rac1	Inhibition of Rac1 function
Simvastatin	HMG CoA reductase	Inhibits the isoprenoid biosynthetic pathway	Decreased protein prenylation
GGTI2147	GGTase-I	Blocks protein geranylgeranylation	Decreased protein geranygeranylation
2-bromopalmitate	Protein acyl transferases	Blocks protein S-palmitoylation	Decreased protein palmitoylation
SB203580	p38MAPK	Blocks kinase activity of p38MAPK	Inhibition of p38MAPK function

Table 1-1: List of pharmacological inhibitors utilized to target Rac1, Nox2 and p38MAPK

CHAPTER 2: MATERIALS AND METHODS

Chemicals and antibodies:

Rabbit polyclonal antibody for phospho-p38MAPK (Thr 180/Tyr 182) and total-p38MAPK were obtained from Santa Cruz Biotechnology [Santa Cruz, CA]. Rabbit monoclonal antibody for phospho-p53 and total-p53 was purchased from Cell Signaling Technology [Danvers, MA]. Mouse monoclonal antibodies for Phospho-ATM (ser-1981) and total-ATM were obtained from Abcam [Cambridge, MA]. NSC23766 and GGTI-2147 were obtained from Calbiochem [San Diego, CA]. EHT1864 was from R&D systems [Minneapolis, MN]. EHop-016 was kindly provided by Dr. Cornelis Vlaar, University of Puerto Rico [San Juan, PR]. Scrambled gp91-ds-tat (inactive) and active gp91-ds-tat were from Anaspec, Inc. [Fremont, CA].). IRDye® 800CW anti-rabbit and anti-mouse secondary antibodies were obtained from LICOR [Lincoln, NE]. Glucose, 2-Bromopalmitate (2-BP), 2', 7'-dichlorofluorescein diacetate (DCFDA), N,-N'-dimethyl-9,-90-bisacridiniumdinitrate (lucigenin) were purchased from Sigma–Aldrich [St. Louis, MO]. All other reagents were obtained from Sigma (St. Louis, MO).

Kits:

Rat insulin ELISA kit was purchased from American Laboratory Products Co [Windham, NH]. Rac1 activation G-LISA kit was from Cytoskeleton Inc. (Denver, CO). NE-PER® Nuclear and Cytoplasmic Extraction Reagents were purchased from Thermo Scientific (Waltham, MA). Cell Death Detection ELISA® were purchased from Sigma (St. Louis, MO). Dead Cell Apoptosis Kit with Annexin V Alexa Fluor® 488 & Propidium Iodide (PI) was from ThermoFischer Scientific.

Insulin secreting INS-1 832/13 cells and culture conditions:

INS-1 832/13 cells were kindly provided by Dr. Chris Newgard, Duke University Medical Center [Durham, NC]. Cells were cultured in RPMI-1640 medium containing 10 % fetal bovine serum (FBS) supplemented with 100 IU penicillin and 100 IU/ml streptomycin, 1 mM sodium pyruvate, 50 mM 2-mercaptoethanol and 10 mM HEPES (pH 7.4) at 37 ° C and 5 % CO_2 in a humidified incubator. Cultured cells were sub cloned twice weekly following trypsinization and

passages 53–61 were used for the studies. Cells were incubated in low glucose-low serum media (LG-LS; 2.5 mM glucose; 2.5 % heat-inactivated FBS) overnight, prior to glucose treatments with low glucose (LG; 2.5 mM) and high glucose (HG; 20 mM) for 24 hours in the absence or presence of pharmacological agents as indicated in the text. At the end of the incubation time, cells were rinsed with PBS and lysed using radio immunoprecipitation assay (RIPA) buffer supplemented with containing protease inhibitor cocktail, 1 mM NaF, 1 mM PMSF and 1 mM Na_3VO_4.

Rodent and human islets and culture conditions:

Sprague-Dawley male rats (6 to 8 weeks old) were purchased from ENVIGO [Indianapolis, IN]. Male Zucker Diabetic Fatty (ZDF) rats (9 to 11 weeks old) and their age-matched lean controls (ZLC) were obtained from Charles River Laboratories [Wilmington, MA], and fed on Purina Diet 5008. All animals were maintained in a 12-h light/dark cycle with free access to water and food. Hyperglycemia in the diabetic animals was confirmed by measuring blood glucose levels by tail vein nick puncture using Freestyle glucometer from Abbott Diabetes Care, Inc [Alameda, CA]. All animal protocols were reviewed and approved by Institutional Animal Care and Use Committee at Wayne State University. Pancreatic islets from Sprague Dawley, ZDF and ZLC rats were isolated using collagenase digestion method as described in **(41, 49).** Briefly, collagenase solution (0.45 mg/ml) is injected into the common bile duct and inflated pancreata are excised. These were then further digested in collagenase (0.9 mg/ml) at 37 ° C followed by density gradient purification using Histopaque 1077. The isolated pancreatic islets were then incubated overnight in in RPMI-1640 medium containing 10% heat-inactivated FBS supplemented with 100 IU/ ml penicillin and 100 IU/ml streptomycin, 1 mM sodium pyruvate and 10 mM HEPES [pH 7.4]. Pancreatic islets isolated from ZLC and ZDF rats were rinsed in PBS and lysed in RIPA buffer supplemented with protease inhibitor cocktail, 1 mM NaF, 1 mM PMSF and 1 mM Na_3VO_4. Islets isolated from normal rats were further incubated in the presence of LG and HG for 24 hours in the absence or presence of pharmacological inhibitors as indicated in the text. Islets were then rinsed in PBS and lysed in RIPA buffer as described above. Human islets [~90-95% purity] from two normal [41-year-old

male and 63-year-old male] donors and culture media was purchased from Prodo Laboratories, Inc. [Irvine, CA]. Islets were then treated with LG (5.8 mM) and HG (30 mM) for 24 hours, harvested and lysed in RIPA buffer.

Glucose-stimulated insulin secretion studies:

For short-term insulin release assays, INS-1 832/13 cells were starved overnight in LG-LS media and then incubated in Krebs-Ringer Bicarbonate buffer (KRB, pH 7.4) for 1 hour. Cells were then stimulated with either 2.5 mM LG or 20 mM HG for 45 min at 37 ° C, and the insulin released into the supernatant was quantified using a sandwich ELISA kit, according to the manufacturer's instructions. Briefly, 5 µL of the supernatants collected were loaded onto microplates pre-coated with insulin monoclonal antibody. The microplates are then incubated at room temperature on a shaker at 700-900 rpm. After washing, TMB substrate is added to the microplate wells and incubated on the shaker at room temperature for another 15 minutes. The reaction is then stopped using a Stop solution provided, and absorbance is read at 450 nm wavelength **(24, 25)**.

For long-term insulin release assays, following overnight starvation, cells were incubated with glucose (2.5 mM, LG and 20 mM, HG) for 24 h. Cells were then pre-incubated in KRB buffer and further stimulated with either LG or HG for 45 min at 37 ° C. The supernatants were then collected and insulin released was quantified using the ELISA kit **(119).**

Quantification of ROS:

Following overnight starvation in LG-LS, INS-1 832/13 cells were incubated in the presence of LG and HG in the absence and presence of gp91-ds-tat (2.5µM) or its inactive scrambled peptide analog (2.5µM) for 24 hours. Cells were then rinsed in PBS, lysed and homogenized in PBS supplemented with 1mM PMSF and 1mM EDTA. 20-30 ug of protein was then incubated with 2 µM 2',-7'-dichlorofluorescein diacetate (DCFDA) for 10-15 minutes. The resulting fluorescence was then measured at 485nm and 530nm as excitation and emission wavelengths **(49, 120)**.

Nox2 activity assay:

INS-1 832/13 cells treated with LG and HG in the absence and presence of gp91-ds-tat (2.5µM) or its inactive scrambled peptide analog (2.5µM) for 24 hours, were rinsed and homogenized in PBS supplemented with 1mM PMSF and 1mM EDTA. 200-500ug protein was then incubated with 20 µM lucigenin (N, N-dimethyl-9, 9'-biacridinium dinitrate) as electron acceptor for 2 min followed by the addition of NADPH (100 µM). The resulting chemiluminescence was measured and Nox2 activity was expressed as nmoles of NADPH oxidized/min/mg of protein.

Rac1 activation assay:

INS- 832/13 cells treated with LG and HG as indicated in the text were washed in PBS and activated Rac1 was quantified using the GLISA kit according to the manufacturer's instructions **(49)**. Briefly, cells were lysed in the lysis buffer provided and lysates were clarified by centrifugation at 14,000 rpm for 1 min. Equal amounts of protein were loaded into the wells of a Rac1-GTP affinity plate and incubated for 30 min at 4 ° C. The wells were then washed with washing buffer and incubated with Rac1-specific primary antibody and HRP-conjugated secondary antibody. This was followed by incubation with horseradish peroxidase-detection reagent. The reaction was stopped using the stop buffer provided, and the absorbance was measured at 490 nm.

Isolation of nuclear and non-nuclear fractions:

Following incubation with LG and HG, cells were harvested in PBS and cell fractionation was done using NE-PER® Nuclear and Cytoplasmic Extraction Kit according to the manufacturer's instructions. Briefly, pelleted cells were suspended in Cytoplasmic Extraction buffer-1 and incubated on ice for 10 min. After addition of buffer-2, cells were incubated on ice for 1 min and centrifuged at 16,000g for 5 min to pellet the nuclei. The supernatants were collected as non-nuclear fractions. Nuclear proteins were then incubated with Nuclear Extraction buffer for 40 min and centrifuged at 16,000g for 10 min. The supernatants were then collected as nuclear fractions.

Western Blotting:

Lysate protein (30-40 µg) were separated by SDS-PAGE. Proteins were then transferred onto nitrocellulose membranes and blocked in 5 % non-fat dry milk solution in 1X TBST of 0.5 % Casein in 0.2X PBST. The membranes were then incubated with primary antibody directed towards the protein of interest in 5% milk or 0.1% Casein at room temperature for 1 hour or overnight at 4 ° C. After washing, the membranes were probed with the corresponding secondary antibodies. The antibody complexes were then detected using ECL detection kit (CareStream® Imaging system or HyBlot CL® Autoradiography Film) or Odyssey® Imaging Systems. The band intensities were quantified using CareStream® Molecular Imaging Software.

Cell Death Assays:

1. **Dead Cell Apoptosis Kit with Annexin V & Propidium Iodide:** INS-1 832/13 cells incubated with LG or HG for 24 h were first rinsed with PBS. Cells werestained with Annexin V/Propidium Iodide, according to Dead Cell Apoptosis Kit with Annexin V Alexa Fluor® 488 & Propidium Iodide kit protocol, for 15 minutes. Cells were then visualized under Olympus IX71 inverted fluorescence microscope using appropriate filters.

2. **Cell Death Detection:** Following incubation with LG and HG for 24 hours, cells were washed with PBS and analyzed with Cell Death Detection ELISA[plus] according to the manufacturer's instructions. Briefly, cells were lysed with the lysis buffer provided with the kit and centrifuged at 200g for 10 min. Supernatants were collected and incubated in streptavidin-coated plates with immuno-reagent containing anti-histone-biotin and anti-DNA-peroxidase for 2 h. Complexes were then detected photo-metrically using ABTS as substrate. Absorbance was measured at 405nm wavelength (reference wavelength at 490nm) and expressed as fold change over LG.

CHAPTER 3: GLUCOTOXIC CONDITIONS PROMOTE RAC1-NOX2-INDUCED ACTIVATION OF p38MAPK IN PANCREATIC β-CELLS

Portions of this work have been published [copies of the published manuscripts are appended]

- **Sidarala V**, Veluthakal R, Syeda K, Vlaar C, Newsholme P, Kowluru A. Phagocyte-like NADPH oxidase (Nox2) promotes activation of p38MAPK in pancreatic β-cells under glucotoxic conditions: Evidence for a requisite role of Ras-related C3 botulinum toxin substrate 1 (Rac1). *Biochemical Pharmacology* 2015; 95(4):301-10.

- **Sidarala V**, Veluthakal R, Syeda K, Kowluru A. EHT 1864, a small molecule inhibitor of Ras-related C3 botulinum toxin substrate 1 (Rac1), attenuates glucose-stimulated insulin secretion in pancreatic β-cells. *Cell Signalling* 2015; 27(6):1159-67.

Glucose-stimulated insulin secretion (GSIS) is initiated by the entry of glucose into the pancreatic β-cell, followed by a series of metabolic events, leading to translocation of insulin granules towards the membrane for fusion and release. It is evident that small G-proteins such as Rac1, Cdc42 and Arf6 play a critical role in cytoskeletal remodeling to mediate migration of insulin-laden granules **(8, 18)**. Studies in our own laboratory have demonstrated the requisite role of Rac1 activation and prenylation in glucose-induced cytoskeletal remodeling and insulin secretion **(18, 23-25, 34)**. Inhibition of Tiam1, a guanine nucleotide exchange factor for Rac1, with NSC23766, resulted in marked reduction in GSIS **(24)**. We recently have utilized Ehop-016, which targets Vav2-mediated Rac1 activation, and observed alterations in glucose-induced cytoskeletal remodeling and reduction in insulin secretion **(25)**. Similar effects were observed in the presence of GGTI-2147, which blocks geranylgeranylation, demonstrating that Rac1 prenylation is also requisite for GSIS **(34)**. Furthermore, studies from several laboratories have reported the

34

involvement of phagocyte-like NADPH oxidase (Nox2) and physiological levels of ROS in mediating GSIS. Studies by Leloup and associates have reported alterations in calcium mobilization and decreased GSIS in rat pancreatic islets, in presence of anti-oxidants **(38)**. Additionally, studies by Morgan et al. have shown that inhibition of Nox2 function results in reduced insulin secretory response **(36)**.

Type 2 diabetes is characterized by insulin resistance in the peripheral tissues and impaired insulin secretion from the pancreatic β-cell. Exposure of pancreatic β-cells to elevated levels of glucose and free fatty acids (referred to as glucolipotoxicity) has been implicated to be the cause of several complications of diabetes, including loss of β-cell function **(14, 15)**. In the context of β-cell dysfunction, several studies have reported increased activity of Rac1-Nox2 enzyme complex, resulting in excess ROS generation in models of diabetes **(49, 50, 120)**. Studies in the ZDF rat, a model for T2D, and human islets exposed to high glucose concentrations, have indicated marked increase in Rac1-Nox2 activity and ROS generation. Since it has been reported that pancreatic β-cells possess limited levels of anti-oxidant enzymes compared to other tissues, oxidative stress has been suggested as the causal mechanism of β-cell dysfunction under glucotoxic conditions **(45)**. However, the downstream signaling pathways that mediate the deleterious effects of oxidative stress need to be further examined.

Previous studies in our laboratory have implicated regulatory roles of stress kinases JNK1/2 and ERK1/2 in the ZDF rat. Studies have also implicated activation of p38MAPK in β-cells exposed to stress stimuli, culminating in the induction of apoptosis possibly mediated by p53 tumor suppressor **(121)**. Herein, we investigated the involvement of p38MAPK, in Rac1-Nox2-ROS signaling under glucotoxic conditions, resulting in β-cell dysfunction. We examined if glucotoxic conditions promote activation of p38MAPK by dual-phosphorylation in INS-1 832/13 cells and normal rodent islets. Furthermore, we utilized several pharmacological inhibitors to target the Rac1-Nox2 holoenzyme and observed their effects of p38MAPK activation.

Exposure of INS-1 832/13 cells to glucotoxic conditions results in cell death:

Unless stated otherwise, we have utilized 20mM glucose (HG) exposure for 24 h as our model for glucotoxicity, and compared the effects to 2.5mM (LG) basal glucose concentration. INS-1 832/13 cells, when exposed to HG for 24 h, showed increase cell death as indicated by increased Annexin V/Propidium Iodide staining, compared to cells exposed to LG (Figure 3-1; Panel A). Similarly, we quantified cell death using Cell Death Detection® kit as per the manufacturer's instructions, and observed a marked increase in cell death signal when cells were exposed to HG for 24 h. Data shown in Figure 3-1 (Panel B) is representative of three independent studies (* p < 0.05 vs 2.5mM glucose alone).
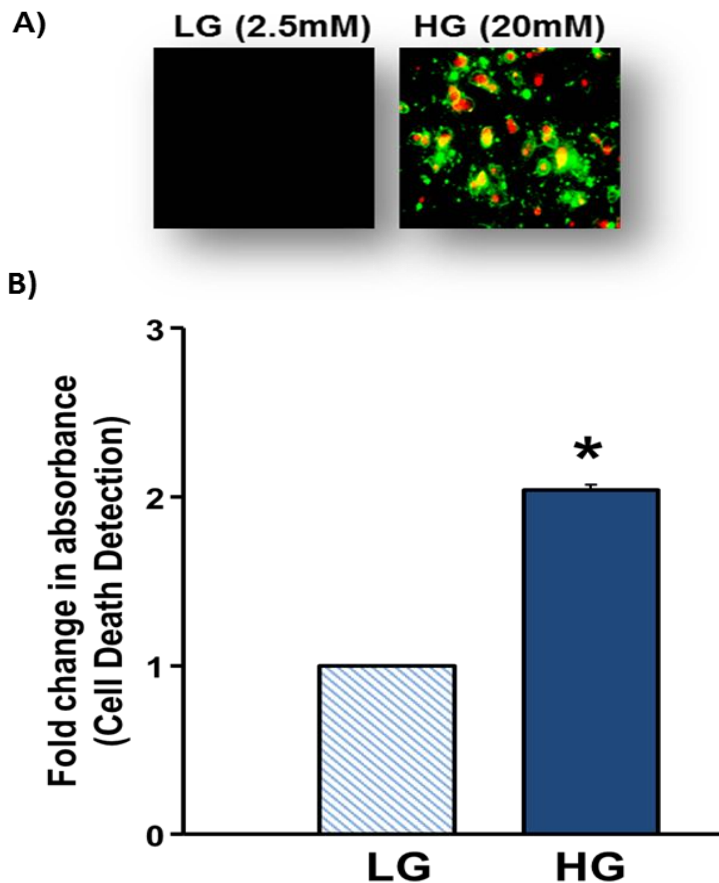
Figure 3-1: Exposure of INS-1 832/13 cells to glucotoxic conditions induces cell death:
Panel A: Following overnight starvation, INS-1 832/13 cells were incubated with LG and HG for 24 h. Cells were then washed and stained with Annexin V/ Propidium Iodide for 15 min. Cells were then visualized under Olympus IX71 inverted fluorescence microscope. **Panel B:** Following incubation with LG (2.5mM) or HG (20mM) for 24 h, INS-1 832/13 cells were washed with PBS and analyzed using Cell Death Detection ELISA^Plus kit according to manufacturer's instructions. Absorbance was measured at 405nm and expressed as fold change over basal LG. Data shown is representative of three independent studies (* p < 0.05 vs 2.5mM glucose alone).

gp91-ds-tat, an inhibitor of Nox2, markedly prevents Nox2 activation, ROS generation and p38MAPK phosphorylation under glucotoxic conditions:

Previous studies by Rey et al. have utilized gp91-ds-tat, a novel peptide inhibitor of NADPH oxidase assembly, to prevent vascular superoxide generation in mice **(122)**. This chimeric peptide interferes with the interaction of cytosolic p47phox and gp91phox in the membrane, thereby, disrupting the holoenzyme assembly. Several studies have utilized this inhibitor and its inactive analog, to study the role of Nox2 in models of various disorders **(123-127)**. At the outset, we utilized this inhibitor and measured its effects in pancreatic β-cells. We incubated INS-1 832/13 cells with LG (2.5mM) and HG (20mM) for 24 hours and quantified Nox2 activation. Data in Figure 3-2 (Panel A) demonstrate a significant increase in Nox2 activation under HG conditions. In addition, gp91-ds-tat, but not its inactive analog, significantly attenuated HG-induced Nox2 activation. Furthermore, we observed a similar increase in ROS generation in INS-1 832/13 cells incubated with HG, which was abrogated in the presence of gp91-ds-tat (Figure 3-2; Panel B).

We, therefore, utilized this inhibitor to determine the involvement of Nox2-derived oxidative stress in HG-induced p38MAPK phosphorylation. Data in Figure 3-2 (Panel C) indicate a marked increase in p38MAPK phosphorylation under HG conditions. However, gp91-ds-tat, but not its inactive analog, significantly attenuated HG-induced p38MAPK activation. Pooled data from multiple experiments is shown in Panel D. Together, these observations suggest upstream regulation by Nox2 activation in HG-induced p38MAPK activation, under glucotoxic conditions.

A)

B)

C)

D)
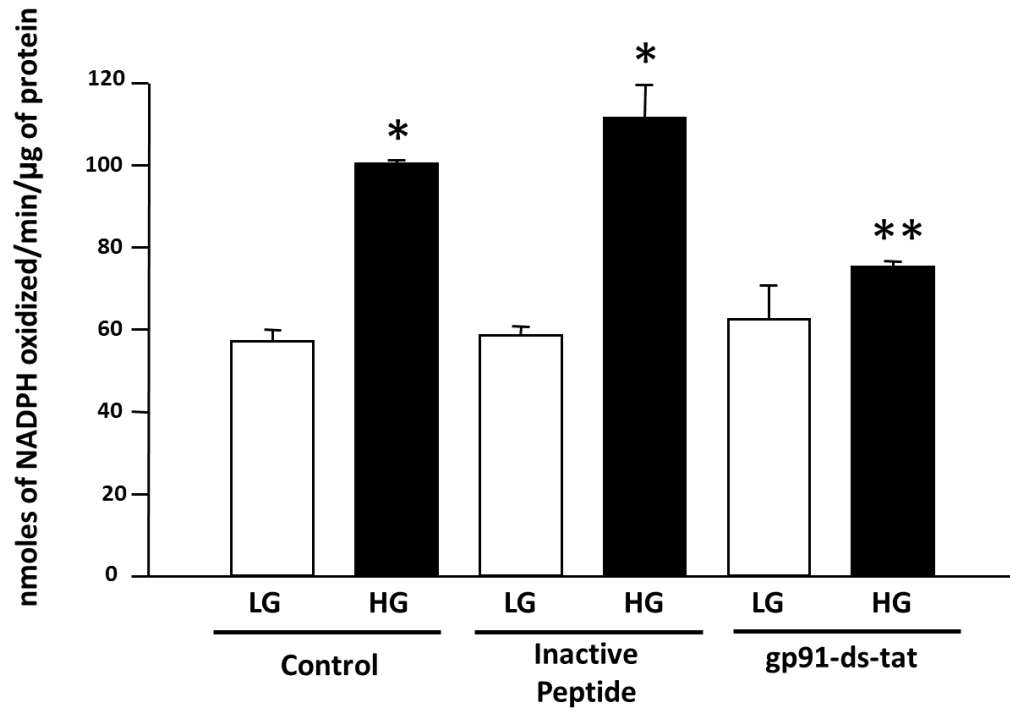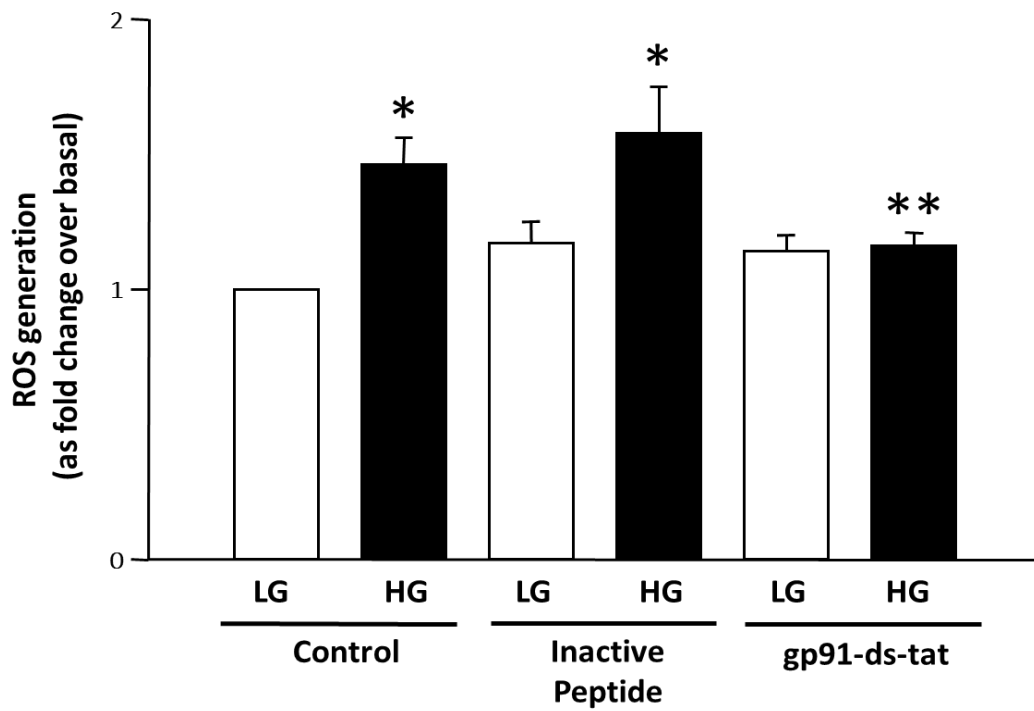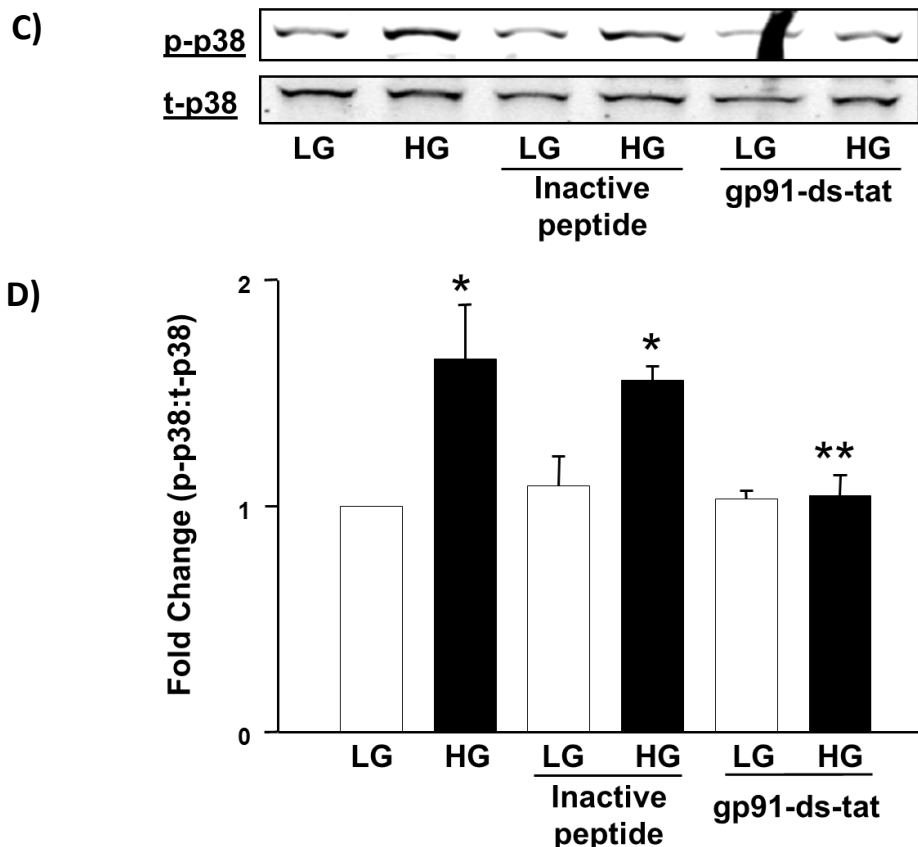
Figure 3-2: gp91-ds-tat peptide a specific inhibitor of Nox2, but not its inactive analog, inhibits HG-induced Nox2 activation, ROS generation and p38MAPK phosphorylation in INS-1 832/13 cells:
Following 1 h pre-incubation with scrambled peptide (2.5 µM) or gp91-ds-tat peptide (2.5 µM), INS-1 832/13 cells were then further treated with glucose (LG and HG) in the presence of scrambled peptide (2.5 µM) or gp91-ds-tat peptide (2.5 µM) for 24 h. **Panel A:** Nox2 activity was quantified as described in Chapter 2: Methods, and the activity was expressed as nmoles of NADPH oxidized/min/mg of protein. * $P < 0.05$ vs. low glucose. ** $P < 0.05$ vs. high glucose alone in presence of inactive peptide (mean ± SEM; n = 6). **Panel B:** After incubation of INS-1 832/13 cells with LG and HG in the absence and presence of scrambled or gp91-ds-tat peptide as described above, intracellular levels of ROS were measured using DCF-DA assay as described in Chapter 2: Methods. ROS generation was expressed as fold change over 2.5 mM glucose. * $P < 0.05$ vs. low glucose. ** $P < 0.05$ vs. high glucose alone or in the presence of inactive peptide (mean ± SEM; n = 6). **Panel C:** After incubation of INS-1 832/13 cells with LG and HG in the absence and presence of scrambled or gp91-ds-tat peptide as described above, cells were lysed and lysate proteins were separated by SDS-PAGE. After separation, proteins were transferred onto nitrocellulose membrane and blocked for 1 h. The membranes were then probed with antibody raised against phosphorylated p38MAPK followed by incubation with rabbit secondary antibody. The immune complexes were then detected using ECL detection kit. The same blots were stripped and reprobed for total p38MAPK. **Panel D:** Band intensities were quantified by densitometric analysis. Results are shown as mean ± SEM from three independent experiments and expressed as fold change of the ratios between phospho-p38MAPK and total p38MAPK. * $P < 0.05$ vs. low glucose, ** $P < 0.05$ vs. high glucose alone or in presence of inactive peptide.

Glucotoxic conditions promote phosphorylation of p38MAPK, which is dependent on Tiam1- and Vav2-mediated Rac1 activation:

Recent studies from our laboratory have demonstrated that inhibition of Rac1 blocks Nox2 activation under glucolipotoxic conditions **(23, 48, 50)**. To determine the involvement of Rac1 activation in p38MAPK activation, we therefore, employed inhibitors of Rac1 function to examine their effects on HG-induced p38MAPK phosphorylation. It is well established that Rac1 is activated by its association with GTP, which is mediated by guanine nucleotide exchange factors (GEF). Studies in our laboratory have identified two GEFs, Tiam1 and Vav2, involved in Rac1 activation in the β-cell **(18)**. We have utilized pharmacological inhibitors of Tiam1-Rac1 (NSC23766) and Vav2-Rac1 (Ehop-016) signaling axis, to assess the role of Rac1 in β-cell dysfunction under diabetic conditions **(24, 25).**

Herein, we assessed the roles of GEF-mediated Rac1 activation in HG-induced p38MAPK phosphorylation. We incubated INS-1 832/13 cells and normal rodent islets with LG and HG for 24 hours in the absence and presence of NSC23766 or EHop-016, and quantified p38MAPK phosphorylation. Data shown in Figure 3-3 (Panel A) demonstrated marked inhibition in p38MAPK phosphorylation in presence of NSC23766 in INS-1 832/13 cells and rat islets. Pooled data from multiple studies is provided in Panel B and C. Together, these data suggest the requisite role of Tiam1-meidated Rac1 activation in HG-induced p38MAPK phosphorylation. Compatible with these findings, we observed significant decrease in HG-induced p38MAPK phosphorylation in the presence of Ehop-016 in INS-1 832/13 cells and rat islets (Figure 3-3; Panel D). Pooled data from multiple studies is provided in Panel E and F. It is interesting, however, that the presence of Ehop-016 significantly increased p38MAPK phosphorylation under basal glucose concentrations in INS-1 832/13 cells and rat islets, suggesting that it might be regulating other signaling pathways. Together, these data suggest that inhibition of Tiam1-Rac1 and Vav2-Rac1 signaling axes prevents HG-induced p38MAPK phosphorylation, demonstrating the involvement of GEF-mediated Rac1 activation in this signaling axis.

A)

	INS-1 832/13 cells				Rat Islets			
Glucose, mM	2.5	2.5	20	20	2.5	2.5	20	20
NSC23766, 20µM	-	+	-	+	-	+	-	+

B)

Glucose, mM: 2.5 | 2.5 | 20 | 20
NSC23766, 20µM: - | + | - | +

C)

Glucose, mM: 2.5 | 2.5 | 20 | 20
NSC23766, 20µM: - | + | - | +

D)

	INS-1 832/13 cells				Rat Islets			
Glucose, mM	2.5	2.5	20	20	2.5	2.5	20	20
Ehop-016, 5µM	-	+	-	+	-	+	-	+

E)

Glucose, mM: 2.5 | 2.5 | 20 | 20
Ehop-016, 5µM: - | + | - | +

F)

Glucose, mM: 2.5 | 2.5 | 20 | 20
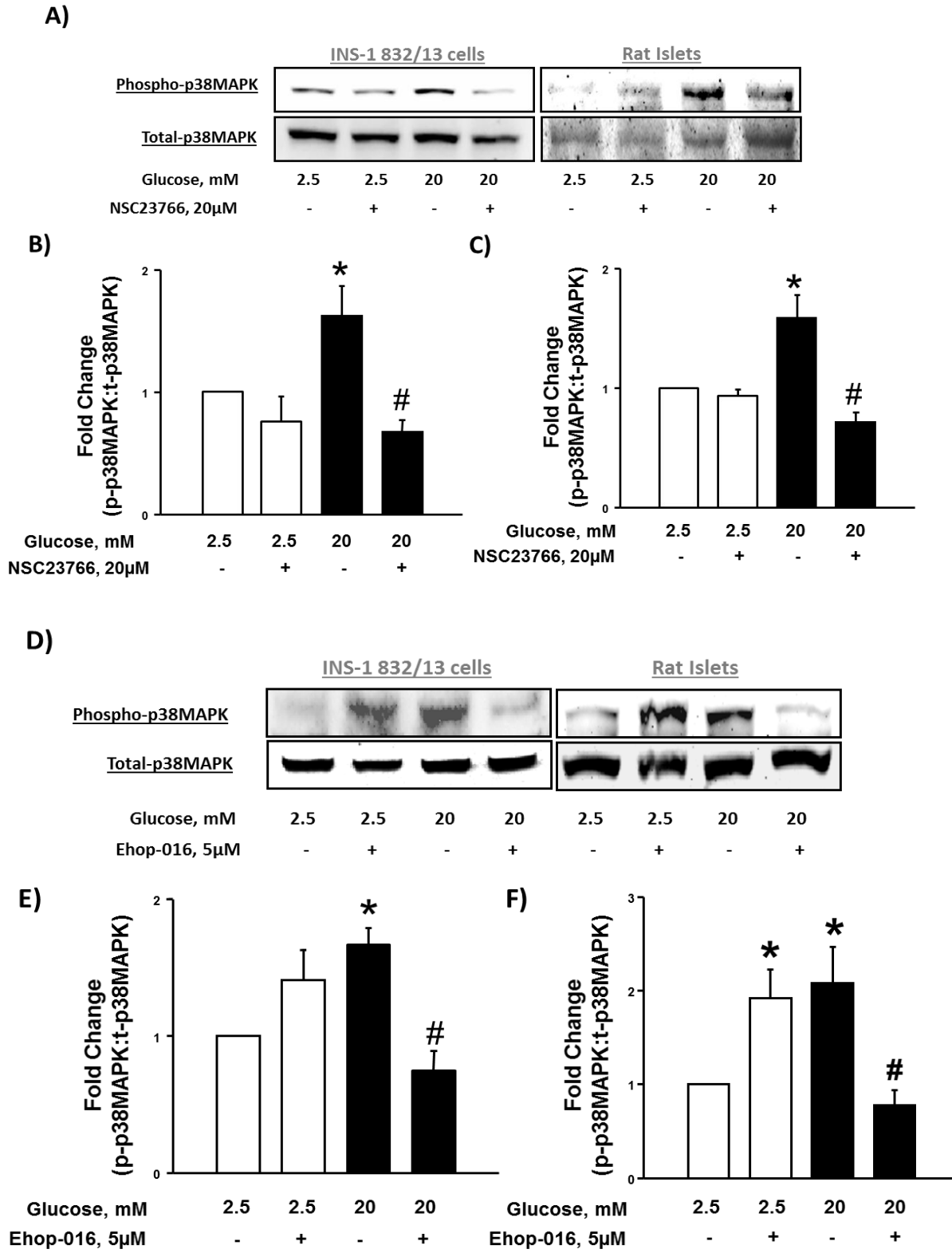Ehop-016, 5µM: - | + | - | +

Figure 3-3: NSC23766 and Ehop-016, which selectively block Tiam1- and Vav2-mediated Rac1 activation, prevent HG-induced p38MAPK phosphorylation in INS-1 832/13 cells and rat pancreatic islets:

Panel A: Rat pancreatic islets and INS-1 832/13 cells, pre-incubated overnight with NSC23766 (20 µM), were further treated with glucose (LG and HG) in the absence or presence of NSC23766 (20 µM) for 24 h. Cells were then lysed and proteins were resolved by SDS-PAGE. Separated proteins were transferred onto nitrocellulose membranes. After blocking for 1 h, the membranes were then probed with phosphorylated p38MAPK antibody followed by incubation with rabbit secondary antibody. The antibody complexes were then detected by ECL detection method. The same blots were stripped and reprobed with antibody against total p38MAPK. **Panel B:** Band intensities of phospho-p38MAPK and total-p38MAPK in INS-1 832/13 cells were quantified by densitometric analysis. Results are shown as mean ± SEM from three independent experiments and expressed as fold change of the ratios between phospho-p38MAPK and total-p38MAPK. * $P < 0.05$ vs. low glucose, # $P < 0.05$ vs. high glucose. **Panel C:** Band intensities of phospho-p38MAPK and total-p38MAPK in rat pancreatic islets were quantified by densitometric analysis. Results are shown as mean ± SEM from three independent experiments and expressed as fold change of the ratios between phospho-p38MAPK and total-p38MAPK. * $P < 0.05$ vs. low glucose, # $P < 0.05$ vs. high glucose. **Panel D:** Rat pancreatic islets and INS-1 832/13 cells, pre-incubated overnight with Ehop-016 (5 µM), were further treated with glucose (LG and HG) in the absence or presence of Ehop-016 (5 µM) for 24 h. Lysate proteins were then resolved by SDS-PAGE, and analyzed by Western Blotting, as described above, for detecting phosphorylated and total p38MAPK. **Panel E:** Band intensities of phospho-p38MAPK and total-p38MAPK in INS-1 832/13 cells were quantified by densitometric analysis. Results are shown as mean ± SEM from three independent experiments and expressed as fold change of the ratios between phospho-p38MAPK and total p38MAPK. * $P < 0.05$ vs. low glucose, # $P < 0.05$ vs. high glucose. **Panel F:** Band intensities of phosphor-p38MAPK and total-p38MAPK in rat pancreatic islets were quantified by densitometric analysis. Results are shown as mean ± SEM from three independent experiments and expressed as fold change of the ratios between phospho-p38MAPK and total p38MAPK. * $P < 0.05$ vs. low glucose, # $P < 0.05$ vs. high glucose.

EHT1864, a novel inhibitor of Rac1, blocks activation and membrane association of Rac1 activation and insulin secretion upon physiological glucose stimulation in INS-1 832/13 β-cells:

Desire and associates have designed a novel small molecular weight inhibitor EHT1864, which blocks Rac1 activation by direct interaction in a GEF-independent manner **(28)**. Studies by Shutes et al. have indicated that EHT1864 binds to Rac1 with a higher affinity than guanine nucleotides (GDP/GTP) thereby displacing GDP/GTP from the Rac1 binding site, retaining Rac1 in an inert, inactive state **(27, 128).** Several studies have utilized this inhibitor to assess the roles of Rac1 in cell physiology and disease **(129-132)**. At the outset, we undertook the study to examine the effects of EHT1864 on Rac1 function and glucose-stimulated insulin secretion under physiological conditions. Following 1 h pre-incubation with EHT1864, we stimulated INS-1 832/13 cells with LG (2.5mM) and HG (20mM) for 20 min in the continuous absence or presence of

EHT1864 and quantified Rac1 activation. Data depicted in Figure 3-4 (Panel A) demonstrate a marked increase in Rac1-GTP levels under stimulatory glucose concentration, which is significantly blocked in the presence of EHT1864. It is noteworthy, however, that EHT1864 caused an increase in Rac1 activation under basal conditions, although such an increase was not statistically significant (Bar1 vs Bar2).

We, next assessed the effects of Rac1 inhibition with EHT1864, on glucose-stimulated insulin secretion. Following pre-incubation with EHT1864 for 1 h as indicated in Figure 3-4 (Panel B), INS-1 832/13 cells were incubated with LG and HG for 30 in the continuous absence or presence of EHT1864, and quantified GSIS. Data depicted in Figure (Panel B) indicate a marked increase in insulin secretory response under stimulatory glucose concentration (20mM). We noticed a modest inhibition in GSIS in presence of EHT1864 at 5 μM concentrations. However, EHT1864 significantly blocked GSIS at 10uM concentrations. It is noteworthy, however, that 10 μM EHT1864 augmented insulin secretion under basal glucose concentrations. Similarly, as depicted in Figure 3-4 (Panel C), we noticed a significant increase in insulin secretion at 5mM glucose concentration in presence of 10 μM EHT1864. Together, these observations demonstrate inhibitory effects of EHT1864 on Rac1 activation and GSIS in INS-1 832/13 cells.

Previous investigations have suggested that membrane targeting of small G-proteins (Rac1 and Cdc42) is required for their optimal interaction with effector proteins and physiological function. We therefore, examined if glucose-induced membrane association of Rac1 is affected in presence of EHT1864. To address this, we first isolated cytosolic and membrane fractions of INS-832/13 cells treated with LG and HG with or without EHT1864 for 20 min. The membrane fractions were further processed by TritonX partitioning, to isolate hydrophilic and hydrophobic compartments. The relative abundance of Rac1 in these fractions was determined by Western Blotting and the purity of the fractions was confirmed by probing for their respective marker proteins. Data depicted in Figure 3-4 (Panel D) indicate that Rac1 is localized in the cytosolic fraction under basal conditions. However, cells treated with 20mM glucose showed marked

increase in Rac1 localized in the hydrophilic and hydrophobic fractions of the membrane. Furthermore, the presence of EHT1864, prevented Rac1 translocation to the membrane fraction induced by 20mM glucose concentration. A representative blot from multiple studies is provided in Panel D. Collectively, these data demonstrate that EHT1864 prevents activation and membrane targeting of Rac1, thereby inhibiting insulin secretion under stimulatory concentrations of glucose.
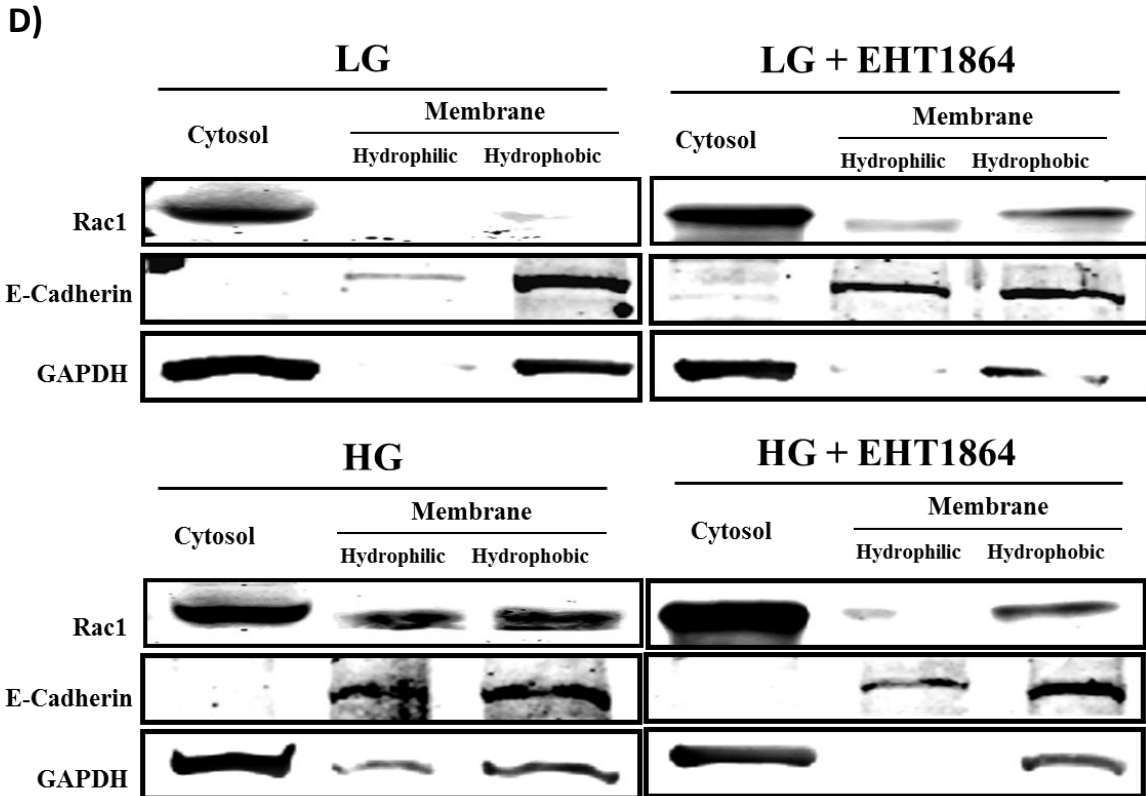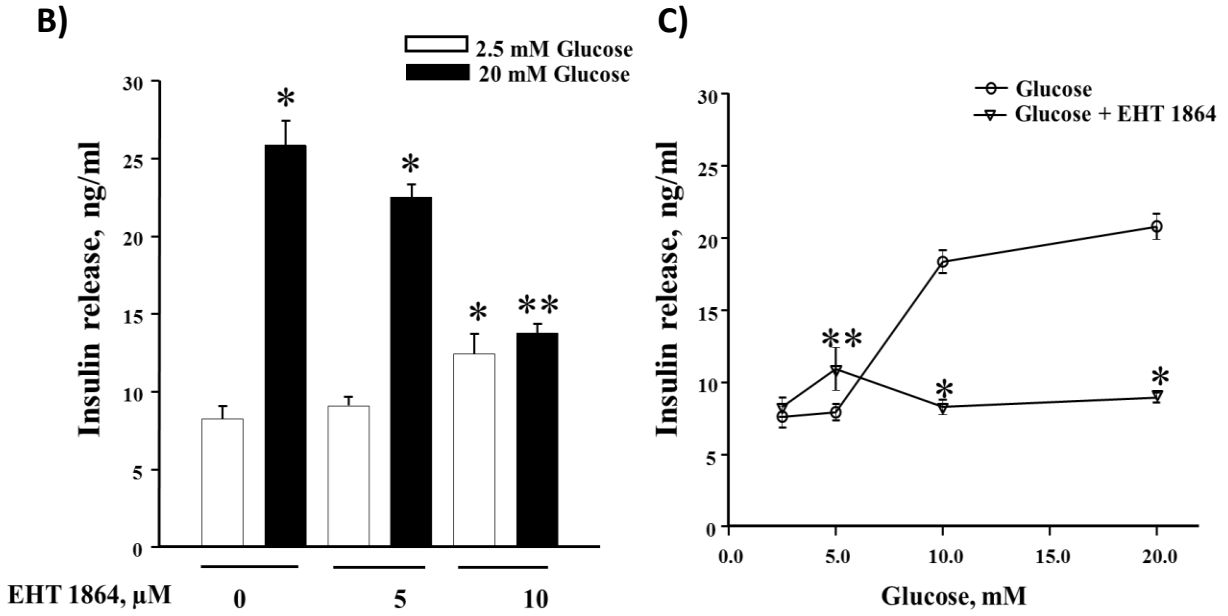
A)

B)

C)

D)
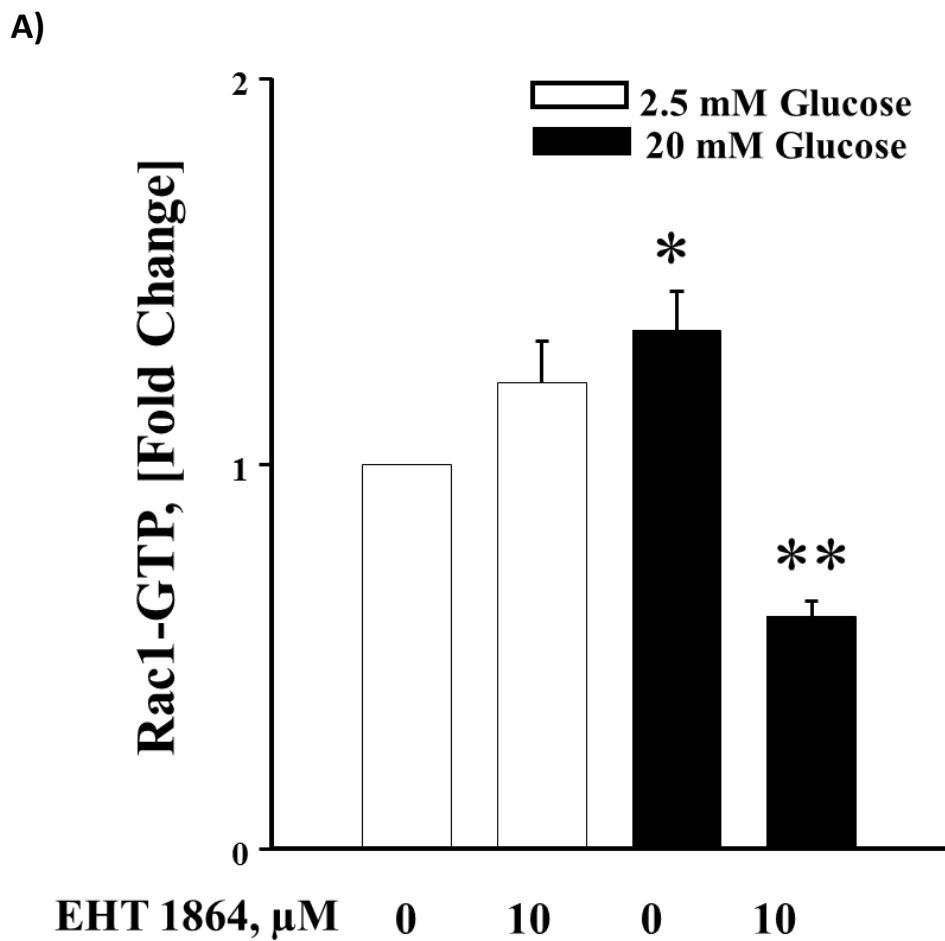
Figure 3-4: EHT 1864 significantly inhibits glucose-induced Rac1 activation, insulin secretion and membrane association of Rac1 in INS-1 832/13 cells:

Panel A: INS-1 832/13 cells were incubated in RPMI media overnight in the presence of 2.5 mM glucose and 2.5 % fetal bovine serum. After pre-incubation with EHT1864 (10 µM) for 1 h, cells were incubated in the presence of low (2.5 mM) or high glucose (20 mM) in the continuous absence or presence of EHT 1864 (10 µM) for 20 min at 37 °C. Rac1 activation was quantified by G-LISA as described in Chapter 2: Methods. Data are shown as mean ± SEM from multiple observations and expressed as fold increase over 2.5 mM glucose, and. * $P < 0.05$ vs. 2.5 mM glucose and ** $P < 0.05$ vs. 20 mM glucose. **Panel B:** Following overnight starvation in RPMI media supplemented with 2.5 mM glucose and 2.5% fetal bovine serum, INS-1 832/13 cells were preincubated with EHT1864 (0–10 µM) for 1 h and then further stimulated with low (2.5 mM) or high glucose (20 mM) in the continuous absence or presence of EHT 1864 for 30 min at 37 °C. Insulin released into the medium was quantified by ELISA. The data was expressed as ng/ml of insulin released ± SEM from multiple experiments. * $P < 0.05$ vs. 2.5 mM glucose and ** $P < 0.05$ vs. 20 mM glucose alone or in the presence of 5 µM of EHT1864. **Panel C:** Following overnight starvation in RPMI media supplemented with 2.5 mM glucose and 2.5% fetal bovine serum, INS-1 832/13 cells were preincubated with EHT1864 (10 µM) for 1 h and further stimulated with different concentrations of glucose (0–20 mM) in the continuous absence or presence of EHT1864 (10 µM) for 30 min at 37 °C. The amount of insulin released was quantified by ELISA. The data was expressed as ng/ml ± SEM from multiple observation. * $P < 0.05$ vs. 10 mM or 20 mM glucose and ** $P < 0.05$ vs. 5 mM glucose. **Panel D:** After overnight starvation in RPMI media supplemented with 2.5 mM glucose and 2.5% fetal bovine serum and 1 h pre-incubation with EHT1864 (10 µM), cells were stimulated with low (2.5mM) or high glucose (20mM) in the continuous absence or presence of EHT1864 for 20 min at 37 °C. Cells were then lysed and processed by phase partitioning with Triton X-114, to obtain cytosolic and hydrophilic/hydrophobic fractions of the membrane. The fractions were then analyzed to determine Rac1 localization by Western blotting, and a representative blot from three independent experiments is provided. The purity of the cytosolic and hydrophilic/hydrophobic membrane fractions was verified by probing for GAPDH (cytosol) and E-Cadherin (Membrane).

Glucotoxicity-induced p38MAPK activation is significantly blocked by EHT1864:

Our observations in Figure 3-4 demonstrate that EHT1864 blocks membrane targeting and activation of Rac1 and insulin secretion in the β-cell under physiological stimulatory conditions. We therefore, employed EHT1864 to observe the effects of Rac1 inhibition on p38MAPK activation under glucotoxic conditions. INS-1 832/13 cells were incubated with LG (2.5mM) and HG (20mM) for 24 h in the continuous absence and presence of EHT1864. As depicted in Figure 3-5 (Panel A), we noticed that inhibition of Rac1 guanine nucleotide association with EHT1864, significantly attenuated HG-induced p38MAPK phosphorylation. Pooled data from multiple experiments is provided in Panel B. Together, these data suggest that Rac1 plays an upstream regulatory role in the cascade of events resulting in p38MAPK phosphorylation under glucotoxic conditions.

A)

p-p38

t-p38

| Glucose, mM | 2.5 | 2.5 | 20 | 20 |
| EHT 1864, 10μM | - | + | - | + |

B)

Fold Change (p-p38:t-p38)

*

#

| Glucose, mM | 2.5 | 2.5 | 20 | 20 |
| EHT 1864, 10μM | - | + | - | + |
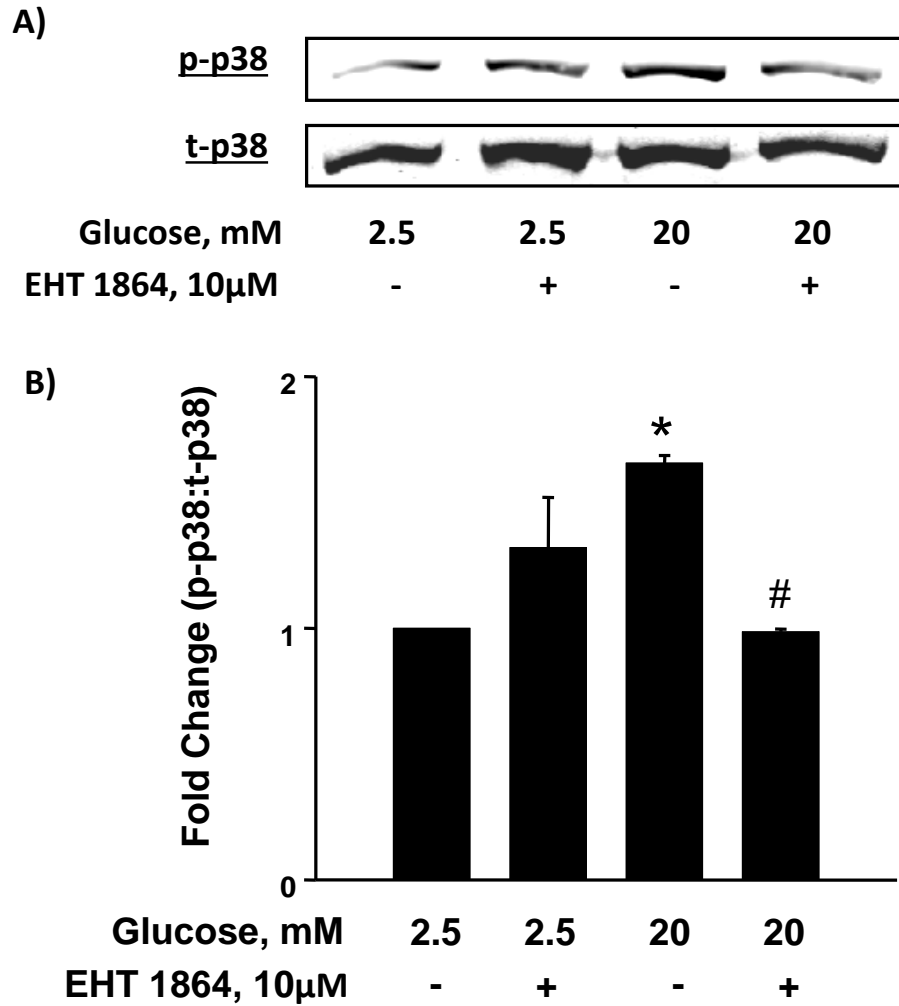
Figure 3-5: EHT1864 attenuates HG-induced p38MAPK phosphorylation in INS-1 832/13 cells:
Panel A: INS-1 832/13 cells were incubated with glucose (2.5 mM and 20 mM) for 24 h in the continuous absence or presence of EHT1864 (10 μM). Cells were then lysed and lysate proteins were then separated by SDS-PAGE, and transferred onto nitrocellulose membranes. The membranes were then blocked and probed with antibody raised against phosphorylated p38MAPK, followed by incubation with rabbit secondary antibody. The immune complexes were detected by ECL detection method. The saem blots were then stripped and reprobed for total p38MAPK. **Panel B:** Band intensities were then quantified by densitometric analysis. Results are shown as mean ± SEM from three independent experiments and expressed as fold change of the ratios between phosphor-p38MAPK and total-p38MAPK. * $P < 0.05$ vs. low glucose, # $P < 0.05$ vs. high glucose.

2-bromopalmitate, an inhibitor of protein palmitoylation, markedly attenuates p38MAPK phosphorylation:

It is well established that small G-proteins undergo a series of post-translational modifications including prenylation, carboxymethylation and palmitoylation. Studies by Navarro-Lerida et al. have demonstrated that Rac1 palmitoylation at cysteine 178, is required for its membrane association and optimal function **(133)**. We therefore, asked if Rac1 palmitoylation is requisite for HG-induced p38MAPK phosphorylation. To address this, we employed 2-bromopalmitate (2-BP), a known inhibitor of protein palmitoylation, to assess the effects on p38MAPK activation. As depicted in Figure 3-6 (Panel A), we noticed a marked inhibition in HG-induced p38MAPK activation in the presence of 2-BP. Pooled data from multiple experiments is provided in Panel B.
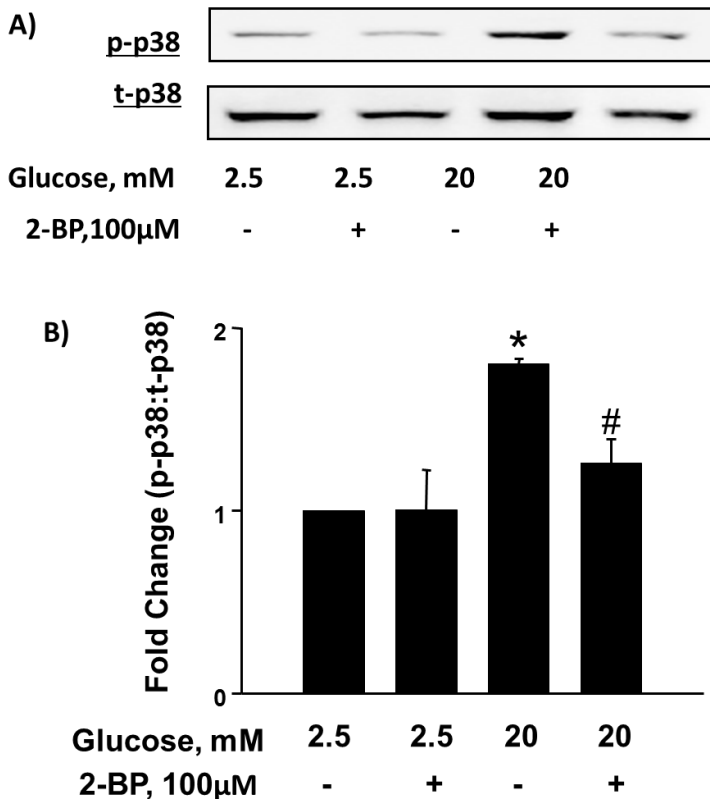
Figure 3-6: 2-bromopalmitate, an inhibitor of protein palmitoylation, prevents HG-induced p38MAPK phosphorylation:
Panel A: INS-1 832/13 cells were incubated with glucose (LG and HG) for 24 h in the continuous presence of 2-BP (100 µM). Cells were then lysed and lysate proteins were analyzed by western blotting. The nitrocellulose membranes were probed with antibody against phospho-p38MAPK followed by incubation with rabbit secondary antibody. The same blots were stripped and analyzed for total p38MAPK. **Panel B:** Band intensities were then quantified by densitometric analysis. Results are shown as mean ± SEM and expressed as fold change of the ratios of phospho- and total p38MAPK. * $P < 0.05$ vs. low glucose, # $P < 0.05$ vs. high glucose.

Collectively, evidence shown in figure 3-8 demonstrate that exposure of pancreatic β-cells to glucotoxic conditions lead to activation of p38MAPK activation. Using pharmacological inhibitors targeting Nox2 enzyme activity and Rac1 activation, we provide the first evidence suggesting the involvement of Rac1-Nox2-derived oxidative stress in the signaling events leading to p38MAPK activation.
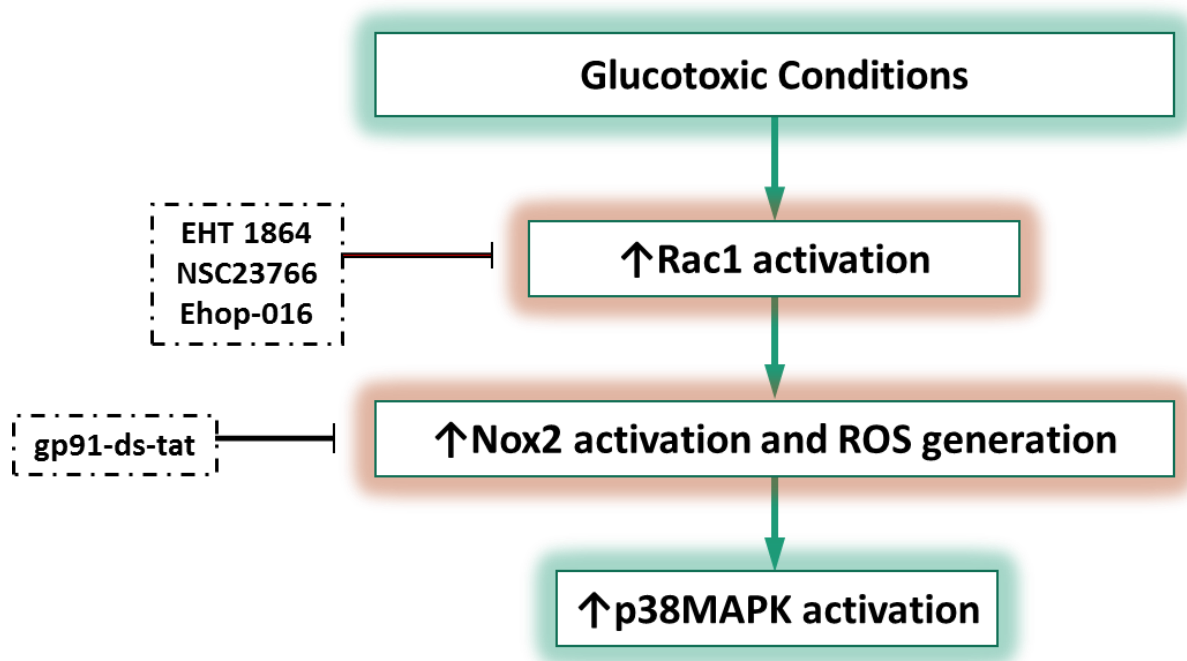
Figure 3-8: Proposed model for Rac1-Nox2-mediated ROS generation and p38MAPK activation under glucotoxic conditions:
Using pharmacological inhibitors of Rac1 (NSC23766, Ehop-016 and EHT1864), we have demonstrated that Rac1 activation is involved in HG-induced p38MAPK phosphorylation. Furthermore, gp91-ds-tat, but not is inactive analog, significantly attenuated HG-induced Nox2 activity, ROS generation and p38MAPK phosphorylation.

CHAPTER 4: GLUCOTOXIC CONDITIONS PROMOTE RAC1-p38MAPK-DEPENDENT ACTIVATION OF p53 TUMOR SUPPRESSOR

p53 tumor suppressor is a transcription factor and consists of several structural and functional domains which regulate its function and stability. Evidence from multiple cell types have implicated activation of the p53 pathway under the duress of oxidative stress and DNA damage, thereby mediating cellular responses to the stress stimuli including cell cycle arrest, DNA repair and apoptosis **(83)**. Studies in multiple cell types have suggested activation of apoptotic genes including Bax, Apaf1, PUMA, Noxa, by p53-mediated mechanisms **(108)**. However, the contributory role of p53 in pancreatic β-cell dysfunction under glucotoxic conditions remains poorly understood. To address this, we herein examined the involvement of p53 in the Rac1-Nox2-p38MAPK signaling cascade in β-cells exposed to glucotoxic conditions.

Several post-translational modification (e.g., Phosphorylation, Acetylation, Ubiquitination) have been shown to regulate p53 functionality and protein levels in the cell **(88).** It has been suggested that phosphorylation of p53 at serine-15 residue in the N-terminal transactivation domain is critical for its stabilization and transcriptional activation **(106)**. Studies have also implicated that serine-15 phosphorylation regulates p53 interaction with MDM2 and CBP/p300 that modulate its stability and DNA binding affinity **(90, 134).** p38MAPK activation has been suggested to result in phosphorylation and stabilization of p53 under specific stress stimuli in multiple cell types **(79, 135).** Additionally, studies by Yoshida and associates have also indicated the involvement of ATM kinase in p53 activation in Doxorubicin-induced cardiotoxicity. Using pharmacological approaches, they have demonstrated the role of Rac1-mediated oxidative stress in ATM kinase and p53 activation resulting in Doxorubicin-induced cardiomyopathy **(136)**. Furthermore, studies by Oleson et al. have also shown that ATM kinase mediates DNA repair in pancreatic β-cells exposed to inflammatory cytokines, but upon extensive dsDNA breaks may be responsible for activating apoptotic pathways primarily through p53-dependent mechanisms **(137)**. Using specific pharmacological inhibitors, we explored the regulatory roles of Rac1-Nox2

enzyme complex and upstream kinases including ATM kinase and p38MAPK in the p53 activation pathway, ultimately resulting in β-cell death.

p53 tumor suppressor is activated by serine-15 phosphorylation in INS-1 832/13 cells and rat islets exposed to glucotoxic conditions:

Phosphorylation of p53 at serine-15 in N-terminus transactivation domain residue has been associated with decreased binding to MDM2 (negative modulator) and increased interaction with p300 (positive modulator), thereby increasing functional activation and stabilization of p53 **(90, 134)**. Therefore, we first determined if exposure to glucotoxic conditions induced p53 activation by serine-15 phosphorylation. We incubated INS-1 832/13 cells and rat islets with LG (2.5 mM) and HG (20 mM) for 24 hours and quantified p53 phosphorylation in these samples. As shown in Figure 4-1, exposure to HG concentrations induced significant increase in p53 phosphorylation at serine-15 in INS-1 832/13 cells (Panel A) and rat islets (Panel C). Data from multiple experiments is shown in Panel B and D.
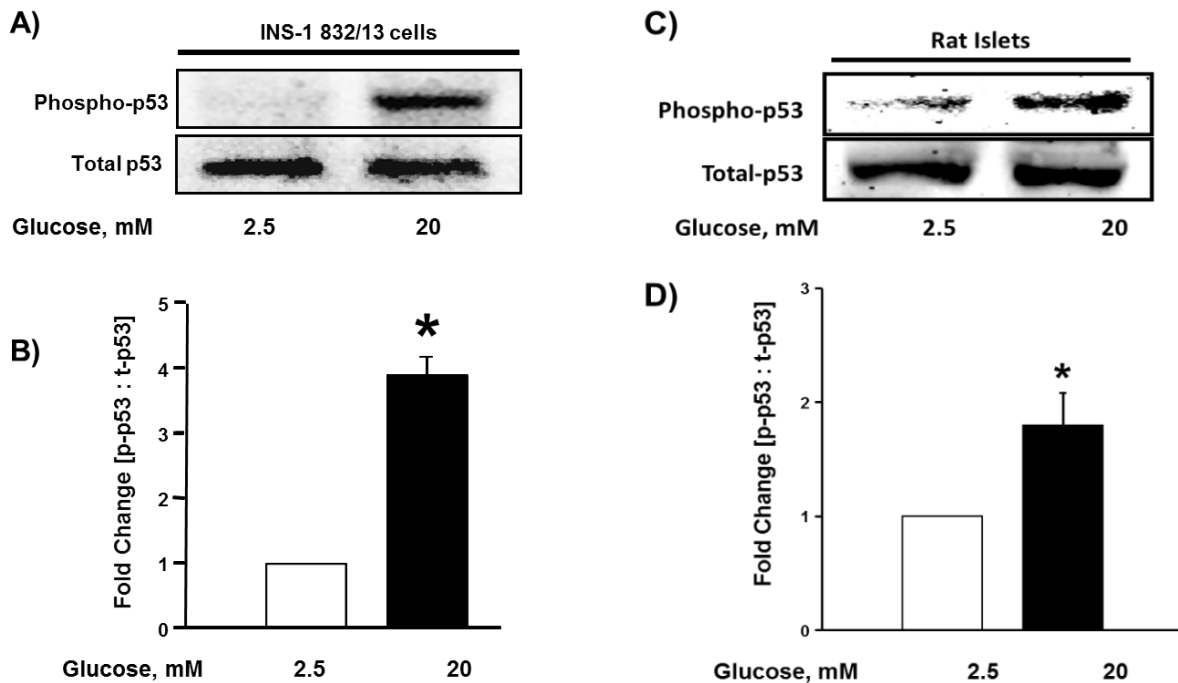
Figure 4-1: Exposure of INS-1 832/13 cells and rodent pancreatic islets to glucotoxic conditions results in p53 phosphorylation:

Panel A: Following overnight starvation in RPMI supplemented with 2.5 mM glucose and 2.5% FBS (LG-LS), INS-1 832/13 cells were incubated with glucose (LG and HG) as indicated for 24 hours. Cell were then harvested and lysates proteins were separated by SDS-PAGE. After transferring onto nitrocellulose membranes, the membranes were then blocked and probed with antibody raised against phosphorylated p53, followed by incubation with rabbit secondary antibody. The immune complexes were detected using ECL detection method. The same blots were stripped and probed for total p53. **Panel B:** Band intensities were analyzed by densitometry. Data from multiple experiments is represented as mean ± SEM and expressed as fold change in ratios between phospho-p53 and total p53. * $P < 0.05$ vs. 2.5mM glucose (LG). **Panel C:** Pancreatic islets isolated from normal Sprague Dawley rats were incubated with glucose (LG and HG) as indicated for 24 hours. Cell were then harvested and lysates proteins were analyzed by Western Blotting for phosphorylated and total p53. **Panel D:** Band intensities were analyzed by densitometry. Data from multiple experiments is represented as mean ± SEM and expressed as fold change in ratios between phospho-p53 and total p53. * $P < 0.05$ vs. 2.5mM glucose (LG).

HG-induced p53 activation is significantly blocked in the presence of EHT1864, Simvastatin and GGTI2147:

Previous experiments in our laboratory have demonstrated the role of Rac1-Nox2 activation and ROS generation in causing β-cell dysfunction in models of diabetes **(49, 50, 52, 120)**. We therefore, examined the involvement of Rac1-Nox2 signaling cascade in the activation of p53 pathway, under glucotoxic stress. We incubated INS-1 832/13 cells with LG and HG for 24 h in the absence and presence of EHT1864, which blocks Rac1 activation by blocking its interaction with GDP/GTP **(128)**. Phosphorylation of p53 under these conditions was then examined by Western Blotting. As represented in Figure 4-2 (Panel A), the presence of EHT1864 significantly suppressed HG-induced p53 phosphorylation, suggesting the involvement of Rac1 in activating p53.

Furthermore, several studies have demonstrated the requisite role of geranylgeranylation in membrane targeting of Rac1, which mediates its optimal interaction with its substrate proteins **(34, 138)**. To examine if Rac1 geranylgeranylation is required for p53 activation, we employed Simvastatin, a global inhibitor of protein prenylation and GGTI-2147, which inhibits protein geranylgeranylation. We incubated INS-1 832/13 cells with LG and HG for 24 h in the absence and presence of Simvastatin and GGTI2147. Data shown in Figure 4-2 (Panel C) demonstrate a marked inhibitory effect of Simvastatin on HG-induced p53 phosphoryaltion. Compatible with

these findings, data shown in Figure 4-2 (Panel E) also demonstrate that GGT-2147 prevents p53 phosphorylation under HG conditions. Data pooled from multiple experiments is provided in Panel D and F. Together, these findings implicate that Rac1 activation and prenylation are necessary for HG-induced activation of the p53 pathway.
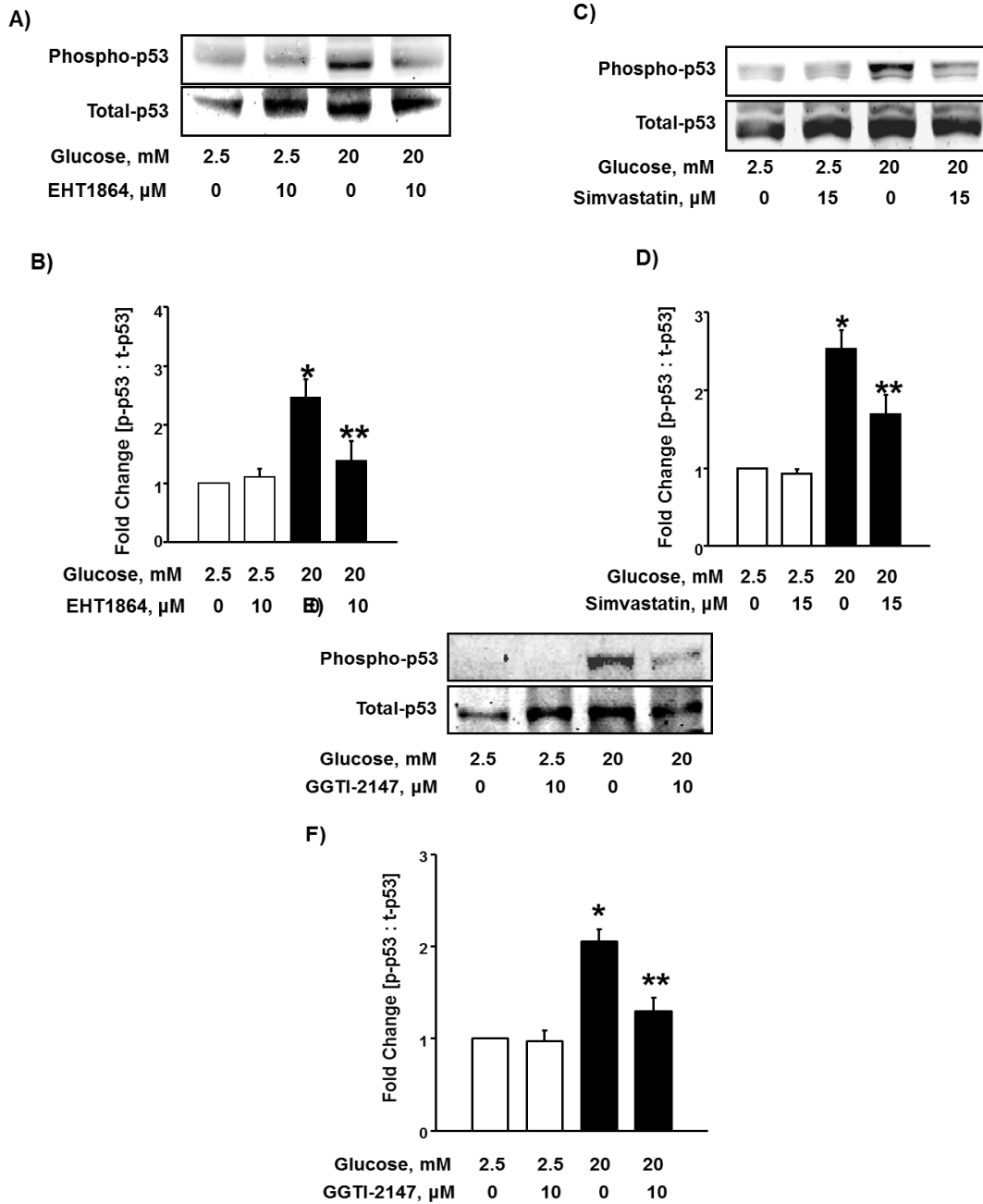
Figure 4-2: Glucotoxicity-induced p53 phosphorylation is attenuated in presence of EHT1864, Simvastatin and GGTI2147:

Panel A: Following overnight starvation in LG-LS, INS-1 832/13 cells were further incubated with LG and HG for 24 hours in the absence and presence of EHT1864. Lysates were then collected, separated by SDS-PAGE and transferred onto nitrocellulose membranes. The membranes were then blocked and probed with antibody raised against phospho-p53, followed by incubation with rabbit secondary antibody. The immune complexes were detected using ECL detection method. The same blots were stripped and probed for total p53. **Panel B:** Band intensities were analyzed by densitometry. Data from multiple experiments is represented as mean ± SEM and expressed as fold change in ratios between phospho-p53 and total p53. * $P < 0.05$ vs. LG alone, ** $P < 0.05$ vs. HG alone. **Panel C:** After overnight starvation, INS-1 832/13 cells were incubated with LG and HG for 24 hours in the absence and presence of Simvastatin. Lysates were then collected and analyzed by Western Blotting as described above. The membranes were probed for phospho-p53 and incubated with rabbit secondary antibody. The same blots were stripped and probed for total p53. **Panel D:** Band intensities were analyzed by densitometry. Data from multiple experiments is represented as mean ± SEM and expressed as fold change in ratios between phospho-p53 and total p53. * $P < 0.05$ vs. LG alone, ** $P < 0.05$ vs. HG alone. **Panel E:** After overnight starvation in LG-LS in the absence and presence of GGTI-2147, INS-1 832/13 cells were incubated with LG and HG for 24 hours in the continuous absence and presence of GGTI-2147. Cell lysates were then collected and analyzed by Western Blotting as described above. The membranes were probed for phospho-p53 and incubated with rabbit secondary antibody. The same blots were stripped and probed for total p53. **Panel F:** Band intensities were analyzed by densitometry. Data from multiple experiments is represented as mean ± SEM and expressed as fold change in ratios between phospho-p53 and total p53. * $P < 0.05$ vs. LG alone, ** $P < 0.05$ vs. HG alone.

EHT1864 had no effect on HG-induced nuclear translocation of p53:

Translocation of p53 to the nucleus has been demonstrated to be critical for its interaction with the DNA, for the transcriptional activation of apoptotic genes **(98, 139)**. To examine if HG conditions promote nuclear localization of p53, we incubated INS-1 832/13 cells with LG and HG in the absence and presence of EHT1864 for 24 hours and isolated the nuclear and non-nuclear fractions using NER-PER® kit. p53 localization was then examined by probing for phosphorylated and total p53 in these fractions. As depicted in Figure 4-3 (Panel A), we observed accumulation of both phosphorylated and total p53 in the nuclear fraction under HG treatment conditions. Furthermore, compatible with our findings in Figure 4-1, the presence of EHT1864 significantly attenuated HG-induced p53 phosphorylation, as demonstrated by the decreased phospho-p53 band intensity in the nuclear fraction. However, the presence of EHT1864 did not seem to affect total p53 localization in the nuclear fraction under HG conditions. These observations suggest

that HG exposure induces p53 translocation to the nucleus, independent of phosphorylation at serine-15 residue.
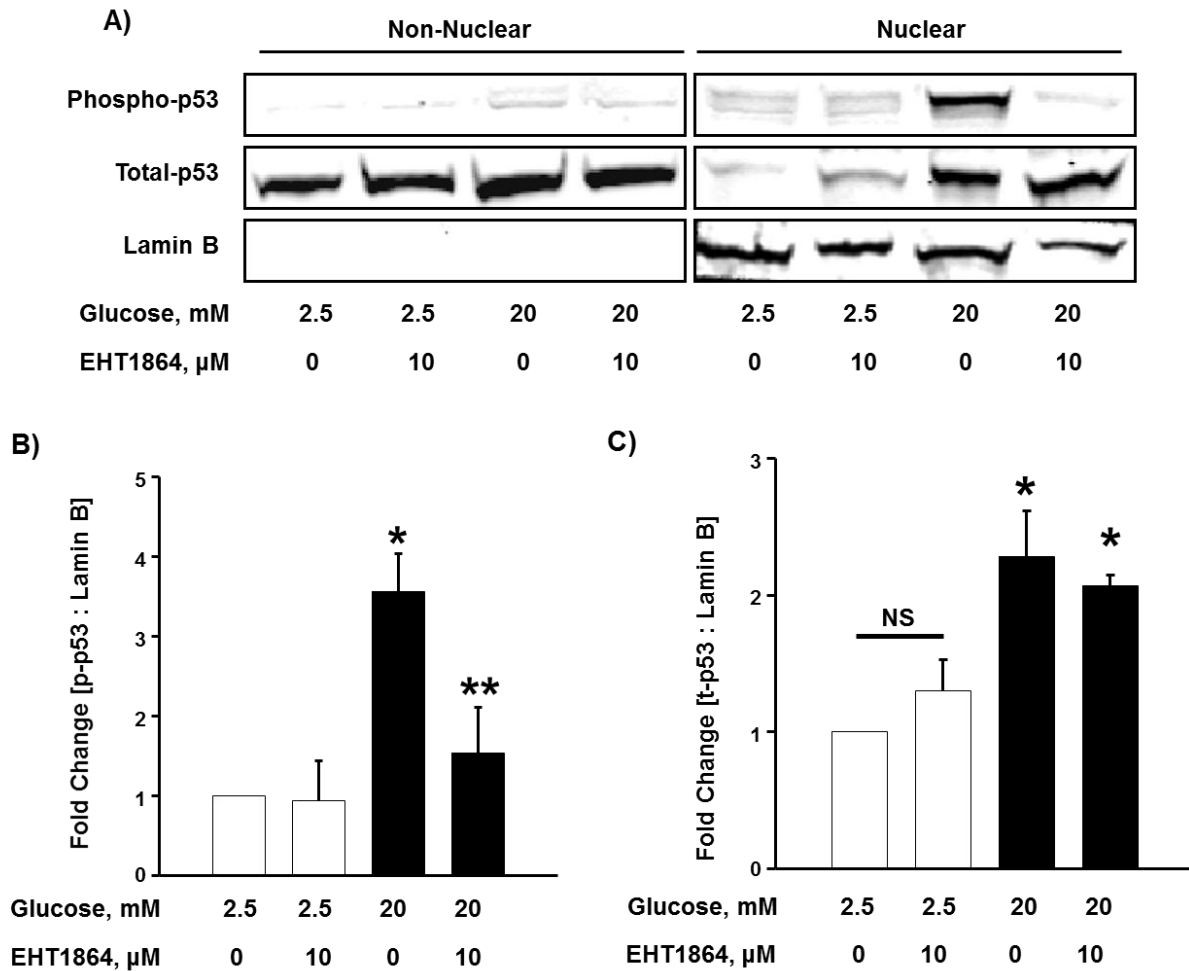
Figure 4-3: Exposure to HG conditions induced nuclear translocation of p53, which is not inhibited by EHT1864:
Panel A: Following overnight incubation in LG-LS media, INS-1 832/13 cells were further incubated with LG and HG for 24 h in the absence and presence of EHT1864. Cells were then rinsed with PBS and nuclear and non-nuclear fractions were isolated using NE-PER® kit according to the manufacturer's instructions. The isolated fractions were then analyzed by Western Blotting for phosphorylated and total p53. The purity of the fractions was analyzed by probing for nuclear Lamin B. **Panel B:** Band intensities for phospho-p53 and Lamin B were determined by densitometric analysis. Data from multiple studies is shown as mean ± SEM and expressed as fold change in the ratios between phospho-p53 and Lamin B. * P < 0.05 vs. LG alone or in the presence of EHT1864, ** P < 0.05 vs. HG alone. **Panel C:** Band intensities for total-p53 and Lamin B were determined by densitometric analysis. Data from multiple studies is shown as mean ± SEM and expressed as fold change in the ratios between total-p53 and Lamin B. * P < 0.05 vs. LG alone. NS: not significant

p53 activation under HG conditions is markedly blocked in the presence of SB203580, a selective inhibitor of p38MAPK:

We next determined the involvement of Rac-Nox2-p38MAPK signaling cascade in the activation of p53 under the duress of glucotoxic conditions. Several lines of evidence have implicated the role of p38MAPK in the activation of p53 in the presence of stress stimuli **(79, 135, 140, 141)**. Therefore, in the next set of experiments, we utilized SB203580, a selective inhibitor of p38MAPK activity, and observed its effects on HG-induced p53 phosphorylation. As depicted in Figure 4-4 (Panel A), the presence of SB203580 blocked p53 phosphorylation in INS-1 832/13 cells incubated with HG. Data from multiple experiments is provided in Panel B. These data collectively demonstrate that Rac-Nox2-p38MAPK module is involved in the activation of p53 under glucotoxic stress.
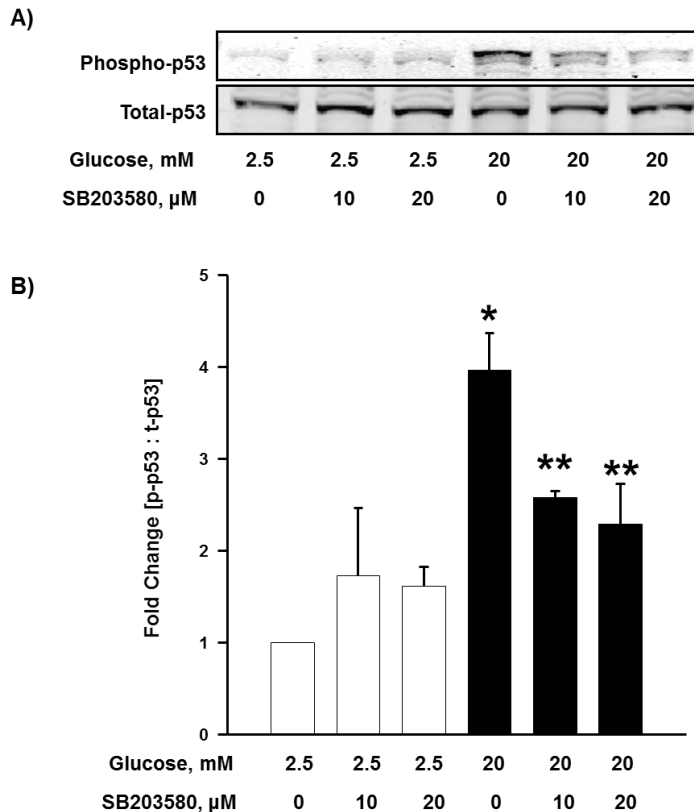
Figure 4-4: SB203580, a selective inhibitor of p38MAPK, attenuates HG-induced p53 phosphorylation:
Panel A: Following overnight starvation in LG-LS, INS-1 832/13 cells were further incubated with LG and HG for 24 hours in the absence and presence of SB203580. Lysates were then collected and analyzed by Western Blotting. The membranes were probed with antibody raised against phospho-p53, followed by incubation with rabbit secondary antibody. The same blots were stripped and probed for total p53. **Panel B:** Band intensities were analyzed by densitometry. Data from multiple experiments is represented as mean ± SEM and expressed as fold change in ratios between phospho-p53 and total p53. * P < 0.05 vs. LG alone, ** P < 0.05 vs. HG alone.

ATM kinase, a known activator of p53, is also activated under HG conditions in a Rac1-dependent manner:

Previous studies in multiple cell types have implicated the involvement of ATM kinase in the activation of p53, induced by Rac1-derived oxidative stress and extensive DNA damage **(136, 137, 142, 143)**. ATM kinase, a cell cycle regulator, is known to be activated by auto-phosphorylation in the presence of double stranded DNA breaks **(144)**. We therefore undertook the study to determine if glucotoxic conditions promote activation of ATM kinase in INS-1 832/13 cells. Data depicted in Figure 4-5 (Panel A) demonstrate a marked increase in ATM kinase phophorylation under HG conditions. Furthermore, the presence of EHT1864, significantly blocked HG-induced ATM kinase activation. Pooled data from multiple experiments is provided in Panel B. These data suggest that HG exposure promotes Rac1-dependent ATM kinase activation.

A)

B)
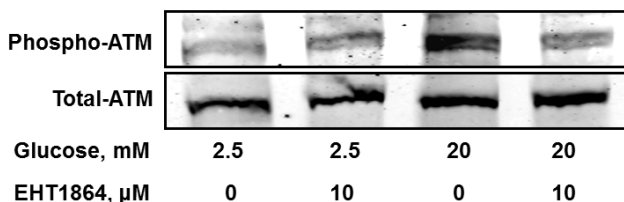
Figure 4-5: Exposure to HG conditions induces ATM kinase phosphorylation, which is inhibited by EHT1864:
Panel A: Following overnight starvation in LG-LS, INS-1 832/13 cells were further incubated with LG and HG for 24 hours in the absence and presence of EHT1864. Lysates were then collected and analyzed by Western Blotting. The membranes were then blocked and probed with antibody raised against phospho-ATM kinase, followed by incubation with rabbit secondary antibody. The same blots were stripped and probed for total ATM kinase. **Panel B:** Band intensities were analyzed by densitometry. Data from multiple experiments is represented as mean ± SEM and expressed as fold change in ratios between phospho- and total ATM kinase. * P < 0.05 vs. LG alone, ** P < 0.05 vs. HG alone.
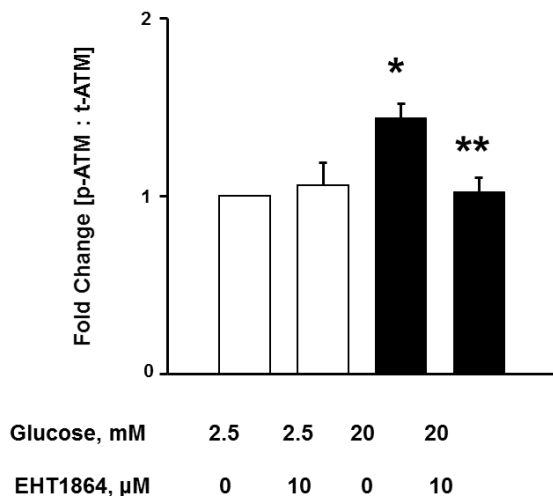
KU-55933, a selective inhibitor of ATM kinase, blocks HG-induced ATM kinase activation but has no effect on p53 activation:

Pharmacological inhibition of ATM kinase has been shown to prevent p53 phosphorylation in cells exposed to various stress stimuli **(145)**. In the next set of experiments, we employed this inhibitor to examine its effects on HG-induced ATM kinase and p53 phosphorylation. Our findings demonstrated a marked decrease in HG-induced ATM kinase phosphorylation in presence of KU55933 in INS-1 832/13 cells, as depicted in Figure 4-6 (Panel A). However, we observed no significant effects of KU55933 in HG-induced p53 phosphorylation. Taken together, these data implicate that ATM kinase does not regulate p53 under glucotoxic stress, and that p53 and ATM kinase, although regulated by Rac1-Nox2 signaling, might be involved in independent downstream pathways.
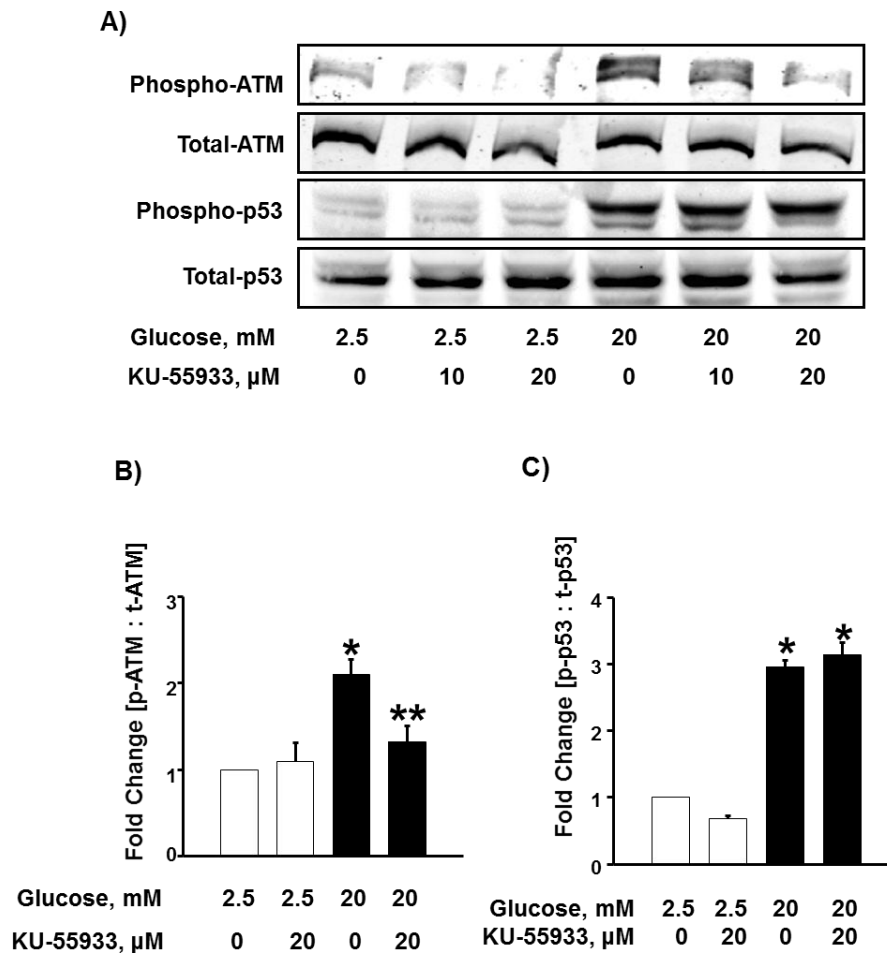
Figure 4-6: KU55933, a selective inhibitor of ATM kinase, prevents HG-induced ATM kinase phosphorylation but has no effect on p53 phosphorylation:

Panel A: Following overnight starvation, INS-1 832/13 cells were incubated with LG or HG in the absence or presence of KU-55933 for 24 h. Cell lysate proteins were separated and analyzed by Western Blotting for phosphorylated ATM kinase and p53. Blots were then stripped and re-probed for total ATM kinase and p53. **Panel B:** Phospho-ATM kinase band intensities were quantified by densitometry and ratios were calculated over total-ATM kinase. Data from multiple studies is shown as mean ± SEM and expressed as fold change in ratios between phosphorylated and total ATM kinase. * $P < 0.05$ vs LG alone, ** $P < 0.05$ vs HG alone. **Panel C:** Phospho-p53 band intensities were quantified by densitometry and ratios were calculated over total-p53. Data from multiple studies is shown as mean ± SEM and expressed as fold change in ratios between phosphorylated and total p53. * $P < 0.05$ vs LG alone.

EHT1864, markedly blocks HG-induced β-cell death:

Our findings have demonstrated that Rac1 activation leads to activation of p38MAPK and p53 signaling pathway, resulting in β-cell death under glucotoxic stress. Therefore, in the last set of experiments, we utilized EHT1864 to determine if pharmacological inhibition of Rac1 prevents HG-induced β-cell death. We incubated INS-1 832/13 cells with LG and HG for 24 h in the continuous absence and presence of EHT1864 and analyzed cell death using Cell Death Detection® kit as per the manufacturer's instructions. Our findings indicated a significant increase in cell death signal under HG conditions as shown in Figure 4-7. We also observed a marked decrease in HG-induced β-cell death in presence of EHT1864, demonstrating protective effects of Rac1 inhibition under glucotoxic stress conditions.
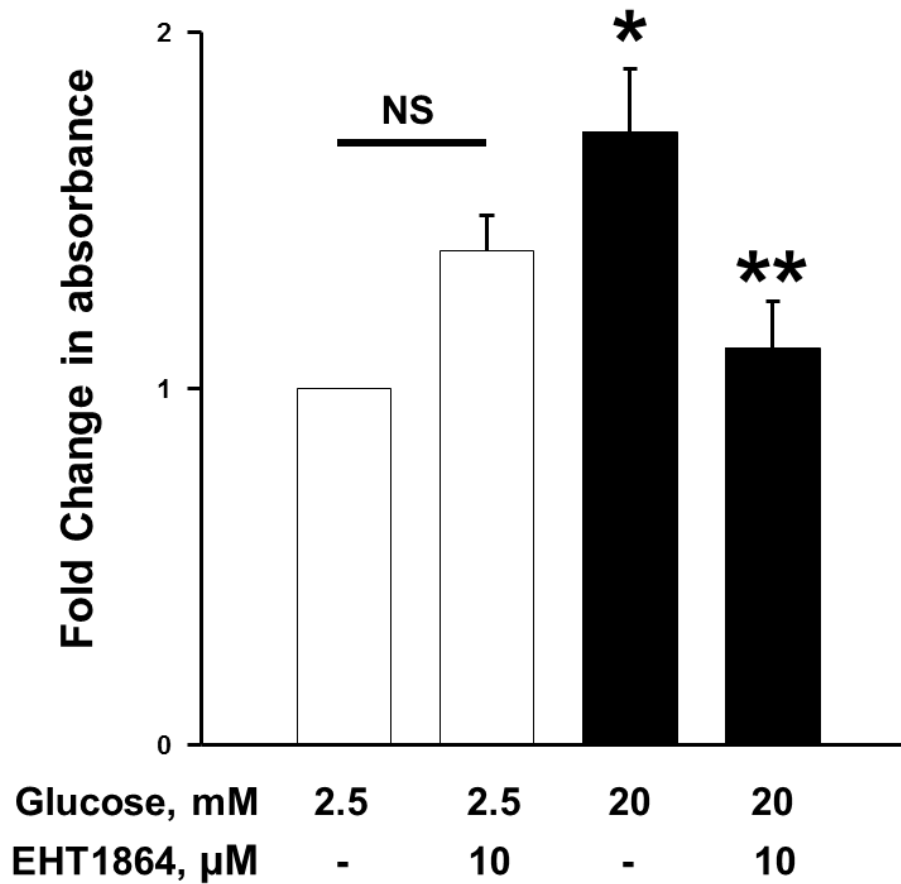
Figure 4-7: EHT1864 prevents HG-induced cell death in INS-1 832/13 cells:
After overnight incubation in LG-LS media, INS-1 832/13 cells were incubated with LG and HG for 24 h in the absence and presence of EHT1864. Cells were then washed with PBS and analyzed using Cell Death Detection ELISA[Plus] kit according to the manufacturer's instructions. Absorbance was measured at 405nm and expressed as fold change over basal LG. Data from multiple studies is shown as mean ± SEM and expressed as fold change over basal LG. * $p < 0.05$ vs LG alone, ** $p < 0.05$ vs HG alone, NS: Not significant.

In conclusion, our findings in chapter 3 and 4 together demonstrate that exposure of pancreatic betake cells to glucotoxic conditions results in increased Rac1-Nox2-derived oxidative stress, leading to activation of p38MAPK-p53 signaling axis that culminates in the induction of apoptotic pathways. Our findings have also indicated activation of ATM kinase under glucotoxic conditions, which might be involved in other signaling pathways.
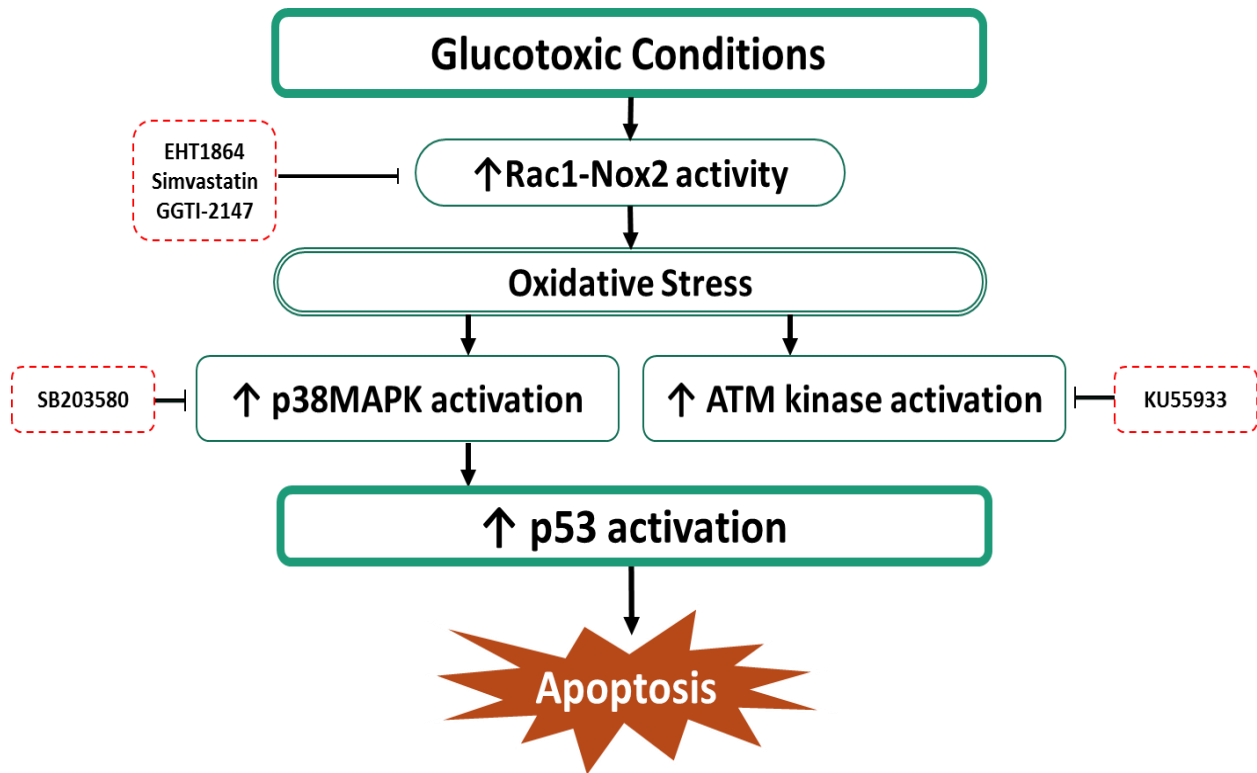
Figure 4-8: Proposed model for Rac1-Nox2-induced oxidative stress and activation of p38MAPK-p53 signaling axis leading to β-cell apoptosis:

Our findings have implicated Rac1-Nox2 activation in p38MAPK activation under glucotoxic stress. Furthermore, using pharmacological inhibitor of Rac1 (EHT1864) and p38MAPK (SB203580) we have demonstrated that activation of Rac1-p38MAPK signaling module is involved in HG-induced p53 phosphorylation.

CHAPTER 5: RAC1-p38MAPK-p53 SIGNALING AXIS IN PANCREATIC ISLETS FROM THE ZDF RAT MODEL AND HUMAN ISLETS

Phagocyte-like NADPH oxidase (Nox2) is composed of several membrane and cytosolic components including the small G-protein, Rac1. Rac1 activation has been demonstrated to play a critical role in the functional assembly and activation of Nox2 holoenzyme complex **(41, 50, 52)**. Although there is ample evidence suggesting the positive regulatory role of Rac1-Nox2 signaling in physiological ROS generation and glucose-stimulated insulin secretion, Nox2 has been shown to play key contributory roles in the pathophysiology of beta-cell dysfunction leading to onset of diabetes. Previous observations in our laboratory have demonstrated that increased Rac1-Nox2-derived ROS generation results in metabolic dysfunction of β-cells when exposed to palmitate **(50)**. Studies have also implicated the involvement of Nox2-induced oxidative stress in models of cytokine-induced beta-cell dysfunction **(52, 120).** Furthermore, exposure to glucotoxic conditions resulted in increased Nox2 activation in INS-1 832/13 cells **(146).** The central objective of this dissertation project is to demonstrate that exposure of pancreatic β-cells to glucotoxic conditions leads to sustained activation of Rac1-Nox2 enzyme complex and the resulting oxidative stress activates p38MAPK-p53 signaling cascade, ultimately causing β-cell death. As discussed in chapters 3 and 4, our *in vitro* studies in INS-1 832/13 cells and rat islets exposed to glucotoxic conditions demonstrates increased activation of p38MAPK and p53. To examine this pathway in an *in vivo* model, we utilized the Zucker diabetic fatty (ZDF) rat, which has been extensively used as a model for obesity, insulin resistance and pancreatic β-cell dysfunction **(147).**

ZDF rats possess a spontaneous mutation of the leptin receptor gene and initially develop obesity. Consequently, these animals spontaneously develop diabetes induced by elevated glucose and free fatty acid levels. Animals which possess a heterozygous leptin receptor mutation (Zucker lean control; ZLC), however, do not exhibit signs of diabetes **(148)**. Previous studies from our laboratory have utilized this model to demonstrate the involvement of increased Rac1-Nox2 activity and ROS generation in mediating β-cell dysfunction. Additionally, exposure of human

pancreatic islets to glucotoxic conditions also resulted in increased Rac1 activation and ROS generation. The downstream signaling pathways in these models, however, remain to be fully understood. Herein, we examined the p38MAPK-p53 signaling axis in pancreatic islets isolated from ZDF rats and in human islets exposed to glucotoxic concentrations.

p38MAPK and p53 are activated in islets isolated from ZDF rats:

We first examined p38MAPK phosphorylation in pancreatic islets isolated from male ZDF rats and compared them to their age-matched ZLC rats. As evidenced in Figure 5-1 (Panel A), the ZDF rats that developed overt diabetes and exhibited elevated blood glucose levels, also showed increased phosphorylation of p38MAPK. Data pooled from four ZDF rats is shown in Panel B. Furthermore, in a separate set of studies, we examined levels of phosphorylated p53 in two ZDF rats. We noticed a marked increase in p53 phosphorylation in islets isolated from ZDF rats compared to their age-matched controls, as depicted in Figure 5-1 (Panel C). Data pooled from two ZDF and two ZLC rats is provided in Panel D.

A)
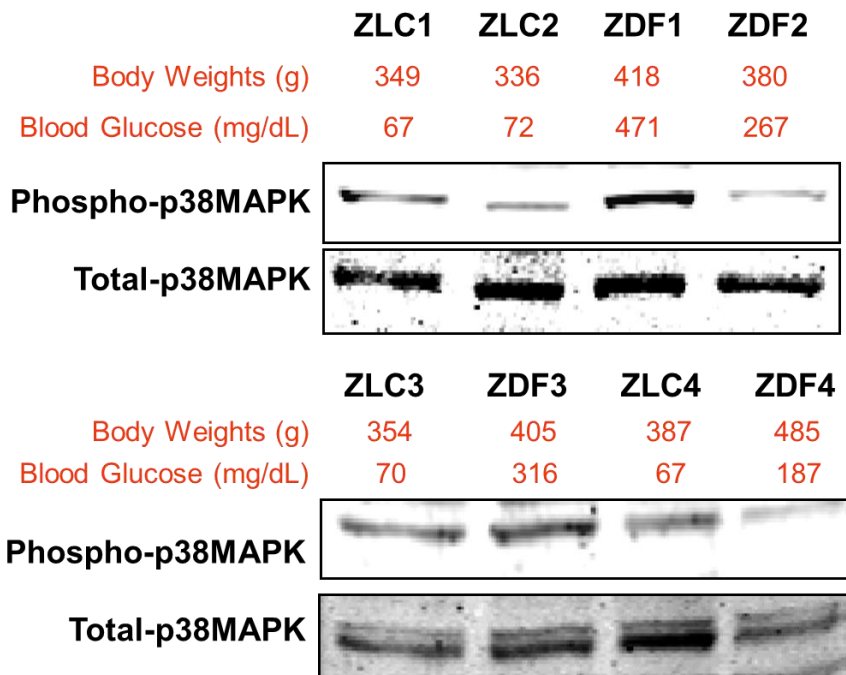
B)
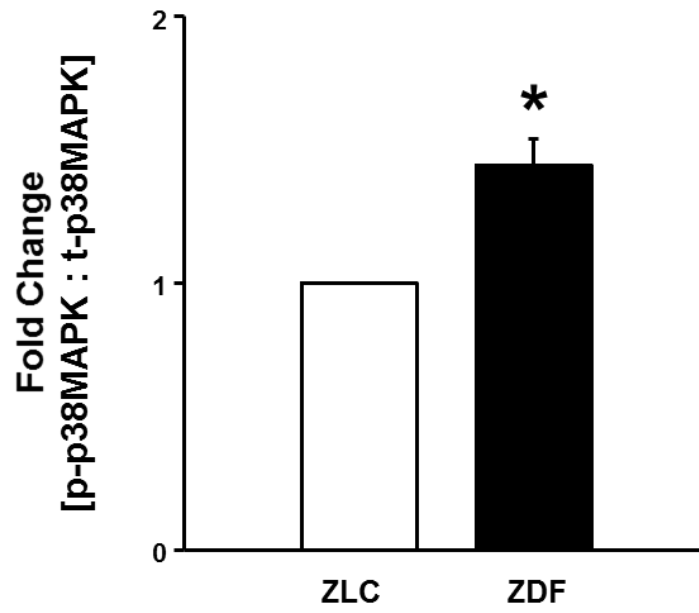
C)
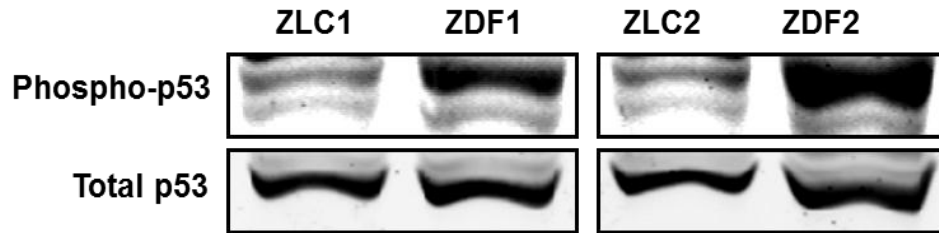
D)
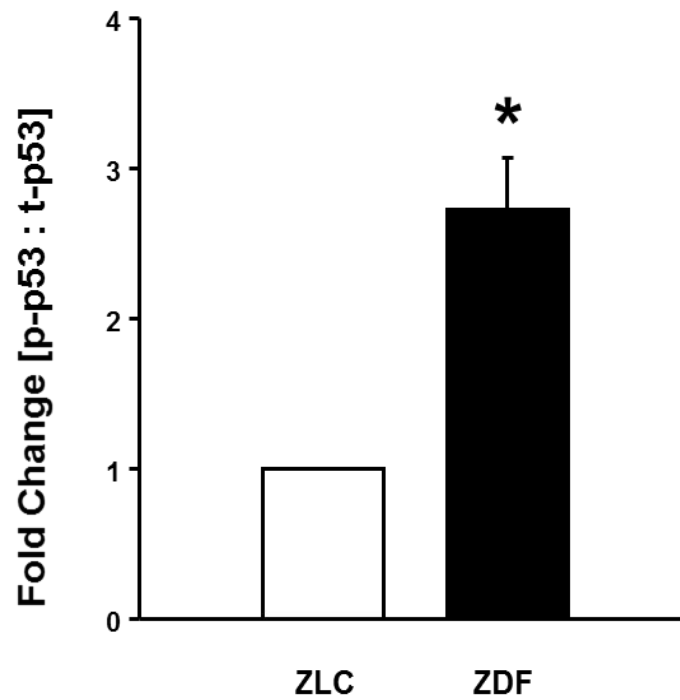
Figure 5-1: Pancreatic islets from ZDF rats show elevated levels of phosphorylated p38MAPK and p53:
Panel A: Pancreatic islets were isolated from ZDF rats and their age-matched controls by collagenase digestion. After overnight incubation in RPMI media, islets were lysed and lysate proteins were separated by SDS-PAGE. Proteins were then transferred onto nitrocellulose membranes and blocked for 1 h. The membranes were then probed for phosphorylated p38MAPK followed by incubation with IR-Dye conjugated rabbit secondary antibody. The immune complexes were detected by Odyssey® Imaging Systems. The same blots were stripped and probed for total p38MAPK. **Panel B:** Band intensities were determined and analyzed by densitometric analysis. Data shown as mean ± SEM are from four rats in each group and expressed as fold change in the ratios between phospho- and total p38MAPK. * $P < 0.05$ vs ZLC rat islets. **Panel C:** Pancreatic islets were isolated from ZLC and ZDF rats and analyzed by Western Blotting as described above. The membranes were probed with antibody raised against phospho-p53 followed by incubation with rabbit IR-Dye conjugated secondary antibody. The same blots were stripped and probed for total p53. **Panel D:** Band intensities were determined and analyzed by densitometric analysis. Data shown as mean ± variance from two rats in each group and expressed as fold change in the ratios between phospho- and total p38MAPK.

Exposure of normal human islets to glucotoxic conditions activates p38MAPK and p53:

We next determined if exposure of pancreatic islets from normal human donors to glucotoxic conditions promote p38MAPK and p53 phosphorylation. We incubated human islets to LG (5.8 mM) and HG (30 mM) for 24 h and quantified p38MAPK and p53 phosphorylation. As depicted in Figure 5-2 (Panel A), we noticed a marked increase in p38MAPK phosphorylation in HG-treated islets (1.61 fold increase). Furthermore, our findings also indicated a 1.97 fold increase in p53 phosphorylation in HG-treated islet samples. These data are compatible to our findings in INS-1 832/13 cells, normal rat islets (Chapters 3 and 4) and ZDF rat islets (Figure 5-1), together demonstrating increased activation of p38MAPK-p53 signaling pathway upon exposure of β-cells to glucotoxic conditions.

A)

B)
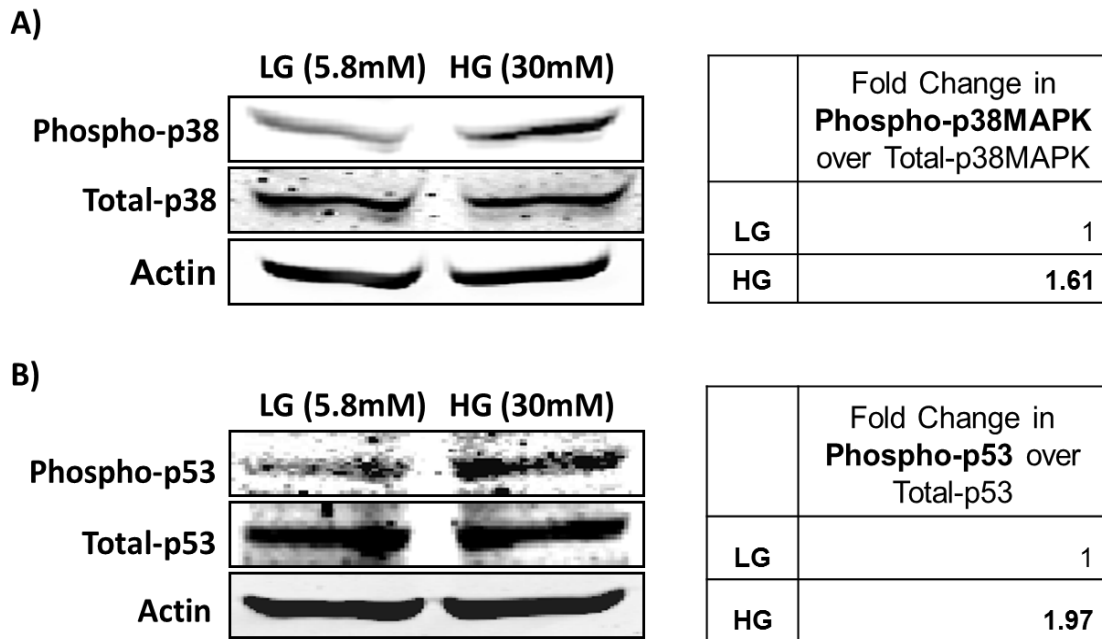
Figure 5-2: p38MAPK and p53 activation in human islets exposed to glucotoxic conditions:
Pancreatic islets from non-diabetic human donors were incubated with LG (5.8 mM) and HG (30 mM) for 24 h. Islets were then lysed and analyzed by Western Blotting for p38MAPK (**Panel A**) and p53 (**Panel B**). The membranes were probed for phospho-p38MAPK and phospho-p53, followed by incubation with anti-rabbit secondary antibodies. The immune complexes were then detected by Odyssey® Imaging Systems. The same blots were stripped and probed for total p38MAPK and p53. Data shown are expressed as fold change in the ratios between phospho- over total p38MAPK and phospho- over total p53.

Exposure to glucotoxic conditions promote nuclear localization of p53 in human islets:

As described in Chapter 4, our studies in INS-1 832/13 cells treated with LG and HG for 24 h indicated accumulation of p53 in the nuclear fractions under HG conditions. We therefore, incubated human pancreatic islets with LG (5.8 mM) and HG (30 mM) for 24 h and isolated nuclear and non-nuclear fractions using NER-PER® kit. In line with our observations in INS-1 832/13 cells, we found increased localization of phospho- and total p53 in the nuclear fractions of HG-treated samples (Figure 5-3).
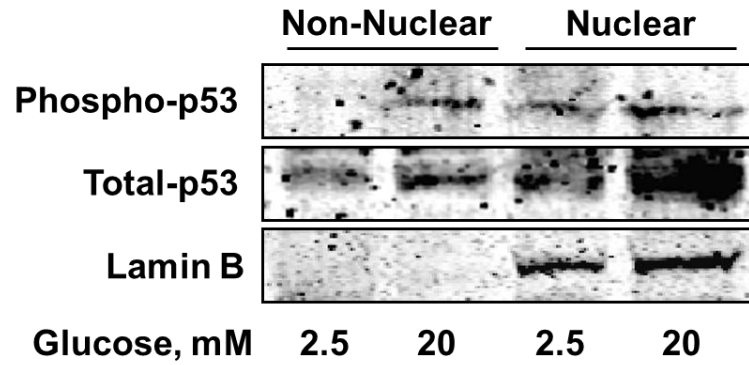
Figure 5-3: Glucotoxic conditions promote nuclear localization of p53 in human islets:
Pancreatic islets from non-diabetic human donors were incubated with LG and HG for 24 h. Cells were then rinsed with PBS and nuclear and non-nuclear fractions were isolated using NE-PER® kit according to the manufacturer's instructions. The isolated fractions were then analyzed by Western Blotting for phosphorylated and total p53. The purity of the fractions was analyzed by probing for nuclear Lamin B.

CHAPTER 6: DISCUSSION

Insulin resistance caused by various factors such as obesity, results in decreased glucose uptake and utilization in the peripheral tissues. This is initially compensated by the pancreatic β-cells, which secrete more insulin to normalize the elevated blood glucose levels. However, the chronic exposure of β-cells to elevated glucose concentrations or glucotoxicity eventually leads to decreased function and ultimately cell demise, culminating in the onset of diabetes. Recently, we reported that exposure of INS-1 832/13 cells, rodent and human pancreatic islets to glucotoxic conditions results in activation of executioner caspases and degradation of nuclear lamins **(119, 149)**. In addition, studies have implicated the role of Rac1-Nox2 enzyme complex and associated oxidative stress in the pathology of β-cell dysfunction **(49, 50, 52)**. However, the precise signaling mechanisms involved in mediating loss in glucose-stimulated insulin secretion (GSIS) and β-cell death under glucotoxic conditions, remain to be poorly understood.

Apart from the negative modulatory roles in the induction of oxidative stress, several lines of evidence have demonstrated the requisite role of Rac1 and Nox2 signaling in GSIS **(18, 35).** Glucose enters the β-cell via GLUT-2 transporter, where it is metabolized to generate ATP. The resulting increase in ATP/ADP ratio causes closure of ATP-sensitive K^+ channels resulting in membrane depolarization. This causes the opening of voltage-gated Ca^{+2} channels and increased intracellular Ca^+ concentration. In presence of Ca^+, insulin-laden secretory granules are then mobilized towards the membrane for fusion and release. This process of translocation of insulin granules to the plasma membrane is mediated by vesicle-associated and t-SNARE proteins at target docking sites, and requires cytoskeletal reorganization **(8)**. Studies by Asahara and associates have demonstrated the critical role of Rac1 in F-actin remodeling and GSIS, using a beta-cell specific Rac1-/- mice model **(22)**. Furthermore, previous studies from our laboratory have also utilized several pharmacological agents to demonstrate that Rac1 activation is required for GSIS. Using NSC23766, we demonstrated that inhibition of Tiam1, a GEF mediating Rac1 activation, results in marked reduction in GSIS in the presence of the inhibitor **(24)**. We also

examined the effects of Ehop-016, a specific inhibitor of Vav2- mediated Rac1 activation, in pancreatic β-cells **(25)**. We observed alterations in F-actin remodeling and a significant decrease in GSIS in the presence of Ehop-016, demonstrating the role of Rac1 in cytoskeletal reorganization and insulin secretion.

Furthermore, several investigations have implicated the involvement of Nox2 and reactive oxygen species (ROS) in GSIS **(35, 36)**. Nox2 holoenzyme is composed of several membrane-bound (gp91^{phox} and p22^{phox}) and cytosolic (p40^{phox}, p47^{phox}, p67^{phox} and Rac1) components. Upon stimulation, the cytosolic components translocate towards the membrane thereby mediating the holoenzyme assembly. The functionally active Nox2 enzyme complex catalyzes the one electron reduction of molecular oxygen to generate superoxide. Emerging evidence implicate that a tonic increase in Rac1-Nox2-mediated ROS generation is necessary for nutrient-induced insulin secretion **(38, 39)**. Studies by Leloup and associates have demonstrated that co-provision of antioxidants suppresses ROS generation induced by glucose, resulting in alterations in calcium mobilization and decreased GSIS, in rodent pancreatic islets **(38)**. Moreover, studies by Morgan and associates have demonstrated the involvement of Nox2-derived ROS in GSIS in rodent pancreatic islets **(36)**.

As demonstrated by these studies, Rac1-Nox2 activity and associated generation of ROS is required for physiological functioning of the β-cell. However, evidence from studies in pancreatic β-cells, retinal endothelial cells and cardiomyocytes suggests the involvement of Rac1-Nox2 signaling axis in causing oxidative stress under diabetic conditions **(48, 150, 151)**. Previous studies in our laboratory have demonstrated that sustained activation of Rac1-Nox2 and ROS generation in pancreatic β-cells exposed to glucolipotoxic conditions and inflammatory cytokines, leads to loss in β-cell function and apoptosis **(49, 50, 52)**. Our observations in the ZDF rat model and type2 diabetic islets have also suggested that Rac1-Nox2-ROS signaling plays a key role in causing β-cell dysfunction **(49)**. However, the underlying mechanisms mediating the effects of Rac1-Nox2-induced oxidative stress remain poorly understood. Using pharmacological

2

2

approaches to target the Rac1-Nox2 signaling cascade, my doctoral work focusses on identifying the effector proteins activated by increased Rac1-Nox2-ROS signaling, that are involved in activation of apoptotic factors leading to β-cell death.

Desire et al. have developed a small molecule inhibitor, EHT1864, which inhibits Rac1 activation in vivo **(28)**. Further characterization by Shutes *et al.* demonstrated that the effect of EHT1864 is independent of GEFs (Tiam1, Vav2) since they observed inhibition of cellular transformation induced by constitutively active mutant of Rac1 (61L) **(128)**. EHT1864 binds directly to Rac1 with a greater affinity than guanine nucleotides (GDP/GTP) thereby retaining Rac1 in an inert, inactive state by displacing pre-bound GDP/GTP. We first tested this Rac1 inhibitor to examine the role of Rac1 in physiological GSIS in INS-1 832/13 cells. Our results have indicated a marked reduction in glucose-induced activation and membrane targeting of Rac1 in the presence of EHT1864. Under these conditions, we also observed a marked reduction in GSIS. Several studies in multiple cell types have utilized EHT1864 to understand Rac1 function in health and disease **(29-32)**. We have further utilized EHT1864, to deduce roles of Rac1-Nox2-signaling axis in activating the downstream apoptotic pathways and β-cell death under glucotoxic conditions.

To identify the downstream signaling proteins mediating the effects of Rac1-Nox2-induced oxidative stress, we examined the activation status of stress-activated protein kinases (SAPK/MAPK). Several lines of evidence have implicated the role of stress kinases, JNK1/2 and p38MAPK in the activation of apoptotic pathways **(55)**. Previous studies in our laboratory in ZDF and human pancreatic islets, have coupled increased Rac1 activation and Nox2 subunit expression with increased activation of JNK1/2 **(49)**. Studies by Flores-Lopez and associates have also suggested that p38MAPK is activated in β-cells exposed to glucotoxic conditions, resulting in apoptosis **(121)**. Additionally, studies in mice lacking an isoform of p38MAPK, showed improved glucose tolerance as a result of improved insulin secretion from the β-cell **(75).** Our findings have also demonstrated increased activation of p38MAPK in insulin-secreting INS-1

832/13 cells, normal rodent and human islets exposed to glucotoxic conditions, and in islets isolated from ZDF rats.
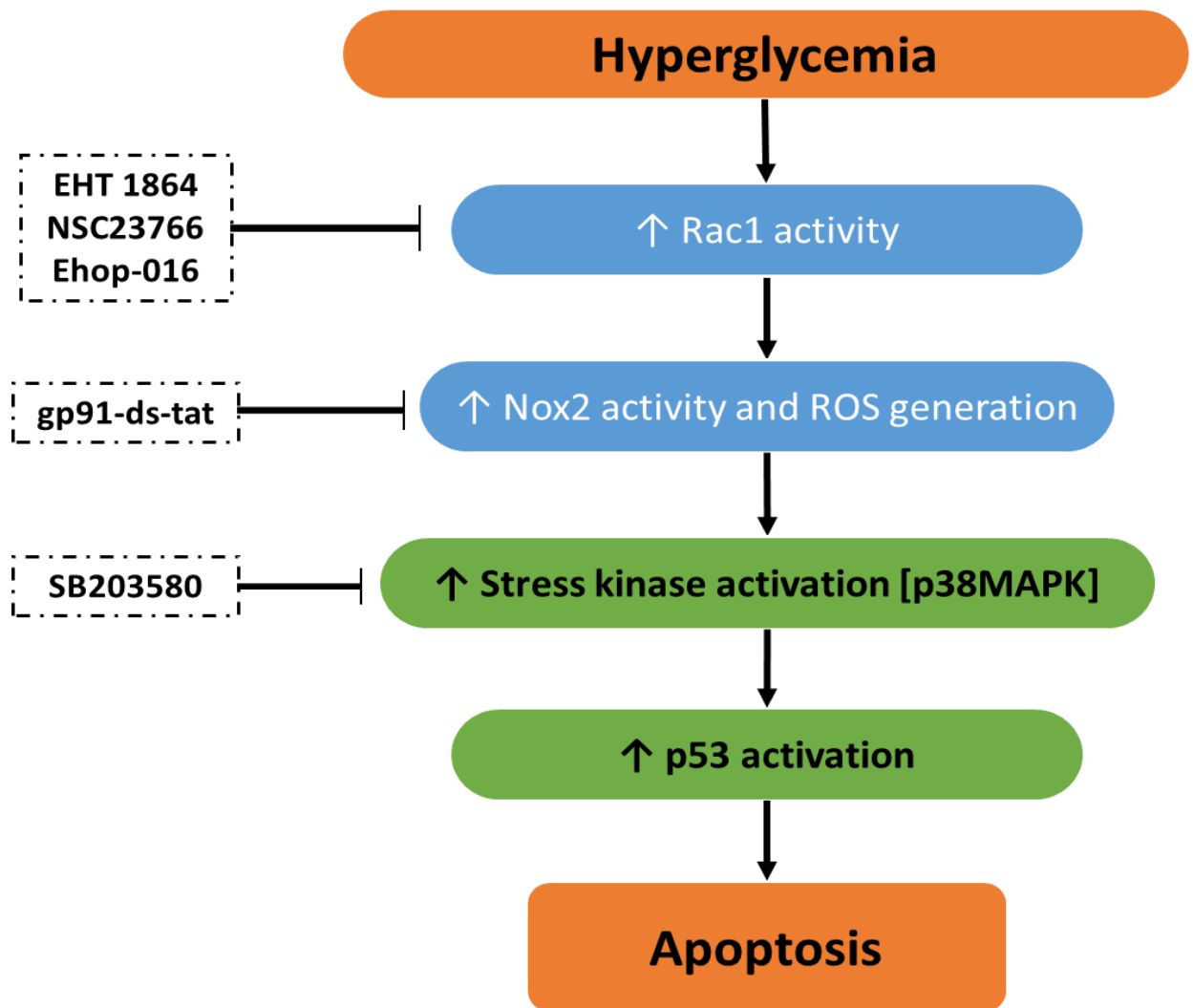
Figure 6-1: Our working model illustrating the involvement of Rac1-Nox2 signaling axis and associated oxidative stress in the activation of p38MAPK and p53, culminating in β-cell apoptosis: We demonstrated that exposure of pancreatic β-cells to glucotoxic conditions leads to sustained activation of Rac1-Nox2 enzyme complex and excess ROS generation. The resulting oxidative stress leads to p38MAPK-mediated activation of p53, which, in turn, activates the transcription of apoptotic proteins and causes β-cell death. Our finding also demonstrate the potential cytoprotective effects of pharmacological inhibitors of Rac1 (EHT1864, NSC23766, Ehop-016), Nox2 (gp91-ds-tat) and p38MAPK (SB203580) in the β-cell, exposed to glucotoxic conditions.

Based on this evidence, we examined if Rac1-Nox2 driven oxidative stress causes β-cell dysfunction under glucotoxic conditions, mediated by p38 family of stress kinases. Several studies including from those from our own laboratory, have utilized diphenyleneiodonium (DPI) and Apocynin, which block Nox2 activation and ROS generation in models of cellular dysfunction **(152)**. However, it has been suggested that DPI also interacts with other flavin-dependent enzymes including nitric oxide synthase and xanthine oxidase **(153)**. In addition, studies have also indicated that Apocynin has anti-oxidant properties, independent of its inhibitory effects on Nox2 **(154).** Recently, Rey et al. have identified a Nox2-specifc peptide-based inhibitor, gp91-ds-tat, which prevents the interaction of the cytosolic p47phox with gp91phox in the membrane **(122)**, thereby inhibiting Nox2 assembly and functional activation. Several studies have demonstrated the specificity of gp91-ds-tat to Nox2, compared to its inactive scrambled analog **(123-127)**. To determine the role of Nox2 in p38MAPK activation under HG conditions in the β-cell, we first utilized this peptide inhibitor and quantified HG-induced Nox2 activity and ROS generation. We observed significant blockade in HG-induced Nox2 activation and ROS generation in the presence of gp91-ds-tat, a specific inhibitor of Nox2, but not its inactive analog. We also demonstrated that HG-induced p38MAPK phosphorylation is significantly blocked in the presence of gp91-ds-tat, but not its inactive analog. Thus, our studies provide the first evidence linking HG-induced Nox2 activation and ROS generation to p38MAPK activation.

Recent *in vitro* and *in vivo* studies have demonstrated that NSC23766, an inhibitor of Tiam1-mediated Rac1 activation, prevents cellular dysfunction in pancreatic β-cells, retinal endothelial cells and cardiomyocytes upon exposure to diabetic conditions **(50, 150, 151)**. Our studies with NSC23766 and Ehop-016 have also shown that inhibition of Tiam-Rac1 signaling blocks HG-induced p38MAPK activation in INS-1 832/13 cells and rodent islets, indicating that regulation of Rac1 function by Tiam1 and Vav2 are requisite for p38MAPK activation under HG conditions. These observations are supported by a recent finding by Liu and associates where they showed that while Vav2 mediates GTP loading of Rac1, Tiam1 functions as an adapter in a

VE-cadherin-p67phox-Par3 polarity complex that mediates localized activation of Rac1. They concluded that Tiam1 and Vav2 play a dual regulatory role in inducing localized Rac1 activation required for Nox2 activation and ROS generation **(155)**. Moreover, the presence of EHT1864, which disrupts Rac1 interaction with GTP/GDP in a GEF-independent manner, also attenuated HG-induced p38MAPK phosphorylation. Together, these results demonstrate the involvement of Rac1 in p38MAPK activation under HG conditions. It is noteworthy that our studies with Ehop-016 showed activation of p38MAPK under basal LG conditions. These effects could be as a result of activation of other signaling mechanisms in presence of Ehop-016. Studies by Montalvo-Ortiz et al. suggest that other Rho-family G –proteins such as RhoA, which has been previously shown to activate p38MAPK **(156)**, are activated in presence of Ehop-016. Additional studies are needed to understand these observations.

In the next set of studies, we examined the downstream effects of p38MAPK activation. Indeed, studies in multiple cell types have documented the role of p38MAPK in cell cycle arrest and apoptosis **(53, 65).** For example, evidence from multiple cell types have reported that p38MAPK activates p53 tumor suppressor in response to stress stimuli to mediate apoptosis **(121).** Previous studies by Karunakaran and associates have analyzed the effects of 1-methyl-4-phenyl-1, 2, 3, 6-tetrahydropyridine (MPTP)-induced ROS generation on the regulation of p38MAPK-p53 pathway. They observed that treatment of dopaminergic neurons with MPTP-activated p38MAPK which in turn activated p53 and p53-dependent transcription of apoptotic Bax and PUMA. Moreover, the presence of pharmacological inhibitors of p38MAPK and p53 protected primary neurons from MPTP-induced cell death **(157).** Furthermore, earlier studies by Bulavin et al. have also shown that p38MAPK activates p53 tumor suppressor by phosphorylation of serine-33 and serine-46 residues in cancer cell lines upon UV radiation **(79).** These phosphorylation sites are required for phosphorylation at serine-15, which has been implicated as the critical step in the transcriptional activation and stabilization of p53 **(88, 106)**. Loughery and associates have suggested that serine-15 phosphorylation of p53 is essential for its interaction with transcriptional

proteins and target gene expression **(106)**. They reported that substitution of serine-15 with alanine results in decreased p53-dependent transcriptional activity which is rescued by substitution with an aspartate that mimics serine residue. This is further supported by evidence from multiple studies indicating that phosphorylation at serine-15 also modulated the interaction of p53 with its regulators including Mdm2 and p300 **(90, 91).**

In the context of pancreatic β-cells, studies by Hoshino et al. have examined the role of p53 in β-cell dysfunction in models of Type 1 and Type 2 diabetes **(158)**. They observed that loss of p53 function prevented onset of diabetes in streptozotocin-induced type1 and db/db mouse model for type 2 diabetes. Additionally, a proteomic study in type2 diabetic human islets indicated significant increase in apoptotic signaling pathways including the p53 apoptotic pathway **(159)**. Despite these findings, the regulatory factors involved in the activation of p53 in β-cells under diabetic conditions, remain to be fully understood. Recently, Flores-Lopez and associates have reported that p38MAPK co-localizes with p53 under HG conditions and mediates p53 phosphorylation, resulting in β-cell apoptosis **(121)**.

We therefore, tested if p53 is activated by Rac1-Nox2-p38MAPK signaling axis in β-cells exposed to HG conditions by quantifying phosphorylation at serine-15 residue. Our observations have indicated increased serine-15 phosphorylation of p53 in INS-1 832/13 cells and human islets exposed to HG conditions, and in diabetic ZDF rats compared to their age-matched ZLC control animals. However, the presence of Rac1 inhibitor (EHT1864) and p38MAPK inhibitor (SB203580) markedly attenuated HG-induced p53 phosphorylation in INS-1 832/13 cells, suggesting the involvement of Rac1-p38MAPK signaling in p53 activation. Furthermore, we isolated nuclear and non-nuclear fractions from INS-1 832/13 cells incubated with LG and HG. We observed increased accumulation of p53 in the nucleus under HG conditions, which is requisite for its interaction with specific DNA sites to promote the transcription of apoptotic genes **(139)**. However, our results show that the presence of EHT1864 had no significant effect on nuclear accumulation of p53, indicating that nuclear localization is regulated by other mechanisms but not phosphorylation **(98)**.

75

Previous studies from our own laboratory, have shown that post-translational prenylation of Rac1 (geranylgeranylation) is requisite for its localization in the membrane fraction, thereby, facilitating its interaction with downstream substrates. Pharmacological and siRNA-mediated inhibition of prenylation resulted in decreased GSIS, demonstrating the critical role of these modifications in β-cell function **(34)**. The presence of FTI-277 and GGTI-2147, inhibitors of protein farnesylation and geranylgeranylation, significantly attenuated Nox2-induced ROS generation under stimulatory glucose concentration, suggesting the importance of protein prenylation (Rac1) in Nox2-mediated ROS generation **(41)**. Studies from our laboratory have also reported that increased Nox2 activation in presence of inflammatory cytokines, is attenuated in the presence of 2-bromopalmitate, suggesting that Rac1 palmitoylation is also requisite for Nox2-induced oxidative stress **(120)**. Therefore, we next asked the question if post-translational modifications of Rac1 are required for p38MAPK and p53 activation. We observed a significant inhibition in p38MAPK activation under HG conditions in presence 2-bromopalmitate (2-BP), a specific inhibitor of protein palmitoylation **(160)**.

Additionally, we tested the effects of GGTI-2147, which inhibits geranylgeranylation, on HG-induced p38MAPK phosphorylation. We observed no effects of GGTI-2147 on HG-induced p38MAPK activation implying that Rac1 geranylgeranylation is not necessary for p38MAPK activation. However, our studies with Simvastatin, a global inhibitor of protein prenylation, and GGTI2147, suggested a marked decrease in HG-induced p53 phosphorylation. It has been suggested that bisphosphonates, which inhibit prenylation by blocking mevalonate pathway, activate p38MAPK before eliciting their effects on G-protein prenylation, independent of Rac1 activation **(161)**. Further studies are required to understand the effects of GGTI-2147 on HG-induced p38MAPK phosphorylation.

As a logical extension of these studies, we tested if inhibition of Rac1 with EHT1864 had any effect on glucotoxicity-induced β-cell death. Our observations showed a significant decrease in cell death in INS-1 832/13 cells exposed to glucotoxic conditions. Together, our observations

in INS-1 832/13 cells, rodent and human pancreatic islets have demonstrated that sustained activation of Rac1-Nox2 signaling module and associated oxidative stress, results in p38MAPK-dependent activation of p53, culminating in β-cell death, under glucotoxic conditions.

We also examined the involvement of ATM kinase, a known regulator of p53, in the Rac1-p38MAPK-p53 signaling cascade. Evidence from multiple studies have shown that ATM kinase is activated upon DNA damage, mainly by auto-phosphorylation **(144)**. Studies by Oleson *et al.* have implicated that ATM kinase is activated in pancreatic β-cells exposed to inflammatory cytokines and mediated DNA damage response (DDR). However, upon excessive DNA damage, ATM kinase activates cellular apoptotic mechanism mainly by p53-dependent mechanisms **(137)**. Furthermore, Yoshida et al. have reported that ATM kinase activates p53 upon DNA damage caused by Doxorubicin, which was prevented in presence of inhibitor of protein prenylation (pitavastatin) and Rac1 (NSC23766) **(136)**. We therefore, asked if ATM kinase is activated in β-cells exposed to HG conditions. We observed a marked increase in activation of ATM kinase, when INS-1 832/13 cells were exposed to HG conditions, which was significantly blocked upon Rac1 inhibition by EHT1864. To determine the role of ATM kinase in the regulation of p53, we utilized KU55933, a known inhibitor of ATM kinase activity, to examine the effects on HG-induced signaling events. Our observations indicated a marked reduction in ATM kinase activation under HG conditions. However, the presence of KU55933 had no significant effect on p53 activation, suggesting that ATM kinase, although regulated by Rac1 signaling, might be involved in other signaling pathways **(83)**. Since multiple studies, including those in ATM deficient mice, have indicated a unique role of ATM kinase in glucose homeostasis, it is possible that it is involved in DNA damage response mechanisms activated as a result of Rac1-induced oxidative stress. Further studies are required to understand the regulatory role of ATM kinase in β-cells under glucotoxic stress.

Pharmacological agent	Effect	p38MAPK phosphorylation	p53 phosphorylation
EHT1864	↓ Rac1 activity	Inhibition	Inhibition
gp91-ds-tat	↓ Nox2 activity	Inhibition	Not determined
NSC23766	↓ Rac1 activity	Inhibition	Not determined
Ehop-016	↓ Rac1 activity	Inhibition	Not determined
Simvastatin	↓ Protein prenylation	Not determined	Inhibition
GGTI2147	↓ Protein geranylgeranylation	No effect	Inhibition
2-bromopalmitate	↓ Protein palmitoylation	Inhibition	Not determined
SB203580	↓ p38MAPK activity	Not determined	Inhibition

Table 6-1: Summary of effects of pharmacological inhibitors on HG-induced p38MAPK and p53 activation

CHAPTER 7: CONCLUSIONS AND FUTURE DIRECTIONS

The central objective of my Ph.D. dissertation project is to assess the role of sustained activation of Rac1 and Nox2 holoenzyme in induction of oxidative stress, resulting in the activation of p38MAPK and p53 signaling axis, culminating in pancreatic β-cell dysfunction. Previous observations in our laboratory have demonstrated contributory roles of increased Rac1-Nox2 activity and ROS generation in mediating metabolic dysfunction of the β-cell in models of diabetes **(49, 50, 52)**. As a logical extension to these studies, this project focuses on examining the downstream apoptotic pathways, activated by Rac1-Nox2-derived oxidative stress. These data can be summarized as follows:

1. Exposure of pancreatic β-cells (INS-1 832/13 cells, rodent and human islets) to glucotoxic conditions results in activation of pro-apoptotic p38MAPK and p53 signaling pathway. Pancreatic islets isolated from Zucker diabetic fatty (ZDF) rat, a model for type 2 diabetes, also exhibit increased activation of p38MAPK and p53.

2. gp91-ds-tat, but not its inactive analog, attenuated HG-induced p38MAPK phosphorylation, suggesting that HG-induced Nox2 activation and ROS generation are upstream to p38MAPK activation.

3. NSC23766 and Ehop-016, which target Tiam1-Rac1 and Vav2-Rac1 interaction respectively, attenuated HG-induced p38MAPK phosphorylation. Additionally, EHT1864 which blocks Rac1 activation in a GEF-independent manner, blocked p38MAPK phosphorylation. These findings implicate the contributory role of Rac1 activation in HG-induced phosphorylation of p38MAPK.

4. Our findings also suggested that HG-induced p53 phosphorylation is also regulated by Rac1, which is attenuated in presence of the Rac1 inhibitor, EHT1864. However, EHT1864 did not block p53 translocation to the nucleus suggesting that HG-induced p53 nuclear localization is independent of its activation step.

5. Rac1 prenylation is also requisite for HG-induced p53 activation in INS-1 832/13 cells, since the presence of GGTI-2147, which blocks geranylgeranylation, and Simvastatin, a global inhibitor of protein prenylation, prevented p53 phosphorylation.

6. SB203580, a selective inhibitor for p38MAPK, blocked HG-induced p53 phosphorylation, confirming the involvement of p38MAPK in activating p53 apoptotic pathway, under glucotoxic stress.

7. EHT1864, which blocked HG-induced p38MAPK and p53 activation, also prevented β-cell death, confirming the role of Rac1-p38MAPK-p53 signaling cascade in β-cell apoptosis under glucotoxic conditions.

8. Our findings also indicated marked activation of ATM kinase, a known activator of p53 and a cell cycle regulator, under HG exposure conditions, which was attenuated in the presence of EHT1864 and ATM kinase inhibitor, KU55933. However, KU55933 exerted no effect on HG-induced p53 phosphorylation, suggesting that ATM kinase might be involved in other regulatory pathways.

Based on these findings, I conclude that chronic exposure of pancreatic β-cells to elevated glucose concentrations lead to sustained activation of Rac1-Nox2 enzyme complex and excess generation of intracellular ROS. The resulting oxidative stress leads to nuclear accumulation and p38MAPK-dependent phosphorylation of p53 tumor suppressor. These events, in turn, lead to transcription of several apoptotic genes mediated by p53, culminating in activation of apoptotic pathways and loss of β-cell mass. These studies provide the first evidence suggesting that therapeutic intervention of this signaling pathway prevents β-cell dysfunction under the duress of hyperglycemic conditions.

Future Directions:

These finding have provided valuable insights into the role of Rac1-Nox2 holoenzyme and associated oxidative stress in mediating β-cell dysfunction under glucotoxic stress. However, studies are needed to further verify these findings in other invivo models of T2DM and human patients, and also fill several knowledge gaps. Some of these are listed below:

➤ We have utilized the ZDF rat, as an animal model for T2DM, to verify our findings. However, since the ZDF rat develops diabetes as a result of genetic manipulations, we need to examine this pathway in a model for diabetes induced by diet/environment, as commonly seen in human populations. This can be addressed by utilizing the high-fat (45% kilocalories from fat) fed C57BL/6 mice model for diabetes to examine the activity levels of Rac1-Nox2 and p38MAPK-p53 signaling axes in the pancreatic islet. Furthermore, studies in pancreatic islets from Type2 diabetic patients would provide valuable evidence demonstrating the role of Rac1-p38MAPK-p53 module in human diabetic patients.

➤ Our findings have implicated that Rac1 prenylation is requisite for HG-induced p53 phosphorylation but not p38MAPK. Although, there is some evidence implicating the effects of prenylation inhibitors on p38MAPK activation, independent of their effects on Rac1, the involvement of Rac1 prenylation in mediating HG-induced effects needs to further examined. This can be addressed by utilizing Rac1 C189A (non-prenylatable) and V12Rac1 SAAX (non-prenylatable, constitutively active) mutants of Rac1.

➤ Our studies have also suggested a possible role of ATM kinase in HG-induced effects. Activation of ATM kinase, which also seems to be regulated by Rac1, might be involved in other signaling mechanisms including DNA repair pathways. Studies by Oleson et al. have implicated ATM kinase activation in H2AX phosphorylation leading to DNA repair response in β-cells exposed to inflammatory cytokines **(137)**. These mechanisms need to be examined in β-cells exposed to glucotoxic conditions.

➢ Lastly, we need to investigate if the Rac1-p38MAPK-p53 signlaing module is involved in β-cell dysfunction induced by exposure to saturated fatty acids (Palmitate) and glucolipotoxic conditions. Previous studies in our laboratory have shown increased Rac1-Nox2 activity and oxidative stress in β-cells exposed to palmitate **(50)**. Additional studies are need to examine activation of p38MAPK and p53, regulated by Rac1-Nox2 enzyme complex, under glucolipotoxic conditions.

APPENDIX A

Phagocyte-like NADPH oxidase (Nox2) promotes activation of p38MAPK in pancreatic β-cells under glucotoxic conditions: Evidence for a requisite role of Ras-related C3 botulinum toxin substrate 1 (Rac1)

CrossMark

Vaibhav Sidarala [a], Rajakrishnan Veluthakal [a], Khadija Syeda [a], Cornelis Vlaar [b], Philip Newsholme [c], Anjaneyulu Kowluru [a,*]

[a] Beta-Cell Biochemistry Laboratory, John D. Dingell VA Medical Center, and Department of Pharmaceutical Sciences, Wayne State University, Detroit, MI 48201, USA
[b] Department of Pharmaceutical Sciences, School of Pharmacy, University of Puerto Rico Medical School Campus, Post Office Box 365067, San Juan, PR 00936-5067, USA
[c] School of Biomedical Sciences, Curtin Health Sciences Innovation Research Institute, Curtin University, Perth, WA 6845, Australia

ARTICLE INFO

ABSTRACT

It is well established that glucotoxicity (caused by high glucose concentrations; HG) underlies pathogenesis of islet dysfunction in diabetes. We have recently demonstrated that Nox2 plays a requisite role in the generation of reactive oxygen species (ROS) under HG conditions, resulting in mitochondrial dysregulation and loss of islet β-cell function. Herein, we investigated roles of Nox2 in the regulation of downstream stress kinase (p38MAPK) activation under HG conditions (20 mM; 24 h) in normal rodent islets and INS-1 832/13 cells. We observed that gp91-ds-tat, a specific inhibitor of Nox2, but not its inactive analog, significantly attenuated HG-induced Nox2 activation, ROS generation and p38MAPK activation, thus suggesting that Nox2 activation couples with p38MAPK activation. Since Rac1, is an integral member of the Nox2 holoenzyme, we also assessed the effects of Rac1 inhibitors (EHT 1864, NSC23766 and Ehop-016) on HG-induced p38MAPK activation in isolated β-cells. We report a significant inhibition of p38MAPK phosphorylation by Rac1 inhibitors, implying a regulatory role for Rac1 in promoting the Nox2-p38MAPK signaling axis in the β-cell under the duress of HG. 2-Bromopalmitate, a known inhibitor of protein (Rac1) palmitoylation, significantly reduced HG-induced p38MAPK phosphorylation. However, GGTI-2147, a specific inhibitor of geranylgeranylation of Rac1, failed to exert any significant effects on HG-induced p38MAPK activation. In conclusion, we present the first evidence that the Rac1-Nox2 signaling module plays novel regulatory roles in HG-induced p38MAPK activation and loss in glucose-stimulated insulin secretion (GSIS) culminating in metabolic dysfunction and the onset of diabetes.

© 2015 Published by Elsevier Inc.

83

1. Introduction

Glucose-stimulated insulin secretion (GSIS) is initiated by the entry of glucose into the pancreatic β-cell and subsequent glucose metabolism which results in the formation of metabolic stimulus-secretion coupling factors, thereby, promoting several intracellular events which facilitate the movement of insulin granules toward the membrane for fusion and release [1]. Small G proteins such as Rac1 and Cdc42 have been implicated to play a critical role in cytoskeletal remodeling and GSIS, as shown in several in vitro and in vivo studies [2–7]. A growing body of evidence suggests that alterations in the function of these G proteins could represent plausible mechanisms underlying impaired insulin secretion, commonly associated with type 2 diabetes (T2D) [7,8].

In the context of physiological function of the islet β-cell, evidence from several laboratories, has shown that physiological and relatively low levels of intracellular reactive oxygen species (ROS) are requisite for GSIS [9]. Studies by Leloup et al. have demonstrated that suppression of ROS generation with antioxidants resulted in altered calcium mobilization and decreased GSIS, in rodent pancreatic islets [10]. Although several intracellular processes including the mitochondrial electron-transport chain play a role in generating ROS, recent investigations have focused on the phagocyte-like NADPH oxidase (Nox2), which is a major source of extra-mitochondrial superoxide in the pancreatic β-cell. Nox2 is a trans-membrane protein complex consisting of several membrane-associated and cytosolic components. This holoenzyme complex catalyzes one electron reduction of oxygen, accompanied by oxidation of cytosolic NADPH, resulting in the generation of intracellular superoxide. The superoxide molecule is rapidly converted to the more stable hydrogen peroxide by superoxide dismutase. While the Nox2 membrane associated components include gp91^{phox} and p22^{phox}, the cytosolic components include p47^{phox}, p67^{phox}, p40^{phox} and a small G-protein, Rac1. Recent evidence from our own laboratory has demonstrated activation of Nox2 and the involvement of Rac1 in the generation of ROS, facilitating GSIS [11,12].

Insulin resistance and decreased glucose utilization, in T2D, results in chronic exposure of pancreatic β-cells to elevated levels of glucose and free-fatty acids (termed as glucolipotoxicity). Glucolipotoxicity has been demonstrated to be the central cause for several T2D complications, including β-cell dysfunction and cell death [13]. In this context, several studies have implicated hyperactivity of Rac1 and Nox2, leading to excess ROS generation and oxidative stress, to play a mediatory role in β-cell dysfunction and apoptosis [14]. Studies from our own laboratory have demonstrated increased Nox2 activity in the ZDF rat, a model for T2D and human islets exposed to glucotoxic conditions [15]. However, the signaling mechanisms that mediate the deleterious effects of glucotoxic conditions and consequent abnormal Rac1-Nox2 activity need to be further elucidated.

To further investigate the downstream effects of Nox2-derived ROS generation under glucotoxic conditions, we investigated the involvement of p38 mitogen-activated protein kinase (p38MAPK) in the metabolic dysfunction of the pancreatic β-cell. As demonstrated in various cell types, p38MAPK undergoes activation by phosphorylation at Thr180/Tyr182 residues, and mediates cellular responses to stress stimuli, which include cell proliferation, senescence and apoptosis [16]. It has been suggested that activation of p38MAPK upon prolonged exposure of β-cells to stress stimuli results in apoptosis, possibly mediated by downstream pro-apoptotic signaling targets including p53 transcription factor and caspases [17,18]. Additionally, in vivo studies with mice lacking p38δ, an isoform of p38MAPK, have shown that genetic

depletion of this stress kinase resulted in prevention of high-fat diet-induced insulin resistance and β-cell dysfunction [19]. These observations indicate a mediatory role of p38MAPK in oxidative-stress induced β-cell dysfunction and cell death. Based on this evidence, in this study, we primarily focused on demonstrating the role of Rac1-Nox2 driven ROS generation in metabolic dysfunction and apoptosis of the pancreatic β-cell under glucotoxic conditions, mediated by the p38 family of stress kinases. We have utilized several pharmacological inhibitors with distinct mechanisms of action (listed in Table 1), targeting various signaling steps involved in activation of the Rac1-Nox2 enzyme complex, to study their effects on p38MAPK activation.

2. Materials and methods

2.1. Materials

Rabbit polyclonal antibody for phospho-p38MAPK (Thr 180/Tyr 182) and total-p38MAPK were obtained from Santa Cruz Biotechnology (Santa Cruz, CA). Cleaved caspase-3 and lamin B antibodies were purchased from Cell Signaling (Danvers, MA). Actin antibody was from Sigma–Aldrich (St. Louis, MO). Anti-rabbit IgG-horseradish peroxidase conjugate and enhanced chemiluminescence (ECL) kits were from Amersham Biosciences (Piscataway, NJ). IRDye® 800CW anti-rabbit was obtained from LICOR (Lincoln, NE). NSC23766 and GGTI-2147 were purchased from Calbiochem (San Diego, CA). Ehop-016 was synthesized as we described in [20]. EHT1864 was from R&D systems (Minneapolis, MN). Scrambled gp91-ds-tat (inactive) and active gp91-ds-tat were from Anaspec, Inc. (Fremont, CA). 2-Bromo-palmitate (2-BP), 2′,7′-dichlorofluorescein diacetate (DCFDA), N,-N′-dimethyl-9,-9′-bisacridiniumdinitrate (lucigenin), were from Sigma–Aldrich (St. Louis, MO). The rat insulin ELISA kit was purchased from American Laboratory Products Co (Windham, NH). All other reagents used in the studies were obtained from Sigma–Aldrich (St. Louis, MO).

2.2. Insulin-secreting cells: isolation, culture and incubations

Pancreatic islets were isolated from 6 to 8 weeks old Sprague-Dawley male rats (Harlan laboratories, Oxford) by collagenase digestion method as previously described [15]. Rat islets and INS-1 832/13 cells were cultured in RPMI 1640 medium containing 10% heat-inactivated FBS supplemented with 100 IU penicillin and 100 IU/ml streptomycin, 1 mM sodium pyruvate, 50 μM 2-mercaptoethanol (not added in medium for rat islets) and 10 mM HEPES (pH 7.4) at 37 °C and 5% CO_2 in a humidified incubator. INS-1 832/123 cells were sub cloned twice weekly following trypsinization and passages 53–61 were used for the studies. Following overnight incubation in 2.5 mM glucose and 2.5% serum RPMI media, the cells were treated with glucose (2.5 mM, low glucose; LG or 20 mM, high glucose; HG) in absence

Table 1
Small molecule inhibitors used in the current studies.

Inhibitor used	Modes of action
gp91-ds-tat peptide	Inhibits Nox2 activation by inhibiting holoenzyme assembly [33]
EHT 1864	Inhibits guanine nucleotide binding and activation of Rac1 [24,25]
NSC23766	Inhibits Tiam1-mediated activation of Rac1 [4]
Ehop-016	Attenuates Vav2-mediated activation of Rac1 [20]
GGTI-2147	Inhibits geranylgeranylation and membrane targeting of Rac1 [29]
2-Bromopalmitate	Inhibits palmitoylation and membrane anchoring of Rac1 [27]

or presence of gp91-ds-tat peptide (2.5 μM) or scrambled peptide (2.5 μM), EHT 1864 (10 μM), NSC23766 (20 μM), Ehop-016 (5 μM), GGTI-2147 (10 μM) and 2-bromopalmitate (2-BP; 100 μM) for the indicated time. After harvesting, samples were separated by SDS-PAGE and processed by Western Blotting.

2.3. Quantification of glucose-stimulated insulin release

Following overnight starving, INS-1 832/13 cells were incubated with glucose (2.5 mM, LG and 20 mM, HG) for 24 h. Cells were then pre-incubated in Krebs-Ringer Bicarbonate buffer (KRB, pH 7.4) and further stimulated with either 2.5 mM LG or 20 mM HG for 45 min at 37 °C. The supernatants were then collected and insulin released into the medium was quantified using ELISA kit, as we described previously [4].

2.4. Western Blotting

After incubation with glucose (2.5 mM, LG and 20 mM, HG) in the absence or presence of various inhibitors as indicated, cells were lysed using RIPA buffer containing protease inhibitor cocktail, 1 mM NaF, 1 mM PMSF and 1 mM Na$_3$VO$_4$. Cell lysates (~40 μg for INS-1 832/13 cells and ~25 μg for rat islets) were then resolved by SDS-PAGE, and transferred onto nitrocellulose membranes. Membranes were blocked in 5% non-fat dry milk in TBS-T buffer (10 mM Tris–HCl pH-7.6, 1.5 M NaCl and 0.1% Tween 20) or 0.1% Casein in PBS and then incubated with appropriate primary antibody (cleaved Caspase-3, Lamin B, phospho-p38MAPK and total-p38MAPK) diluted with 5% non-fat dry milk in TBS-T or 0.1% Casein in PBS-T, for 1 h at room temperature. The membranes were then washed 5× for 5 min with TBS-T or PBS-T, and then probed with the appropriate secondary antibody (Anti-rabbit IgG-horseradish peroxidase conjugate or IRDye® 800CW anti-rabbit). The immune complexes were then detected using ECL detection kit (CareStream® Imaging system or HyBlot CL® Autoradiography Film) or Odyssey® Imaging Systems. The band intensities were quantified using CareStream® Molecular Imaging Software.

2.5. Quantification of ROS generation

Total ROS levels were quantified fluorometrically using 2′,-7′-dichlorofluorescein diacetate (DCFDA; Sigma–Aldrich, St. Louis, MO, USA). Briefly, 20–30 μg of protein derived from INS-1 832/13 cells treated with glucose (LG and HG) alone or in the presence of gp91-ds-tat peptide (2.5 μM) or scrambled peptide (2.5 μM), was incubated with 2 μM of DCHFDA for 10 min and the resulting fluorescence was measured at 485 nm and 530 nm as excitation and emission wavelengths, respectively.

2.6. Determination of Nox2 activity

Nox2 activity was measured in lysates derived from INS-1 832/13 cells treated with glucose (LG and HG) in absence or presence of gp91-ds-tat peptide (2.5 μM) or scrambled peptide (2.5 μM) by luminescence assay using 20 μM lucigenin as electron acceptor and 100 μM NADPH. The Nox2 activity was expressed as nmoles of NADPH oxidized/min/μg of protein.

2.7. Statistical analysis of experimental data

Results are expressed as means with their standard errors as indicated. The statistical significance of differences between control and experimental groups was evaluated by ANOVA followed by SNK Post Hoc test where appropriate. $P < 0.05$ was considered to be statistically significant.

3. Results

3.1. Our in vitro experimental model for glucotoxicity of the islet β-cell

The overall objective of the current study was to assess the contributory roles of Nox2 in promotion of stress kinase (p38MAPK) activation in pancreatic β-cells exposed to glucotoxic conditions. Unless stated otherwise, as a model for glucotoxicity, pancreatic β-cells were incubated in the presence of either 2.5 mM or 20 mM glucose for 24 h. We have chosen these experimental conditions since we observed a significant increase in mitochondrial dysfunction which promotes caspase 3 activation (Fig. 1; Panel A). Furthermore, as we reported recently [21], a significant increase in caspase 3-mediated lamin degradation was also seen under these conditions (Fig. 1; Panel A), culminating in metabolic dysfunction and loss in GSIS (Fig. 1; Panel B). To accomplish our objectives, we utilized gp91-ds-tat, a specific inhibitor of Nox2, and its scrambled peptide (as a negative control) to delineate the regulatory roles of Nox2 in HG-induced p38MAPK activation. Furthermore, we tested specific inhibitors of Rac1, which is a component of the Nox2 holoenzyme to further assess the contributory roles of the Rac1-Nox2 cascade in the induction of islet dysfunction under conditions of glucotoxicity. For brevity, specific details of pharmacological inhibitors and their modes of action are described in Table 1.
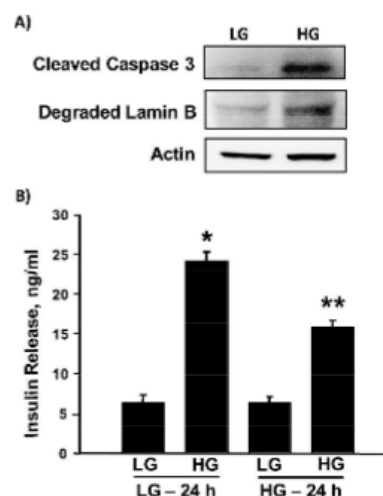
Fig. 1. Glucotoxic conditions promote caspase 3 activation, lamin B degradation and loss in GSIS in INS-1 832/13 cells.
Panel A: INS-1 832/13 cells were incubated in the presence of low (2.5 mM; LG) or high (20 mM; HG) glucose for 24 h and protein lysates (~40 μg) were resolved by SDS-PAGE and transferred to a nitrocellulose membrane. The membrane was probed for cleaved (active) caspase 3 and lamin B, and immune complexes were identified using ECL detection kit. To check equal protein loading, the membranes were stripped and reprobed for actin. A representative blot is shown here. These findings confirm our original observations in [21].
Panel B: INS-1 832/13 cells were cultured in the presence of low (2.5 mM; LG) or high (20 mM; HG) glucose for 24 h following which they were stimulated with low (2.5 mM) or high (20 mM) glucose for 45 min. Insulin released into the medium was quantified by ELISA (as described in Section 2). The data are expressed as insulin release (ng/ml) and are mean ± SEM from two independent experiments. $*P < 0.05$ vs. LG under 24 h low glucose treatment; $**P < 0.05$ vs. HG under 24 h low glucose treatment.

3.2. gp91-ds-tat peptide, a specific inhibitor of Nox2, but not its inactive congener, markedly attenuates HG-induced Nox2 activation and ROS generation in INS-1 832/13 cells

At the outset, we determined whether HG conditions induce Nox2 activation in INS-1 832/13 cells. To accomplish this, we quantified Nox2 activity in these cells exposed to LG (2.5 mM) or HG (20 mM) conditions for 24 h. Data in Fig. 2 (Panel A) demonstrate a significant increase in Nox2 activity under these experimental conditions. Further, gp91-ds-tat peptide, a specific inhibitor of Nox2 activation, markedly attenuated HG-induced Nox2 activation. These inhibitory effects of gp91-ds-tat peptide were specific, since its inactive analog failed to inhibit HG-induced Nox2 activity in these cells. Compatible with these findings are our observations, which suggested a significant increase in ROS generation in INS-1 832/13 cells incubated under HG conditions (Fig. 2; Panel B). In addition, HG-induced ROS generation was significantly suppressed by gp91-ds-tat peptide (bar 4 vs. bar 6), but not by its inactive analog. Taken together, our findings (Fig. 2) indicate a significant increase in Nox2 activity and associated ROS generation in INS-1 832/13 cells following exposure to HG conditions.

3.3. Nox2 activation is upstream to p38MAPK activation in pancreatic β-cells exposed to HG conditions

We next asked whether HG-induced activation of Nox2 and associated generation of ROS promote activation of p38MAPK, which has been implicated in cellular dysfunction under the duress of HG conditions in multiple cell types, including the islet β-cell. To address this, we quantified p38MAPK phosphorylation under basal or HG conditions in the absence or presence of gp91-ds-tat peptide. Data depicted in Fig. 3 demonstrate significant increase in p38MAPK phosphorylation under HG conditions, which was suppressed significantly by gp91-ds-tat peptide (Panel A). In line with our observations in Figs. 1 and 2, the inactive analog of gp91-ds-tat peptide exerted no inhibitory effects on HG-induced p38MAPK activation (Panel A). Pooled data from multiple experiments are provided in Panel B. Together, these data suggest Nox2 activation is upstream to p38MAPK activation in the cascade of events leading to loss of β-cell function, including GSIS under the duress of HG conditions.

3.4. Inhibition of guanine nucleotide association with Rac1 results in inhibition of HG-induced p38MAPK activation

The Nox2 holoenzyme complex is comprised of membranous (gp91^{phox}, p22^{phox}) and cytosolic (p47^{phox}, p67^{phox}) and the small
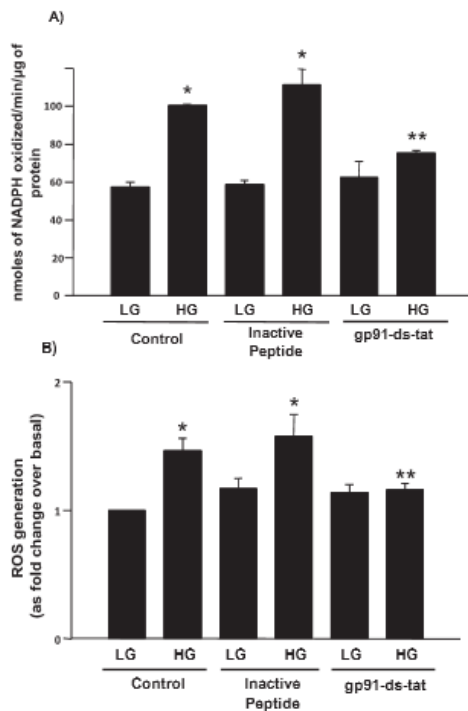
Fig. 2. gp91-ds-tat peptide a specific inhibitor of Nox2, but not its inactive analog, inhibits HG-induced Nox2 activation and ROS generation in INS-1 832/13 cells.
Panel A: INS-1 832/13 cells were pre-incubated with scrambled peptide (2.5 μM) or gp91-ds-tat peptide (2.5 μM) for 1 h and then treated with LG and HG in the continuous presence of scrambled peptide (2.5 μM) or gp91-ds-tat peptide (2.5 μM) for 24 h. Nox2 activity was quantified as described under Methods, and the activity was expressed as nmoles of NADPH oxidized/min/μg of protein. *$P < 0.05$ vs. low glucose. **$P < 0.05$ vs. high glucose alone or in the presence of inactive peptide (mean ± SEM; $n = 6$).
Panel B: INS-1 832/13 cells were cultured and treatments were performed as described under Panel A. Intracellular levels of ROS were then measured using DCF-DA assay as described under Methods. ROS generation was expressed as fold change over 2.5 mM glucose. *$P < 0.05$ vs. low glucose. **$P < 0.05$ vs. high glucose alone or in the presence of inactive peptide (mean ± SEM; $n = 6$).
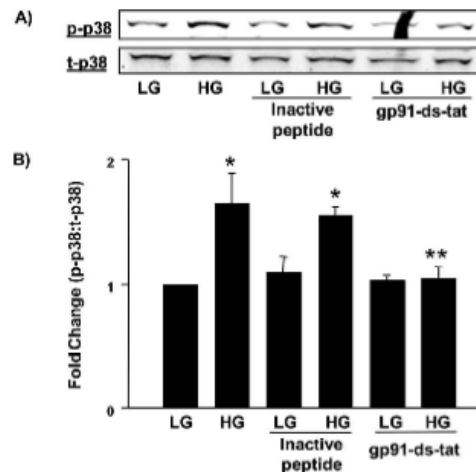
Fig. 3. Glucose induced p38MAPK activation is inhibited by gp91-ds-tat.
Panel A: INS-1 832/13 cells were pre incubated with scrambled peptide (2.5 μM) or gp91-ds-tat peptide (2.5 μM) for 1 h and then further treated with glucose (LG and HG) in the presence of scrambled peptide (2.5 μM) or gp91-ds-tat peptide (2.5 μM) for 24 h. Lysate proteins were then separated by SDS-PAGE, and levels of phosphorylated p38MAPK were determined by Western Blotting. After separation, proteins were transferred onto nitrocellulose membranes. The membranes were then blocked and probed with antibody raised against phosphorylated p38MAPK followed by incubation with anti-rabbit secondary antibody. The immune complexes were then detected using ECL detection kit. To ensure equal protein loading, phospho-p38MAPK was normalized with total p38MAPK, as loading control.
Panel B: Band intensities of phospho-p38MAPK and total-p38MAPK were quantified by densitometric analysis. Results are shown as mean ± SEM from three independent experiments and expressed as fold change of the ratios between phospho-p38MAPK and total p38MAPK. *$P < 0.05$ vs. low glucose, **$P < 0.05$ vs. high glucose alone or in presence of inactive peptide.
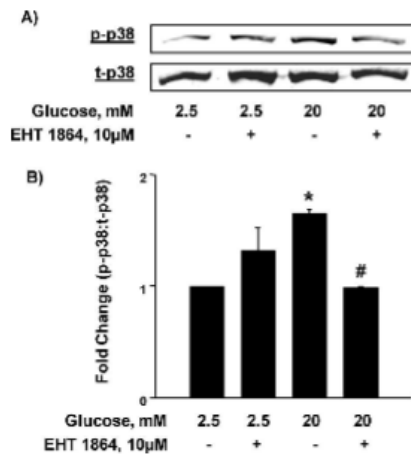
Fig. 4. Glucose-induced p38MAPK activation is inhibited by EHT 1864.
Panel A: Following treatment with glucose (LC and HG) in the absence or presence of EHT 1864 (10 μM) for 24 h, INS-1 832/13 cells were lysed and proteins were separated by SDS-PAGE. Lysate proteins were then transferred onto nitrocellulose membranes. The membranes were then blocked and incubated with antibody against phosphorylated p38MAPK followed by incubation with anti-rabbit secondary antibody. The same blots were stripped and reprobed with antibody raised against total p38MAPK.
Panel B: Band intensities of phospho-p38MAPK and total-p38MAPK were quantified by densitometric analysis. Results are shown as mean ± SEM from three independent experiments and expressed as fold change of the ratios between phospho-p38MAPK and total-p38MAPK. *$P < 0.05$ vs. low glucose. #$P < 0.05$ vs. high glucose.

molecular weight G-protein Rac1 [7,22]. Recent evidence from our laboratory has suggested that pharmacological or molecular biological inhibition of Rac1 prevents the activation of Nox2 under the duress of HG and high lipid exposure conditions [22,23]. Therefore, in the next series of experiments, we employed specific inhibitors of Rac1 function (Table 1) to further assess the regulatory roles of this G-protein in HG-induced p38MAPK activation in INS-1 832/13 cells. The first inhibitor we tested was EHT 1864, a small molecule inhibitor, which inhibits Rac1 activation via inhibition of guanine nucleotide association. Consequently, EHT 1864 retains Rac1 in an inactive/inert conformation [24,25]. Data in Fig. 4 (Panel A) demonstrate a marked reduction of HG-induced p38MAPK activation by EHT 1864, thus suggesting a regulatory role for Rac1 in the cascade of events leading to HG-induced p38MAPK activation. Data from multiple experiments confirming the inhibitory effects of EHT 1864 are provided in Fig. 4; Panel B.

3.5. Inhibition of GDP/GTP exchange on Rac1 suppresses HG-induced p38MAPK in pancreatic β-cells

It is well established that biological activation-inactivation of small G-proteins (e.g., Rac1) is mediated by a variety of highly specific regulatory proteins/factors [7]. One such regulatory class of proteins are the guanine nucleotide exchange factors (GEFs), which promote activation of G-proteins via GDP/GTP exchange. Recent studies from our laboratory have identified two GEFs for Rac1 in pancreatic β-cells. They are Tiam1 [4] and Vav2 [20]. Using siRNA and pharmacological approaches (e.g., NSC23766 for Tiam1 and Ehop-016 for Vav2), we defined novel roles for Tiam1-Rac1 and Vav2-Rac1 signaling pathways in islet function, including GSIS [4, unpublished data]. More recent investigations from our

laboratory have implicated the Tiam1-Rac1 signaling pathway in the metabolic dysregulation of pancreatic β-cells under the duress of glucolipotoxic, ceramide and pro-inflammatory cytokine exposure conditions [22,23,26]. We also reported regulatory roles of the Tiam1-Rac1 axis at the level of Nox2 activation [23,26]. Therefore, in the next set of studies, we examined the contributory roles of Tiam1-Rac1 and Vav2-Rac1 axes on HG-induced p38MAPK activation.

Data depicted in Fig. 5; Panel A demonstrates significant inhibition of HG-induced p38MAPK activation by NSC23766 in INS-1 832/13 cells. NSC23766 exerted no effects on basal p38MAPK. Data from multiple studies are pooled and presented in Fig. 5; Panel B. It is noteworthy that NSC23766 completely abolished HG-induced p38MAPK activation in normal rodent islets without significantly affecting basal activation (Fig. 5; Panel C). Pooled data from multiple studies are provided in Fig. 5; Panel D. Taken together, our findings in INS-1 832/13 cells and normal rodent islets indicate that functional inactivation of Tiam1-Rac1 signaling pathway, presumably, upstream to Nox2 activation [22,23,26], relieves HG-induced stress kinase (p38MAPK) activation.

In the next series of studies, we asked whether the Vav2-Rac1 signaling module mediates HG-induced p38MAPK activation in pancreatic β-cells. To accomplish this, we utilized Ehop-016, a specific inhibitor of Vav2-mediated activation of Rac1 [20]. Data in Fig. 6; Panel A demonstrate a significant inhibition of p38MAPK activation by Ehop-016 under glucotoxic conditions. However, unlike other Rac1 inhibitors tested above, we observed a significant stimulation of p38MAPK by Ehop-016 under basal glucose conditions (Fig. 6; Panel B; bar 1 vs. bar 2). Data accrued in multiple studies are included in Panel B. We observed similar inhibitory effects of Ehop-016 on p38MAPK phosphorylation in normal rodent islets exposed to glucotoxic conditions (Fig. 6; Panels C and D). Furthermore, akin to our findings in INS-1 832/13 cells (Fig. 6; Panels A and B) Ehop-016 significantly increased p38MAPK phosphorylation in rat islets under basal glucose conditions (Fig. 6; Panels C and D), raising a potential possibility that it might be regulating additional signaling mechanisms (see Section 4). Taken together, our findings shown in Figs. 5 and 6 suggest novel regulatory roles of GEFs (Tiam1 and Vav2) in Rac1-mediated activation of p38MAPK in pancreatic β-cells exposed to glucotoxic conditions. To the best of our knowledge this is the first evidence in support of involvement of more than one GEF in modulation of G-protein-mediated metabolic dysfunction of the islet β-cell. We speculate that these two GEFs might mediate HG-induced activation of Rac1-sensitive Nox2 (see Section 4).

3.6. Geranylgeranylation of Rac1 is not essential for HG-induced p38MAPK activation in INS-1 832/13 cells

It is well established in multiple cell types, including in our own observations in the islet β-cell, that small molecular weight G-proteins (e.g., Rac1) undergo a series of post-translational modifications at their C-terminal cysteine residues (prenylation, carboxylmethylation and palmitoylation). It has been shown that these modifications increase the hydrophobicity of modified G-proteins, thereby promoting their membrane targeting and effector activation [7,27–29]. Recent pharmacological and molecular biological evidence from our laboratory in human islets, rat islets and INS-1 832/13 cells implicate novel regulatory roles for these modifications in islet function, including GSIS [28–30]. Herein, we first investigated whether geranylgeranylation of Rac1 is critical for promoting p38MAPK activation in INS-1 832/13 cells exposed to HG conditions. To address this, we quantified HG-induced p38MAPK phosphorylation in INS-1 832/13 cells incubated in the absence or presence of GGTI-2147, a known inhibitor of
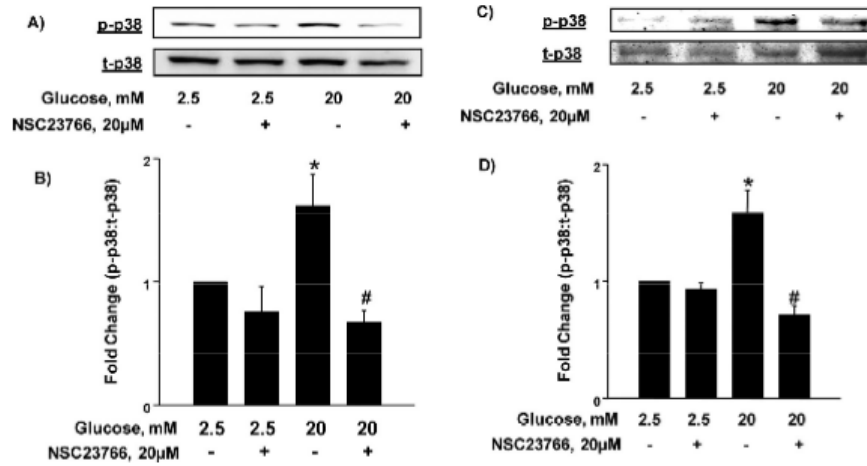
Fig. 5. NSC23766, a known inhibitor of Tiam1-Rac1 signaling pathway suppresses HG-induced p38MAPK activation in INS-1 832/13 cells and normal rodent islets.

Panel A: INS-1 832/13 cells, pre-incubated overnight with NSC23766 (20 μM), were further treated with glucose (LG and HG) in the absence or presence of NSC23766 (20 μM) for 24 h. Cells were then lysed and proteins were resolved by SDS-PAGE. Separated proteins were transferred onto nitrocellulose membranes. The membranes were then blocked and probed with antibody for detecting phosphorylated p38MAPK. The same blots were stripped and reprobed with antibody against total p38MAPK.

Panel B: Band intensities of phospho-p38MAPK and total-p38MAPK were quantified by densitometric analysis. Results are shown as mean ± SEM from three independent experiments and expressed as fold change of the ratios between phospho-p38MAPK and total-p38MAPK. $^{*}P < 0.05$ vs. low glucose, $^{\#}P < 0.05$ vs. high glucose.

Panel C: After isolation, rat pancreatic islets were pre incubated overnight with NSC23766 (20 μM) and further treated with glucose (LG and HG) in the absence or presence of NSC23766 (20 μM) for 24 h. Lysate proteins (~25 μg) were then resolved by SDS-PAGE, and analyzed by Western Blotting, as described above, for detecting phosphorylated and total p38MAPK.

Panel D: Band intensities of phospho-p38MAPK and total-p38MAPK were quantified by densitometric analysis. Results are shown as mean ± SEM from three independent experiments and expressed as fold change of the ratios between phospho-p38MAPK and total p38MAPK. $^{*}P < 0.05$ vs. low glucose, $^{\#}P < 0.05$ vs. high glucose.
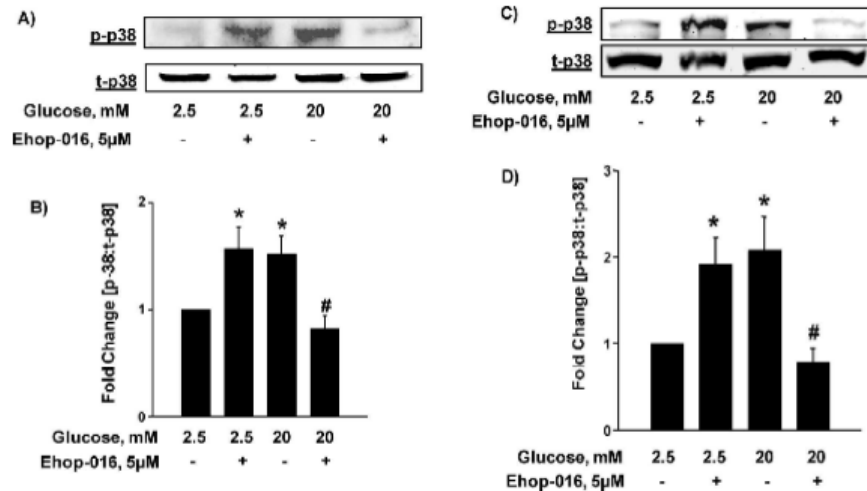
Fig. 6. Ehop-016, a specific inhibitor of Vav2-mediated activation of Rac1 attenuates HG-induced p38MAPK activation in INS-1 832/13 cells and normal rodent islets.

Panel A: INS-1 832/13 cells, pre incubated overnight with Ehop-016 (5 μM) were further treated with LG and HG in the absence or presence of Ehop-016 (5 μM) for 24 h. Cell lysate proteins were then separated and analyzed by Western Blotting as described above. After separation by SDS-PAGE, proteins were transferred onto nitrocellulose membranes. The membranes were blocked and probed with anti-phosphorylated p38MAPK followed by incubation with anti-rabbit secondary antibody. The same blots were stripped and reprobed with anti-total p38MAPK.

Panel B: Band intensities of phospho-p38MAPK and total-p38MAPK were quantified by densitometric analysis. Results are shown as mean ± SEM from five independent experiments and expressed as fold change of the ratios between phospho-p38MAPK and total-p38MAPK. $^{*}P < 0.05$ vs. low glucose, $^{\#}P < 0.05$ vs. high glucose.

Panel C: Pancreatic islets isolated from normal rodents, were pre-incubated with Ehop-016 (5 μM) overnight and further incubated with glucose (LG and HG) in the continuous absence or presence of Ehop-016, for 24 h. Islets were then lysed and lysate proteins were separated by SDS-PAGE. Phosphorylated and total p38MAPK were then detected by Western Blot analysis.

Panel D: Band intensities of phospho-p38MAPK and total-p38MAPK were quantified by densitometric analysis. Results are shown as mean ± SEM from three independent studies and expressed as fold change in the ratios between phosphorylated and total p38MAPK. $^{*}P < 0.05$ vs. low glucose, $^{\#}P < 0.05$ vs. high glucose.
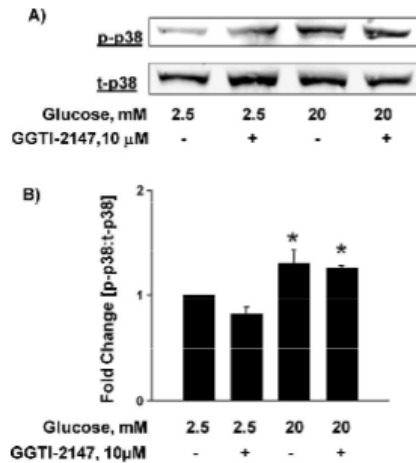
Fig. 7. Inhibition of geranylgeranylation by GGTI-2147 fails to exert significant effects on HG-induced p38MAPK activation.
Panel A: INS-1 832/13 were treated with LG and HG in the absence or presence of GGTI-2147 (10 μM) for 24 h. Cells were then lysed and proteins were separated by SDS-PAGE, and then transferred onto a nitrocellulose membrane. The membranes were then blocked and probed with anti-phosphorylated p38MAPK followed by incubation with anti-rabbit secondary antibody. The same blots were stripped and reprobed with anti-total p38MAPK.
Panel B: Band intensities of phospho-p38MAPK and total-p38MAPK were quantified by densitometric analysis. Results are shown as mean ± SEM from three independent experiments and expressed as fold change of the ratios between phospho-p38MAPK and total-p38MAPK. $*P < 0.05$ vs. low glucose.

Fig. 8. Inhibition of protein palmitoylation by 2-bromopalmitate results in inhibition of HG-induced p38MAPK activation.
Panel A: INS-1 832/13 were treated with LG and HG in the absence or presence of 2-BP (100 μM) for 24 h. Cells were then lysed and proteins were separated by SDS-PAGE, and then transferred onto a nitrocellulose membrane. The membranes were then blocked and probed with anti-phosphorylated p38MAPK followed by incubation with anti-rabbit secondary antibody. The same blots were stripped and reprobed with anti-total p38MAPK.
Panel B: Band intensities of phospho-p38MAPK and total-p38MAPK were quantified by densitometric analysis. Results are shown as mean ± SEM from three independent experiments and expressed as fold change of the ratios between phospho-p38MAPK and total-p38MAPK. $*P < 0.05$ vs. low glucose, $#P < 0.05$ vs. high glucose.

geranylgeranylation of Rac1. Data in Fig. 7 demonstrate no significant effects of this inhibitor on glucose-induced p38MAPK (Panel A). Pooled data from multiple experiments are included in Fig. 7; Panel B. Taken together, these findings indicate that geranylgeranylation of Rac1 may not be necessary for HG-induced p38MAPK activation.

3.7. Protein palmitoylation is requisite for HG-induced p38MAPK in INS-1 832/13 cells

In the last set of experiments, we determined whether protein (*e.g.*, Rac1) palmitoylation underlies HG-induced p38MAPK activation. To address this, we employed 2-bromopalmitate (2-BP), a selective inhibitor of palmitoyl transferase, which incorporates palmitate into the cysteine residues, which is upstream to the prenylated cysteine [7]. Data in Fig. 8; Panel A (representative Western blot) and Panel B (pooled data from multiple studies) demonstrate significant attenuation of HG-induced p38MAPK activation by 2-BP (Fig. 8; Panel B) suggesting that protein palmitoylation represents one of the signaling events leading to HG-mediated stress kinase activation and metabolic dysregulation of the islet β-cell.

4. Discussion

It is well established that chronic exposure of pancreatic β-cells to elevated glucose concentrations (glucotoxicity) results in severe metabolic dysregulation including inhibition of GSIS [13,14]. The current study was based on the hypothesis that HG induces Nox2 activation leading to subsequent activation of the downstream stress kinase signaling pathway culminating in the loss of GSIS in pancreatic β-cells. We have tested this hypothesis using small

molecule inhibitors of Nox2 and Rac1 activation (Table 1) in insulin-secreting pancreatic β-cells and normal rodent islets. Salient findings are discussed below.

Our current findings suggest that high glucose-induced p38MAPK activation is a consequence of increased Nox2 activation and associated ROS generation, since gp91-ds-tat peptide, but not its inactive (sgp91-ds-tat, scrambled) analog, markedly reduced HG-induced Nox2 activation (Fig. 2A), ROS generation (Fig. 2B) and p38MAPK activation (Fig. 3A and B). Data accrued from previously published studies and our current investigations also suggest that p38MAPK activation by HG results in increased β-cell apoptosis. For example, recent studies have provided evidence to suggest that glucotoxic conditions increase stress kinase activation, including p38MAPK [18,31] resulting in increased apoptosis. In support of this, our recent findings have also suggested that glucotoxic conditions (identical to those employed in the current studies) significantly attenuated HG-stimulated insulin secretion and loss in metabolic cell viability [32,33]. Compatible with these findings are our current data (Fig. 1) indicating significant activation of caspase-3 and lamin B degradation in INS-1 832/13 cells under conditions of glucotoxicity.

Several lines of evidence in multiple cell types, specifically in the islet β-cell, suggests that Nox2 activation results in the generation of ROS under conditions of glucolipotoxicity and exposure to pro-inflammatory cytokines (IL-1β, TNFα and IFNγ) and biologically active sphingolipids (ceramide) [22,23,26]. The majority of the studies employed relatively selective inhibitors of Nox2, such as apocynin and DPI, to deduce its roles in the onset of cellular dysfunction [34,35]. In the current studies, we have utilized gp91-ds-tat peptide, a specific inhibitor of Nox2; this peptide has been shown to interfere with binding of the cytosolic

[5] S. Asahara, Y. Shibutani, K. Teruyama, H.Y. Inoue, Y. Kawada, H. Etoh, et al., Ras-related C3 botulinum toxin substrate 1 (RAC1) regulates glucose-stimulated insulin secretion via modulation of F-actin, Diabetologia 56 (2013) 1088–1097.

[6] A. Kowluru, S.E. Seavey, G. Li, R.L. Sorenson, A.J. Weinhaus, R. Nesher, et al., Glucose- and GTP-dependent stimulation of the carboxylmethylation of Cdc42 in rodent and human pancreatic islets and pure β cells: evidence for an essential role for GTP-binding proteins in nutrient-induced insulin secretion, J. Clin. Invest. 98 (1996) 540–555.

[7] A. Kowluru, Small G proteins in islet beta-cell function, Endocr. Rev. 31 (2010) 52–78.

[8] S.A. Metz, M. Meredith, J. Vadakekalam, M.E. Rabaglia, A. Kowluru, A defect late in stimulus-secretion coupling impairs insulin secretion in Goto-Kakizaki diabetic rats, Diabetes 48 (1999) 1754–1762.

[9] P. Newsholme, D. Morgan, E. Rebelato, H.C. Oliveira-Emilio, J. Procopio, R. Curi, et al., Insights into the critical role of NADPH oxidase(s) in the normal and dysregulated pancreatic beta cell, Diabetologia 52 (2009) 2489–2498.

[10] C. Leloup, C. Tourrel-Cuzin, C. Magnan, A. Karaca, J. Castel, L. Carneiro, et al., Mitochondrial reactive oxygen species are obligatory signals for glucose-induced insulin secretion, Diabetes 58 (2009) 673–681.

[11] I. Syed, C.N. Kyathanahalli, A. Kowluru, Phagocyte-like NADPH oxidase generates ROS in INS 832/13 cells and rat islets: role of protein prenylation, Am. J. Physiol. Regul. Integr. Comp. Physiol. 300 (2011) R756–R762.

[12] A. Matti, C. Kyathanahalli, A. Kowluru, Protein farnesylation is requisite for mitochondrial fuel-induced insulin release: further evidence to link reactive oxygen species generation to insulin secretion in pancreatic β-cells, Islets 4 (2012) 74–77.

[13] V. Poitout, R.P. Robertson, Glucolipotoxicity: fuel excess and beta-cell dysfunction, Endocr. Rev. 29 (2008) 351–366.

[14] A. Kowluru, R.A. Kowluru, Phagocyte-like NADPH oxidase [Nox2] in cellular dysfunction in models of glucolipotoxicity and diabetes, Biochem. Pharmacol. 88 (2014) 275–283.

[15] I. Syed, C.N. Kyathanahalli, B. Jayaram, S. Govind, C.J. Rhodes, R.A. Kowluru, et al., Increased phagocyte-like NADPH oxidase and ROS generation in type 2 diabetic ZDF rat and human islets: role of Rac1-JNK1/2 signaling pathway in mitochondrial dysregulation in the diabetic islet, Diabetes 60 (2011) 2843–2852.

[16] T. Zarubin, J. Han, Activation and signaling of the p38 MAP kinase pathway, Cell Res. 15 (2005) 11–18.

[17] J.L. Evans, I.D. Goldfine, B.A. Maddux, G.M. Grodsky, Oxidative stress and stress-activated signaling pathways: a unifying hypothesis of type 2 diabetes, Endocr. Rev. 23 (2002) 599–622.

[18] L.A. Flores-López, M. Díaz-Flores, R. García-Macedo, A. Ávalos-Rodríguez, M. Vergara-Onofre, M. Cruz, et al., High glucose induces mitochondrial p53 phosphorylation by p38 MAPK in pancreatic RINm5F cells, Mol. Biol. Rep. 40 (2013) 4947–4958.

[19] G. Sumara, I. Formentini, S. Collins, I. Sumara, R. Windak, B. Bodenmiller, et al., Regulation of PKD by the MAPK p38delta in insulin secretion and glucose homeostasis, Cell 136 (2009) 235–248.

[20] B.L. Montalvo-Ortiz, L. Castillo-Pichardo, E. Hernández, T. Humphries-Bickley, A. De la Mota-Peynado, L.A. Cubano, et al., Characterization of EHop-016, novel small molecule inhibitor of Rac GTPase, J. Biol. Chem. 287 (2012) 13228–13238.

[21] K. Syeda, A.M. Mohammed, D.K. Arora, A. Kowluru, Glucotoxic conditions induce endoplasmic reticulum stress to cause caspase 3 mediated lamin B degradation in pancreatic β-cells: protection by nifedipine, Biochem. Pharmacol. 86 (2013) 1338–1346.

[22] A. Kowluru, Friendly, and not so friendly, roles of Rac1 in islet β-cell function: lessons learnt from pharmacological and molecular biological approaches, Biochem. Pharmacol. 81 (2011) 965–975.

[23] I. Syed, B. Jayaram, W. Subasinghe, A. Kowluru, Tiam1/Rac1 signaling pathway mediates palmitate-induced, ceramide-sensitive generation of superoxides and lipid peroxides and the loss of mitochondrial membrane potential in pancreatic beta-cells, Biochem. Pharmacol. 80 (2010) 874–883.

[24] V. Sidarala, R. Veluthakal, K. Syeda, A. Kowluru, EHT 1864, a small molecule inhibitor of Ras-related C3 botulinum toxin substrate 1 (Rac1), attenuates glucose-stimulated insulin secretion in pancreatic β-cells, Cell. Signal. 27 (2015) 1159–1167.

[25] L. Désiré, J. Bourdin, N. Loiseau, H. Peillon, V. Picard, C. De Oliveira, et al., RAC1 inhibition targets amyloid precursor protein processing by gamma-secretase and decreases Abeta production in vitro and in vivo, J. Biol. Chem. 280 (2005) 37516–37525.

[26] W. Subasinghe, I. Syed, A. Kowluru, Phagocyte like NADPH oxidase promotes cytokine-induced mitochondrial dysfunction in pancreatic β-cells: evidence for regulation by Rac1, Am. J. Physiol. Regul. Integr. Comp. Physiol. 300 (2011) R12–R20.

[27] A.M. Mohammed, F. Chen, A. Kowluru, The two faces of protein palmitoylation in islet β-cell function: potential implications in the pathophysiology of islet metabolic dysregulation and diabetes, Recent Pat. Endocr. Metab. Immune Drug Discov. 7 (2013) 203–212.

[28] B. Jayaram, I. Syed, A. Singh, W. Subasinghe, C.N. Kyathanahalli, A. Kowluru, Isoprenylcysteine carboxyl methyltransferase facilitates glucose-induced Rac1 activation, ROS generation and insulin secretion in INS 832/13 β-cells, Islets 3 (2011) 48–57.

[29] R. Veluthakal, H. Kaur, M. Goalstone, A. Kowluru, Dominant negative α-subunit of farnesyl- and geranyl geranyltransferase inhibits glucose-stimulated, but not KCl-stimulated, insulin secretion in INS 832/13 cells, Diabetes 56 (2007) 204–210.

[30] A. Kowluru, S.E. Seavey, G. Li, R.L. Sorenson, A.J. Weinhaus, R. Nesher, et al., Glucose- and GTP-dependent stimulation of the carboxyl methylation of CDC42 in rodent and human pancreatic islets and pure beta cells: evidence for an essential role of GTP-binding proteins in nutrient-induced insulin secretion, J. Clin. Invest. 98 (1996) 540–555.

[31] H. Yuan, Y. Lu, X. Huang, Q. He, Y. Man, Y. Zhou, et al., Suppression of NADPH oxidase 2 substantially restores glucose-induced dysfunction of pancreatic NIT-1 cells, FEBS J. 277 (2010) 5061–5071.

[32] D.K. Arora, D. Machhadieh, A. Matti, B.E. Wadzinski, S. Ramanadham, A. Kowluru, High glucose exposure promotes activation of protein phosphatase 2A in rodent islets and INS-1 832/13 β-cells by increasing the posttranslational carboxylmethylation of its catalytic subunit, Endocrinology 155 (2014) 380–391.

[33] S. Khadija, V. Veluthakal, A. Kowluru, Glucotoxic and diabetic conditions induce caspase 6-mediated degradation of nuclear lamin A in human islets, rodent islets and INS-1 832/13 cells, Apoptosis 19 (2014) 1691–1701.

[34] A.M. Mohammed, A. Kowluru, Activation of apocynin-sensitive NADPH oxidase (Nox2) activity in INS-1 832/13 cells under glucotoxic conditions, Islets 5 (2013) 129–131.

[35] D. Morgan, E. Rebelato, F. Abdulkader, M.F. Graciano, H.R. Oliveira-Emilio, A.E. Hirata, et al., Association of NAD(P)H oxidase with glucose-induced insulin secretion by pancreatic beta-cells, Endocrinology 150 (2009) 2197–2201.

[36] F.E. Rey, M.E. Cifuentes, A. Kiarash, M.T. Quinn, P.J. Pagano, Novel competitive inhibitor of NAD(P)H oxidase assembly attenuates vascular O(2)(−) and systolic blood pressure in mice, Circ. Res. 89 (2001) 408–414.

[37] R.A. Kowluru, A. Kowluru, R. Veluthakal, G. Mohammad, I. Syed, J.M. Santos, et al., TIAM1-RAC1 signalling axis-mediated activation of NADPH oxidase-2 initiates mitochondrial damage in the development of diabetic retinopathy, Diabetologia 57 (2014) 1047–1056.

[38] E. Shen, Y. Li, Y. Li, L. Shan, H. Zhu, Q. Feng, et al., Rac1 is required for cardiomyocyte apoptosis during hyperglycemia, Diabetes 58 (2009) 2386–2395.

[39] Y. Liu, C. Collins, W.B. Kiosses, A.M. Murray, M. Joshi, T.R. Shepherd, et al., A novel pathway spatiotemporally activates Rac1 and redox signaling in response to fluid shear stress, J. Cell Biol. 201 (2013) 863–873.

[40] O.M. Khan, M.X. Ibrahim, I.M. Jonsson, C. Karlsson, M. Liu, A.K. Sjogren, et al., Geranylgeranyltransferase type I (GGTase-I) deficiency hyperactivates macrophages and induces erosive arthritis in mice, J. Clin. Invest. 121 (2011) 628–639.

[41] I. Navarro-Lérida, S. Sánchez-Perales, M. Calvo, C. Rentero, Y. Zheng, C. Enrich, et al., A palmitoylation switch mechanism regulates Rac1 function and membrane organization, EMBO J. 31 (2012) 534–551.
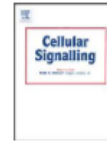
APPENDIX B

EHT 1864, a small molecule inhibitor of Ras-related C3 botulinum toxin substrate 1 (Rac1), attenuates glucose-stimulated insulin secretion in pancreatic β-cells

Vaibhav Sidarala, Rajakrishnan Veluthakal, Khadija Syeda, Anjaneyulu Kowluru *

John D. Dingell VA Medical Center, Detroit, MI 48201, USA
Department of Pharmaceutical Sciences, Eugene Applebaum College of Pharmacy and Health Sciences, Wayne State University, Detroit, MI 48201, USA

ABSTRACT

Glucose-stimulated insulin secretion (GSIS) in the pancreatic β-cells entails a variety of signaling mechanisms including activation of small GTP-binding proteins (G-proteins). Previous studies from our laboratory in human islets, rodent islets and clonal β-cells have demonstrated that G-proteins (e.g., Arf6, Cdc42 and Rac1) play novel roles in cytoskeletal remodeling, which is a critical step in the trafficking of insulin-laden secretory granules for fusion with plasma membrane and release of insulin. To further understand regulatory roles of Rac1 in GSIS, we utilized, herein, EHT 1864, a small molecule inhibitor, which attenuates Rac1 activation by retaining the G-protein in an inert/inactive state, thereby preventing activation of its downstream effector proteins. We demonstrate that EHT 1864 markedly attenuated GSIS in INS-1 832/13 cells. In addition, EHT 1864 significantly reduced glucose-induced activation and membrane targeting of Rac1 in INS-1 832/13 cells. This Rac1 inhibitor also suppressed glucose-induced activation of ERK1/2 and p53, but not Akt. Lastly, unlike the inhibitors of protein prenylation (simvastatin), EHT 1864 did not exert any significant effects on cell morphology (cell rounding) under the conditions it attenuated Rac1-sensitive signaling steps leading to GSIS. Based on these findings, we conclude that EHT 1864 specifically inhibits glucose-induced Rac1 activation and membrane association and associated downstream signaling events culminating in inhibition of GSIS.

Published by Elsevier Inc.

1. Introduction

It is well established that glucose-stimulated insulin secretion (GSIS) from the islet β-cell involves an interplay between a wide range of metabolic events and signal transduction pathways leading to the generation of second messenger molecules (cyclic nucleotides, adenine and guanine nucleotides and soluble second messengers) and mobilization of calcium ions [1–4]. Consequently, insulin-laden secretory granules are transported from distal sites to the plasma membrane for fusion and release of cargo into the circulation. Several lines of evidence suggest critical regulatory roles for small GTP-binding proteins (G-proteins; e.g., Cdc42 and Rac1) in the translocation of secretory vesicles to the plasma membrane [5,6]. In this context, recent studies have

demonstrated regulation of GSIS by small G-proteins including Arf6, Cdc42 and Rac1 [7–14]. Evidence from knockout animal models further affirms key functions of these signaling proteins (Rac1) in physiological insulin secretion [15].

Several mechanisms have been put forth for the regulation of small G-protein function, including post-translational modifications (e.g., prenylation, carboxylmethylation and acylation). These modifications are felt to increase the hydrophobicity of the target proteins thus rendering optimal membrane association [6,12]. Previous studies from our laboratory have demonstrated the requisite nature of these modification steps in GSIS. For example, using specific inhibitors of geranylgeranylation (e.g., GGTI-2147 and GGTI-2368), we reported significant inhibition of GSIS in clonal β-cells and normal rodent islets [6,14]. Specific inhibitors of the carboxylmethylation of G-proteins (e.g., acetyl farnesyl cysteine) have also been shown to suppress GSIS in pancreatic β-cells [13,16,17]. Lastly, selective inhibitors of protein palmitoylation (e.g., cerulenin) also inhibit GSIS [13,18]. These findings were further confirmed via the use of dominant negative mutants or siRNAs of the subunits of prenyltransferases [14] and carboxylmethyltransferases [17]. In addition, we have demonstrated that inhibition of Tiam1, a guanine nucleotide exchange factor (GEF) for Rac1, leads to inhibition of GSIS in insulin-secreting cells [9]. Together, the aforementioned observations implicate roles for small G-proteins (Rac1) in physiological insulin secretion.

V. Sidarala et al. / Cellular Signalling 27 (2015) 1159–1167

Désiré et al. [19] have developed a small molecular weight (~582) inhibitor EHT 1864 [5-(5-(7-(trifluoromethyl) quinolin-4-ylthio) pentyloxy)-2-(morpholinomethyl)-4H-pyran-4-one dihydrochloride; Fig. 1], which inhibited Rac1 function in vivo. Further characterization of EHT 1864 by Shutes et al. [20] suggested that EHT 1864 binds to Rac1 with high affinity, compared to GDP/GTP, and retains Rac1 in an inert and inactive state by displacement of pre-bound guanine nucleotide (GDP/GTP). Several recent studies have utilized EHT 1864 to deduce cellular roles of Rac1 function in health and disease [21–25]. Its unique inhibitory properties on Rac1 function have prompted us to undertake the current study to assess the roles of Rac1 in islet function and insulin secretion. Our findings suggest that EHT 1864 inhibits glucose-induced Rac1 activation and membrane targeting and associated signaling events (e.g., ERK1/2 and p53 activation) culminating in inhibition of GSIS.

2. Materials and methods

2.1. Materials

EHT 1864 and PD0325901 were obtained from R&D systems (Minneapolis, MN). Simvastatin was from Sigma (St. Louis, MO). The rat insulin ELISA kit was purchased from American Laboratory Products Co (Windham, NH). Rac1 activation G-LISA kit was from Cytoskeleton Inc. (Denver, CO). Antibodies against phospho-p44/42 ERK1/2 (Thr202/Tyr204), total p44/42 ERK1/2, phospho-Akt (Ser473), total Akt, phospho-p53 (Ser15) and E-Cadherin were obtained from Cell Signaling Technology (Danvers, MA). Antisera directed against GAPDH and total p53 were from Santa Cruz Biotechnology (Santa Cruz, CA). Mouse monoclonal antibody directed against Rac1 was purchased from BD Bioscience (San Jose, CA).

2.2. GSIS and KSIS from INS-1 832/13 cells

INS-1 832/13 cells (seeded at a density of 2.5×10^5 cells per well in a 24 well plate) were cultured in RPMI media overnight in the presence of 2.5 mM glucose and 2.5% fetal bovine serum. After pre-incubation at varying concentrations of EHT 1864 (0–10 μM) for 1 h, cells were further incubated in the presence of low (2.5 mM) or varying concentrations of glucose (2.5–20 mM) or KCl (40 mM) for 30 min at 37 °C in the continuous absence or presence of EHT 1864 at concentrations indicated in the text. The supernatant was then removed, centrifuged at 300 g for 10 min, and the amount of insulin released was quantified by ELISA as we described previously [10,26].

2.3. Rac1 activation assay

INS-1 832/13 cells were cultured in RPMI media overnight in the presence of 2.5 mM glucose and 2.5% fetal bovine serum. After pre-incubation with EHT 1864 (10 μM) for 1 h, cells were incubated with low (2.5 mM) or high glucose (20 mM) for 20 min at 37 °C in the continuous absence or presence of EHT 1864. Rac1 activation was quantified using a G-LISA kit as described in [27].

2.4. Subcellular fractionation and phase partitioning using Triton X-114

INS-1 832/13 cells were cultured in RPMI media overnight in the presence of 2.5 mM glucose and 2.5% fetal bovine serum. After pre-incubation with EHT 1864 (10 μM) for 1 h, cells were treated with low (2.5 mM) or high glucose (20 mM) in the continuous absence or presence of EHT 1864 for 20 min. Cell lysates were homogenized in a homogenization buffer (20 mM Tris–HCl, pH 7.5, 0.5 mM EGTA, 2 mM MgCl₂ and protease inhibitor cocktail) and subjected to a single-step centrifugation at 100,000 g for 60 min at 4 °C. Total membrane (pellet) and soluble (supernatant) fractions were separated. Hydrophilic and hydrophobic phases of the total membrane fractions were isolated using Triton X-114 as we described earlier [28]. Relative abundance of Rac1 in cytosol and each of the individual hydrophilic and hydrophobic phases derived from the membranous fractions was determined by Western blotting. Additionally, the relative purity of these fractions was verified by probing for marker proteins such as GAPDH (a marker for the cytosolic fraction) and E-Cadherin (a marker for membrane fraction).

2.5. Western blotting

INS-1 832/13 cells were cultured in RPMI media overnight in the presence of 2.5 mM glucose and 2.5% fetal bovine serum. After pre-incubation with EHT 1864 (10 μM) or PD0325901 (1 μM) for 1 h, cells were treated with low (2.5 mM) or high glucose (20 mM) in the continuous absence or presence of EHT 1864 or PD0325901 for 30 min. Cell lysates were separated by SDS-PAGE on 10% (w/v) polyacrylamide gels and electrotransferred to nitrocellulose membrane. The membranes were then blocked with 0.1% Casein in 0.2× PBS for 1 h at room temperature. Blots were then incubated overnight at 4 °C with appropriate primary antibody (Rac1, phospho-ERK1/2 (Thr202/Tyr204), total-ERK1/2, phospho-Akt (Ser473), total Akt, phospho-p53 (Ser15), E-Cadherin and GAPDH) in 0.2× PBS-T containing 0.1% Casein. The membranes were washed 5× for 5 min each with PBS-T and probed with appropriate IRDye® 800CW secondary antibody in 0.1% casein in PBS-T at room temperature for 1 h. After washing, the immune complexes comprised of the target proteins were detected under Odyssey® Imaging Systems.

2.6. Changes in β-cell morphology following inhibition of protein prenylation and Rac1 activation

To observe the effects of EHT 1864 on cell morphology, INS-1 832/13 cells were incubated overnight, in a 6-well plate, with RPMI (2.5 mM glucose and 2.5% fetal bovine serum) in the presence of diluent (de-ionized water) or simvastatin (30 μM). Cells were also incubated with EHT 1864 (10 μM) for 1 h following overnight incubation in RPMI with 2.5 mM
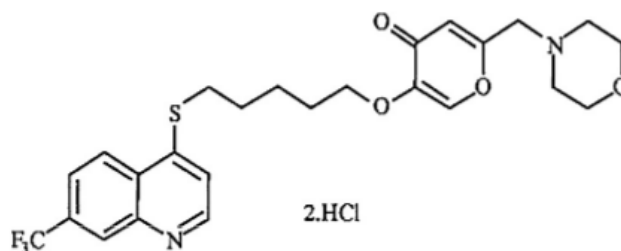

Fig. 1. Structure of EHT 1864. Chemical structure of EHT 1864 is provided here.

www.manaraa.com

glucose and 2.5% fetal bovine serum. Changes in cell morphology were then quantified visually under an Olympus IX71 microscope.

2.7. Statistical analysis of experimental data

The statistical significance of the differences between the experimental conditions was determined by ANOVA. p values <0.05 were considered significant.

3. Results

3.1. EHT 1864 inhibits GSIS in INS-1 832/13 cells

At the outset, we quantified the effects of EHT 1864 on GSIS from INS-1 832/13 cells. Data depicted in Fig. 2 demonstrate a modest (−13%; not significant) inhibition of GSIS following incubation with EHT 1864 at 5 μM concentration. Furthermore, we noticed a complete inhibition of GSIS by EHT 1864 at 10 μM concentration. It should also be noted that, while 5 μM EHT 1864 exerted no significant effects on basal secretion, it did modestly increase the basal secretion at 10 μM concentration (−50%). Therefore, in all the subsequent experiments, we studied the effects of EHT 1864 at 10 μM. Furthermore, EHT 1864 inhibited GSIS in INS-1 832/13 cells elicited at 10–20 mM glucose (Fig. 3). Compatible with findings reported in Fig. 2, a significant increase in insulin secretion was also noted in cells incubated with this inhibitor at 5 mM glucose concentration. Together, data depicted in Figs. 2 and 3 demonstrate significant inhibitory effects of EHT 1864 on GSIS in INS-1 832/13 cells.

3.2. EHT 1864 inhibits glucose-induced Rac1 activation in INS-1 832/13 cells

As stated above, several previous studies have demonstrated requisite roles for Rac1 activation in GSIS. Therefore, we asked if EHT 1864 inhibits glucose-induced Rac1 activation under conditions it inhibited insulin secretion. To test this, INS-1 832/13 cells were incubated in the absence or presence of EHT 1864 and glucose-induced activation of

Rac1 was quantified. Data in Fig. 4 suggested a significant increase in the activation of Rac1 (GTP-bound conformation) by stimulatory glucose (bar 1 vs. 3), which was inhibited by EHT 1864 (bar 3 vs. bar 4). Interestingly, EHT 1864 modestly increased Rac1 activation in the presence of basal glucose (2.5 mM; bar 1 vs. bar 2), but such an activation was not statistically significant. Taken together, these findings indicate that EHT 1864 inhibits glucose-induced Rac1 activation (Fig. 4) resulting in inhibition of GSIS (Figs. 2 and 3).

Fig. 3. Effect of EHT 1864 on insulin secretion at different glucose concentrations in INS-1 832/13 cells. INS-1 832/13 cells were cultured in RPMI media overnight in the presence of 2.5 mM glucose and 2.5% fetal bovine serum. After pre-incubation with EHT 1864 (10 μM) for 1 h, cells were incubated in the presence of different concentrations of glucose (0–20 mM) in the continuous absence or presence of EHT 1864 for 30 min at 37 °C. The amount of insulin released was quantified by ELISA. The data was expressed as ng/ml ± SEM. * $p < 0.05$ vs. 10 mM or 20 mM glucose and ** $p < 0.05$ vs. 5 mM glucose.

Fig. 2. EHT 1864 inhibits GSIS in INS-1 832/13 cells. INS-1 832/13 cells were cultured in RPMI media overnight in the presence of 2.5 mM glucose and 2.5% fetal bovine serum. After pre-incubation with EHT 1864 (0–10 μM) for 1 h, cells were incubated in the presence of low (2.5 mM) or high glucose (20 mM) in the continuous absence or presence of EHT 1864 for 30 min at 37 °C. Insulin released into the medium was quantified by ELISA. The data was expressed as ng/ml of insulin released ± SEM. * $p < 0.05$ vs. 2.5 mM glucose and ** $p < 0.05$ vs. 20 mM glucose alone or in the presence of 5 μM of EHT 1864.
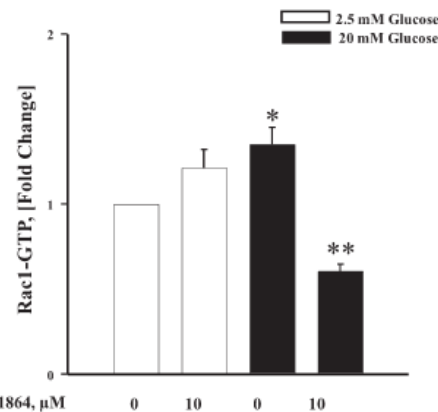
Fig. 4. EHT 1864 significantly inhibits glucose-induced Rac1 activation in INS-1 832/13 cells. INS-1 832/13 cells were incubated in RPMI media overnight in the presence of 2.5 mM glucose and 2.5% fetal bovine serum. After pre-incubation with EHT 1864 (10 μM) for 1 h, cells were incubated in the presence of low (2.5 mM) or high glucose (20 mM) in the continuous absence or presence of EHT 1864 for 20 min at 37 °C. Rac1 activation was quantified by G-LISA method. Data are expressed as fold increase over 2.5 mM glucose, and are mean ± SEM. * $p < 0.05$ vs. 2.5 mM glucose and ** $p < 0.05$ vs. 20 mM glucose.
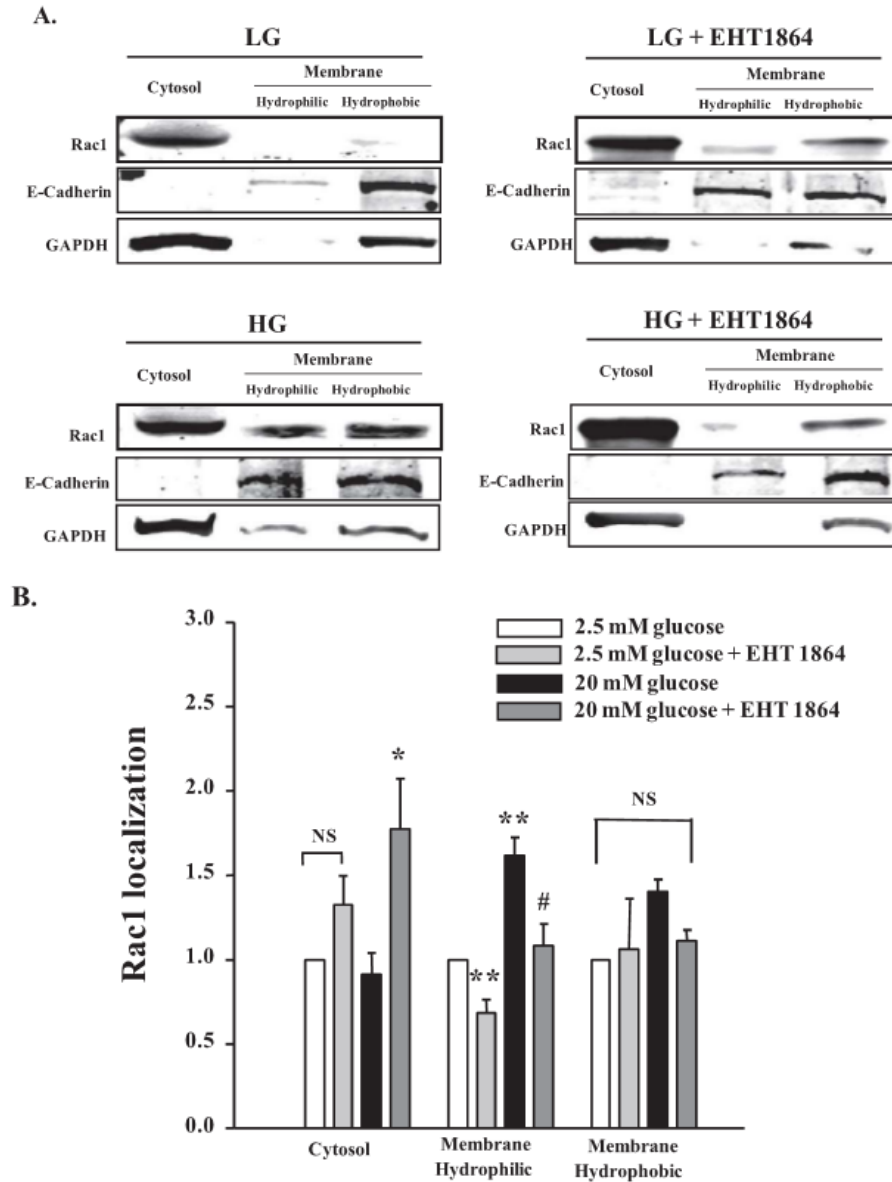
Fig. 5. EHT 1864 significantly inhibits glucose-induced membrane targeting of Rac1. INS-1 832/13 cells were incubated in RPMI media overnight in the presence of 2.5 mM glucose and 2.5% fetal bovine serum. After pre-incubation with EHT 1864 (10 µM) for 1 h, cells were stimulated with low (2.5 mM) or high glucose (20 mM) in the continuous absence or presence of EHT 1864 for 20 min at 37 °C. Cells were then lysed and subjected to phase partitioning with Triton X-114, to obtain cytosolic and hydrophilic/hydrophobic fractions of the membrane. Rac1 localization in these fractions was determined by Western blotting, and a representative blot from three independent experiments is provided (A). The relative purity of cytosolic and hydrophilic/hydrophobic membrane fractions was verified by probing for GAPDH (cytosol) and E-Cadherin (Membrane). Rac1 band intensities were then quantified by densitometry (B). Data represent mean ± SEM from three independent experiments, and expressed as fold change over 2.5 mM glucose for each cell fraction. * $p < 0.05$ vs. 2.5 mM glucose-cytosol. ** $p < 0.05$ vs. 2.5 mM glucose-membrane hydrophilic. # $p < 0.05$ vs. 20 mM glucose-membrane hydrophilic. NS: not significant.

3.3. EHT 1864 inhibits glucose-induced membrane association of Rac1 in INS-1 832/13 cells

Published evidence, including our own in pancreatic β-cells, supports the notion that activation and membrane association of small G-proteins (Cdc42 and Rac1) are necessary for optimal interaction of

these proteins with their effector proteins [5,6]. Therefore, in the next series of experiments, we determined if glucose-induced membrane targeting is inhibited by EHT 1864 in INS-1 832/13 cells. To address this, the hydrophilic and hydrophobic compartments of the membrane fraction were isolated from cells exposed to basal or stimulatory glucose concentrations, incubated in the absence or presence of EHT 1864, by Triton X-114 phase extraction method (see Section 2.4 for additional details). Relative abundance of Rac1 in the cytosolic and hydrophilic and hydrophobic compartments of the membrane fraction (above) was determined by Western blotting. As stated above, purity of the total soluble (cytosolic fraction) and the membrane fraction was assessed by marker proteins for these fractions. Data shown in Fig. 5 (Panel A) indicate that Rac1 is predominantly localized in the cytosolic fraction under basal conditions. Treatment of these cells with EHT 1864 modestly increased the association of Rac1 with the hydrophobic fraction. As has been shown previously, a significant amount of Rac1 translocated to the hydrophobic and hydrophilic compartments from cells incubated with stimulatory glucose. Coprovision of EHT 1864 to these cells significantly inhibited glucose-induced translocation of Rac1 to the membrane fraction. Pooled data from multiple studies are provided in Panel B of Fig. 5. These data indicate that glucose-induced activation and membrane association of Rac1 are prevented by EHT 1864 leading to inhibition of GSIS.

3.4. EHT 1864 inhibits glucose-induced ERK1/2 phosphorylation and activation in INS-1 832/13 cells

Recent evidence from our laboratory [26] and the Thurmond's laboratory [29] implicated ERK1/2 activation as key to cytoskeletal re-modeling, which is requisite for GSIS. Further, these studies suggested key regulatory roles for this signaling step in G-protein (Cdc42 and Rac1)-mediated insulin secretion in glucose-stimulated β-cell. Therefore, we quantified glucose-induced ERK1/2 phosphorylation in INS-1 832/13 cells following exposure to EHT 1864. At the outset, we assessed glucose-induced activation of ERK1/2 phosphorylation in the presence of PD0325901, a known inhibitor of MEK. Data in Fig. 6 (Panel A) indicate complete inhibition by MEK inhibitor of glucose-induced phosphorylation of ERK1/2 in INS-1 832/13 cells. Data from multiple studies demonstrating inhibitory effects of PD 0325901 are provided in Fig. 6 (Panel B). It is noteworthy that data depicted in Fig. 6 (Panel C) demonstrate no significant effects of EHT 1864 on ERK1/2 phosphorylation under basal glucose conditions. However, a marked inhibition of high glucose-induced ERK1/2 phosphorylation was demonstrable in INS-1 832/13 cells exposed to EHT 1864. Pooled data from multiple studies are provided in Panel D of Fig. 6. Based on the findings described above, we conclude that EHT 1864 efficiently inhibits glucose-induced ERK1/2 and Rac1 activation and its membrane association culminating in inhibition of GSIS.

We next assessed if inhibition of glucose-induced Rac1 activation by EHT 1864 results in inhibition of other downstream signaling pathways involved in islet β-cell function. Data depicted in Fig. 7 (Panel A) indicate a significant increase in the phosphorylation of Akt in INS 1-832/13 cells following exposure to stimulatory glucose. Interestingly, glucose-induced Akt phosphorylation was resistant to Rac1 inhibition by EHT 1864. Data from multiple experiments (Fig. 7; Panel
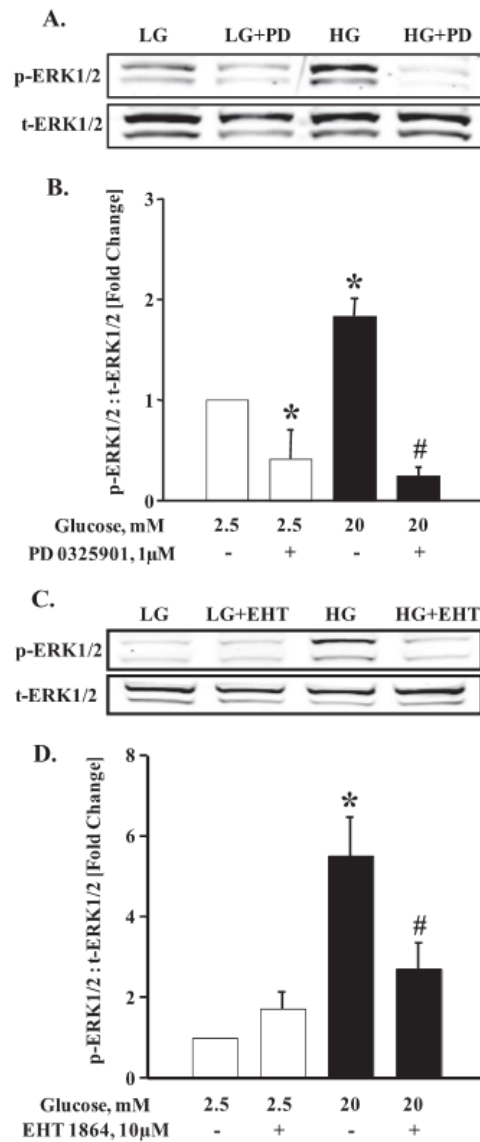
Fig. 6. Glucose-induced ERK1/2 activation is inhibited by PD 0325901 and EHT 1864. INS-1 832/13 cells were starved in RPMI media overnight in the presence of 2.5 mM glucose and 2.5% fetal bovine serum. After pre-incubation with PD 0325901 (1 μM) or EHT 1864 (10 μM) for 1 h, cells were stimulated with low (2.5 mM) or high glucose (20 mM) in the continuous absence or presence of PD 0325901 or EHT 1864 for 30 min at 37 °C. Cell lysate proteins were separated by SDS-PAGE, and then transferred onto a nitrocellulose membrane. The membranes were then blocked and probed with anti-phosphorylated ERK1/2 followed by incubation with anti-rabbit secondary antibody. The same blots were stripped and re-probed with anti-total ERK1/2 (A, C). Band intensities of phospho-ERK1/2 and total-ERK1/2 were quantified by densitometric analysis (B, D). Results are shown as mean ± SEM from three independent experiments and expressed as fold change in the ratios between phospho-ERK1/2 and total-ERK1/2. * $p < 0.05$ vs. 2.5 mM glucose alone or in presence of EHT 1864. # $p < 0.05$ vs. 20 mM glucose.

A.

| | LG | LG+EHT | HG | HG+EHT |

p-Akt

t-Akt

B.

p-Akt : t-Akt [Fold Change]

| Glucose, mM | 2.5 | 2.5 | 20 | 20 |
| EHT 1864, 10 μM | - | + | - | + |

C.

| | LG | LG+EHT | HG | HG+EHT |

p-p53

Actin

D.

p-p53 : Actin [Fold Change]

| Glucose, mM | 2.5 | 2.5 | 20 | 20 |
| EHT 1864, 10 μM | - | + | - | + |
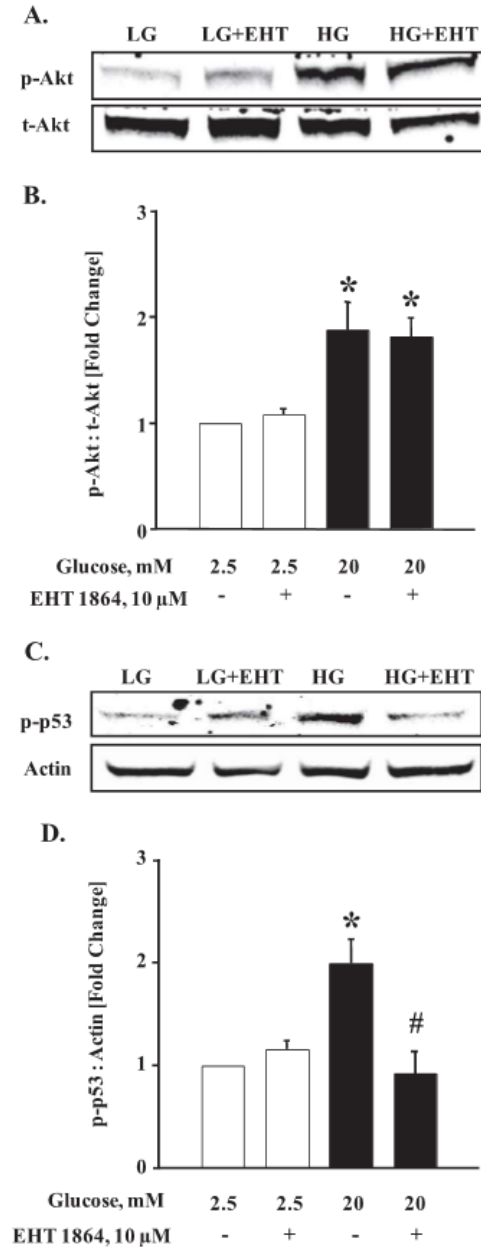
B) suggest that glucose-induced phosphorylation and activation of Akt does not require Rac1 activation signaling step. It is noteworthy, however, that p53 phosphorylation is significantly augmented by glucose in INS 1-832/13 cells (Fig. 7; Panel C), which was abolished by EHT 1864-mediated inhibition of Rac1 (Fig. 7; Panel C and D). Taken together, data in Figs. 6 and 7 suggest specific roles of glucose-induced Rac1 activation in mediating downstream signaling steps (see Section 4).

3.5. EHT 1864 elicits minimal effects on cell morphology under conditions it inhibits GSIS: evidence for a lack of involvement of protein prenylation in the inhibitory effects of EHT 1864

Previous investigations from our laboratory have demonstrated that post-translational prenylation of small G-proteins is necessary for membrane targeting and effector activation in the pancreatic β-cell [6,12]. It has also been suggested that inhibition of small G-protein function results in alterations in cell morphology (cell rounding) following inhibition of protein prenylation [6,12]. Herein, we investigated if EHT 1864 elicits changes on cell morphology under conditions it inhibits ERK1/2-Rac1 activation and GSIS. To address this, we incubated INS-1 832/13 cells in the absence or presence of EHT 1864 and examined alterations in cell morphology by phase contrast microscopy. As a positive control, INS-1 832/13 cells were cultured in the presence of simvastatin, a known inhibitor of mevalonic acid, a precursor for farnesyl and geranylgeranyl pyrophosphates [6,12]. Data shown in Fig. 8 demonstrate significant cell rounding in INS-1 832/13 cells incubated in the presence of simvastatin (~57% of cells), but not in the presence of the diluent (~3% cells). However, incubation of these cells with EHT 1864, under conditions it inhibited cellular signaling events (ERK1/2 and Rac1 activation), led to no significant abnormalities in cell morphology (~3% of cells; Fig. 8). These data indicate that EHT 1864 attenuates ERK1/2 and Rac1 activation and insulin secretion without exerting significant effects on cellular events leading to abnormal cell morphology.

3.6. In contrast to GSIS, KCl-stimulated insulin secretion (KSIS) is augmented by EHT 1864

Previous observations from the laboratories of Thurmond [5,7,8], Kowluru [6,14,28] and Asahara [15] have demonstrated that insulin secretion elicited by a membrane depolarizing concentration of KCl (KSIS) is resistant to Rac1 inhibition. In the last set of experiments, we quantified KSIS in INS-1 832/13 cells following exposure to EHT 1864 (5 or 10 μM). Interestingly, in contrast to GSIS, insulin secretion elicited by KCl was potentiated significantly by EHT 1864 (Fig. 9). Such potentiating effects were more pronounced at 10 μM EHT 1864. These data raise an interesting possibility that Rac1 might mediate additional calcium-regulated signaling pathways, which are inhibitory to exocytotic secretion of insulin (see Section 4).

4. Discussion

The overall objective of this study was to further assess the role of Rac1 in the cascade of events leading to GSIS. To address this, we

Fig. 7. EHT 1864 significantly inhibited glucose-induced p53 phosphorylation but had no effect on phosphorylation of Akt: INS-1 832/13 cells were starved overnight in RPMI media supplemented with 2.5 mM glucose and 2.5% fetal bovine serum. After pre-incubation with EHT 1864 (10 μM), cells were further stimulated with low (2.5 mM) or high glucose (20 mM) in the continuous absence or presence of EHT 1864 for 30 min at 37 °C. Cells were then lysed and lysate proteins were separated by SDS-PAGE. Proteins were then transferred onto a nitrocellulose membrane, blocked and probed with antibody directed against phospho-Akt or phospho-p53. The membranes were then incubated with anti-rabbit secondary antibody. After detection, the same blots were stripped and re-probed with antibody directed against total-Akt or Actin (A, C). Band intensities were quantified by densitometric analysis (B, D). Results are shown as mean ± SEM from three independent experiments and expressed as fold change in the ratios between phospho-Akt and total-Akt or phospho-p53 and Actin. * $p < 0.05$ vs. 2.5 mM glucose alone or in presence of EHT 1864. # $p < 0.05$ vs. 20 mM glucose.
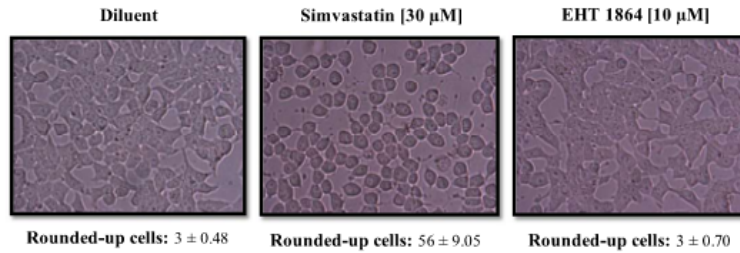
Diluent	Simvastatin [30 µM]	EHT 1864 [10 µM]
Rounded-up cells: 3 ± 0.48	Rounded-up cells: 56 ± 9.05	Rounded-up cells: 3 ± 0.70

Fig. 8. EHT 1864 had no effect on INS-1 832/13 cell morphology. INS-1 832/13 cells were cultured overnight with RPMI (2.5 mM glucose and 2.5% fetal bovine serum) in the presence of diluent (de-ionized water) or Simvastatin (30 µM). The cells were also incubated with EHT 1864 (10 µM) for 1 h after overnight incubation in RPMI with 2.5 mM glucose and 2.5% fetal bovine serum. The cells were then visualized under the microscope to observe changes in morphology. Alterations in cell morphology were quantified by counting cells with morphological abnormalities (rounded-up cells), in the selected areas (0.5 cm²) and expressed as mean ± SEM (n = 6).

employed EHT 1864, a novel small molecule inhibitor, which attenuates Rac1 activation by retaining it in its inert and inactive conformation via inhibition of its association with guanine nucleotides. This class of inhibitors has not been tested before in the islet β-cell. Our findings indicate that EHT 1864 inhibits glucose-induced activation and membrane targeting of Rac1 and associated signaling steps, including ERK1/2, which has been shown to control cytoskeletal remodeling and insulin exocytosis [26,29]. Compatible with these findings, we also observed significant inhibition of GSIS by EHT 1864 in INS-1 832/13 cells. Our findings also suggest no morphological changes in pancreatic β-cells incubated with EHT 1864 at least under conditions it suppressed glucose-sensitive signaling events. Thus, our findings provide the first evidence that inhibition of guanine nucleotide association on Rac1 GTPase impedes activation of key signaling steps necessary for the stimulus-secretion coupling of GSIS.

We demonstrated herein that glucose-induced ERK1/2 activation is inhibited by EHT 1864, thus establishing a link between Rac1 activation and ERK1/2 activation. These findings are supported by two recent studies that investigated regulatory roles of Raf-1 and ERK1/2 in glucose-induced cytoskeletal remodeling. First, using pharmacological approaches, Kalwat and associates demonstrated that glucose-induced activation of Cdc42 promotes activation of a signaling cascade involving activation of PAK1 → Raf-1 → MEK1/2 → ERK1/2 to facilitate F-actin remodeling and insulin secretion [29]. Second, studies from our laboratory suggested that a protein farnesylation step is necessary for glucose-induced activation of Raf-1 → ERK1/2 to promote Rac1 activation [26]. Together, data from the above and current studies place ERK1/2 as one of the key signaling steps in Cdc42/Rac1-mediated insulin secretion in the pancreatic β-cell. It should be noted that other downstream signaling steps involved in GSIS are also under the direct control of Rac1 since we observed in the current studies that glucose-induced phosphorylation of p53, but not Akt, was inhibited by EHT 1864. This will
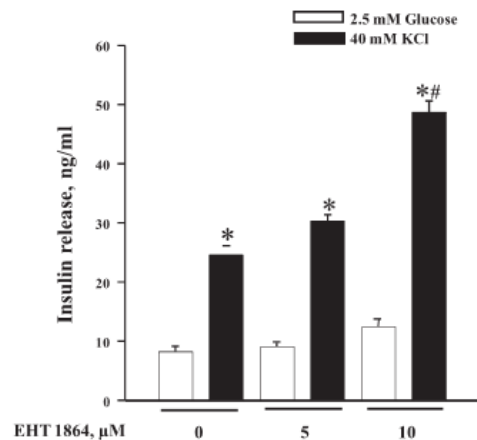
Fig. 9. EHT 1864 potentiates KSIS in INS-1 832/13 cells. INS-1 832/13 cells were cultured in RPMI media overnight in the presence of 2.5 mM glucose and 2.5% fetal bovine serum. After pre-incubation with EHT 1864 (0–10 µM) for 1 h, cells were incubated in the presence of low glucose (2.5 mM) or KCl (40 mM) in the continuous absence or presence of EHT 1864 for 30 min at 37 °C. The amount of insulin released was quantified by ELISA. The data was expressed as ng/ml of insulin released ± SEM and * p < 0.05 vs. 2.5 mM glucose, and # p < 0.05 vs. 40 mM KCl alone or in presence of 5 µM EHT 1864.
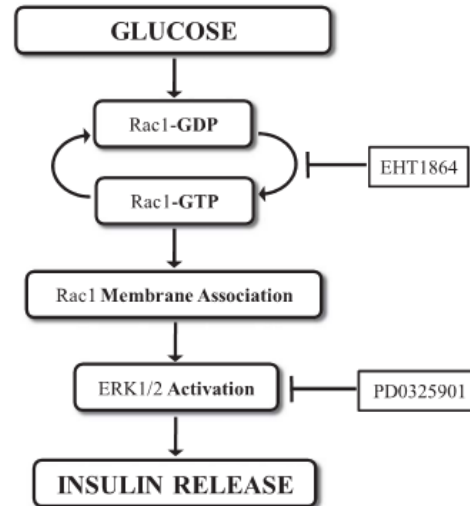
Fig. 10. Proposed model for glucose-stimulated insulin secretion via activation and membrane association of Rac1 and downstream activation of ERK1/2: We propose that acute exposure of INS-1 832/13 cells to stimulatory glucose (20 mM) results in the activation and membrane association of Rac1. This results in the activation of downstream effectors including ERK1/2, culminating in insulin release from the pancreatic β-cell. Our findings suggest that EHT 1864, a selective inhibitor of Rac1 activation, disrupts this signaling mechanism, thereby attenuating GSIS (see Section 4).

serve as one example, and it is likely that several downstream signaling pathways might be regulated by active Rac1. Future studies will address the identity of those signaling cascades.

We also noted no clear changes in the morphology in INS-1 832/13 cells following exposure to EHT 1864 under the conditions it abrogated glucose-mediated signaling events in these cells. Our findings of significant alterations (rounding) in cells exposed to inhibitors of protein prenylation (simvastatin) suggest that they induce significant defects in the actin cytoskeleton leading to alterations in cell morphology (current studies) and inhibition of GSIS as shown earlier [13,30]. It should be noted however that studies by Baier et al. [31] and Shutes et al. [20] demonstrated significant inhibitory effects of EHT 1864 on membrane ruffling in mast cells and lamellipodia formation in U87 MG glioblastoma cells. The observed differences between these studies and our current investigations may, in part, be due to differences in cell types studied and the concentrations of EHT 1864 employed (20 μM in mast cells and 5 μM in glioblastoma cells) [20,31].

It is noteworthy that while EHT 1864 inhibited GSIS at 5–10 μM concentrations (Fig. 2), higher concentrations of this inhibitor potentiated insulin release from INS-1 832/13 cells in the absence (basal) or glucose-stimulated conditions. For example, at 20 μM concentration, insulin secretion under basal conditions was increased from 8 ± 0.8 ng/ml to 15 ± 1.2 ng/ml in the absence or presence of EHT 1864, respectively ($n = 8$). Likewise, GSIS values in the absence and presence of EHT 1864 represented 26 ± 1.5 vs. 31.5 ± 1.7 ng/ml ($n = 8$). While potential mechanisms underlying stimulatory effects of this inhibitor on insulin secretion under basal and glucose stimulated conditions remain to be determined, we also observed in the current studies the potentiating effects of this inhibitor on KCl-induced insulin secretion (Fig. 9). These findings suggest that additional Rac1-dependent regulatory mechanisms might underlie potentiation of calcium-induced insulin secretion. For example, previous studies from our laboratory have demonstrated significant potentiation of GSIS from INS-1 832/13 cells following siRNA-mediated knockdown of Tiam1, a GEF for Rac1 [9]. We also demonstrated that such a potentiation of GSIS was sensitive to extracellular calcium [9]. It is also likely that calcium-induced insulin secretion is negatively regulated by Rac1 or its downstream signaling events, inhibition of which by EHT 1864 relieves such an effect thereby further stimulating the secretion. Future studies will address these questions, including regulation, by Rac1, of putative inhibitory G-proteins (G_{Ei}) that regulate exocytosis that we proposed previously [32].

It is becoming increasingly clear that Rac1 contributes significantly towards the pathology of many disease states including diabetes. For example, several recent studies in pancreatic β-cells, retinal endothelial cells, and cardiomyocytes have demonstrated key roles for Rac1 in the induction of oxidative stress under conditions of glucotoxicity and diabetes [33–36]. These studies also demonstrated that such an increase in oxidative stress is due to activation of phagocyte-like NADPH oxidase (Nox2), and Rac1 represents one of the members of the Nox2 holoenzyme [27,33–36]. Interestingly, data from in vitro and in vivo experiments suggested that inhibition of Tiam1, a GEF for Rac1 (using NSC23766), markedly prevented the damaging effects of glucotoxic and diabetic conditions [27,33–37]. These data suggested that GTP/GDP exchange on Rac1 by Tiam1 is critical for Nox2 activation. Future studies will determine if EHT 1864 can prevent effects of high glucose and diabetes by inhibiting the activation of Nox2 and its downstream signaling steps. In this context, recent investigations by Yoshida et al. [38] in cultured mesangial cells demonstrated significant inhibition of high glucose-induced Rac1 activation and mineralocorticoid receptor activation by over expression of dominant negative Rac1 or by coprovision of EHT 1864. Based on these observations, the authors concluded that Rac1 is a therapeutic target for the treatment of nephropathy in obesity-related diabetic population [38]. In addition, recent studies by Katz and associates, using EHT 1864, provided compelling evidence to implicate Rac1 as one of the key signaling proteins in the spread of

human breast cancer [24]. Thus, it appears that Rac1 activation contributes to the pathogenesis of several disease states.

5. Conclusion

In conclusion, we present the first evidence to suggest that EHT 1864, which inhibits Rac1 function *via* inhibition of guanine nucleotide association, impedes glucose-induced Rac1-mediated signaling events leading to inhibition of GSIS. Based on our current findings we present a model detailing our current understanding of the signaling pathways involved in glucose-mediated activation of Rac1 (Fig. 10). We propose that acute exposure of isolated β-cells to stimulatory glucose leads to the conversion of inactive (GDP-bound) Rac1 to its active configuration (GTP-bound) and targeting to the appropriate membranous compartment. Active Rac1 promotes phosphorylation of downstream signaling steps, including phosphorylation of ERK1/2 and p53. It appears that the stimulatory effects of GTP-bound Rac1 are specific, since phosphorylation of Akt was unaffected under conditions of Rac1 inhibition by EHT 1864. Studies are in progress to further determine the utility of this small molecule inhibitor in the prevention of metabolic dysfunction of the islet β-cell under conditions in in vitro and in vivo models of metabolic stress and diabetes.

References

[1] M. Prentki, F.M. Matschinsky, Physiol. Rev. 67 (1987) 1185–1248.
[2] M.J. MacDonald, Diabetes 39 (1990) 1461–1466.
[3] M. Komatsu, M. Takei, H. Ishii, Y. Sato, J. Diabetes Investig. 27 (2013) 511–516.
[4] S.N. Yang, Y. Shi, G. Yang, Y. Li, J. Yu, P.O. Berggren, Cell. Mol. Life Sci. 71 (2014) 4149–4177.
[5] Z. Wang, D.C. Thurmond, J. Cell Sci. 122 (2009) 893–903.
[6] A. Kowluru, Endocr. Rev. 31 (2010) 52–78.
[7] A.K. Nevins, D.C. Thurmond, Am. J. Physiol. Cell Physiol. 285 (2003) C698–C710.
[8] Z. Wang, E. Oh, D.C. Thurmond, J. Biol. Chem. 282 (2007) 9536–9546.
[9] R. Veluthakal, S.V. Madathilparambil, P. McDonald, L.K. Olson, A. Kowluru, Biochem. Pharmacol. 77 (2009) 101–113.
[10] B. Jayaram, I. Syed, C.N. Kyathanahalli, C.J. Rhodes, A. Kowluru, Biochem. Pharmacol. 81 (2011) 1016–1027.
[11] J.T. Lawrence, M.J. Birnbaum, Proc. Natl. Acad. Sci. U. S. A. 100 (2003) 13320–13325.
[12] A. Kowluru, Am. J. Physiol. Endocrinol. Metab. 285 (2003) E669–E684.
[13] S.A. Metz, M.E. Rabaglia, J.B. Stock, A. Kowluru, Biochem. J. 295 (1993) 31–40.
[14] R. Veluthakal, H. Kaur, M. Goalstone, A. Kowluru, Diabetes 56 (2007) 204–210.
[15] S. Asahara, Y. Shibutani, K. Teruyama, H.Y. Inoue, Y. Kawada, H. Etoh, T. Matsuda, M. Kimura-Koyanagi, N. Hashimoto, M. Sakahara, W. Fujimoto, H. Takahashi, S. Ueda, T. Hosooka, T. Satoh, H. Inoue, M. Matsumoto, A. Aiba, M. Kasuga, Y. Kido, Diabetologia 56 (2013) 1088–1097.
[16] A. Kowluru, S.E. Seavey, G. Li, R.L. Sorenson, A.J. Weinhaus, R. Nesher, M.E. Rabaglia, J. Vadakekalam, S.A. Metz, J. Clin. Invest. 98 (1996) 540–555.
[17] B. Jayaram, I. Syed, A. Singh, W. Subasinghe, C.N. Kyathanahalli, A. Kowluru, Islets 3 (2011) 48–57.
[18] A.M. Mohammed, F. Chen, A. Kowluru, Recent Pat. Endocr. Metab. Immune Drug Discov. 7 (2013) 203–212.
[19] L. Désiré, J. Bourdin, N. Loiseau, H. Peillon, V. Picard, C. De Oliveira, F. Bachelot, B. Leblond, T. Taverne, E. Beausoleil, S. Lacombe, D. Drouin, F. Schweighoffer, J. Biol. Chem. 280 (2005) 37516–37525.
[20] A. Shutes, C. Onesto, V. Picard, B. Leblond, F. Schweighoffer, C.J. Der, J. Biol. Chem. 282 (2007) 35666–35678.
[21] B.C. Dipaolo, N. Davidovich, M.G. Kazanietz, S.S. Margulies, Am. J. Physiol. Lung Cell. Mol. Physiol. 305 (2013) 141–153.
[22] L. Stefanini, Y. Boulaftali, T.D. Ouellette, M. Holinstat, L. Désiré, B. Leblond, P. Andre, P.B. Conley, W. Bergmeier, Arterioscler. Thromb. Vasc. Biol. 32 (2012) 434–441.
[23] F. Raynaud, E. Moutin, S. Schmidt, J. Dahl, F. Bertaso, T.M. Boeckers, V. Homburger, L. Fagni, J. Biol. Chem. 289 (2014) 2600–2609.

[24] E. Katz, A.H. Sims, D. Sproul, H. Caldwell, M.J. Dixon, R.R. Meehan, D.J. Harrison, Oncotarget 3 (2012) 608–619.
[25] C. Onesto, A. Shutes, V. Picard, F. Schweighoffer, C.J. Der, Methods Enzymol. 439 (2008) 111–129.
[26] A. Kowluru, R. Veluthakal, C.J. Rhodes, V. Kamath, I. Syed, B.J. Koch, Diabetes 59 (2010) 967–977.
[27] I. Syed, C.N. Kyathanahalli, B. Jayaram, S. Govind, C.J. Rhodes, R.A. Kowluru, A. Kowluru, Diabetes 60 (2011) 2843–2852.
[28] A. Kowluru, R. Veluthakal, Diabetes 54 (2005) 3523–3529.
[29] M.A. Kalwat, S.M. Yoder, Z. Wang, D.C. Thurmond, Biochem. Pharmacol. 85 (2013) 808–816.
[30] G. Li, R. Regazzi, E. Roche, C.B. Wollheim, Biochem. J. 289 (1993) 379–385.
[31] A. Baier, V.N. Ndoh, P. Lacy, G. Eitzen, J. Leukoc. Biol. 95 (2014) 763–774.
[32] A. Kowluru, S.A. Metz, Biochem. J. 297 (1994) 399–406.
[33] A. Kowluru, R.A. Kowluru, Biochem. Pharmacol. 88 (2014) 275–283.
[34] E. Shen, Y. Li, Y. Li, L. Shan, H. Zhu, Q. Feng, J.M. Arnold, T. Peng, Diabetes 58 (2009) 2386–2395.
[35] R.A. Kowluru, A. Kowluru, R. Veluthakal, G. Mohammad, I. Syed, J.M. Santos, M. Mishra, Diabetologia 57 (2014) 1047–1056.
[36] M.T. Elnakish, H.H. Hassanain, P.M. Janssen, M.G. Angelos, M. Khan, J. Pathol. 231 (2013) 290–300.
[37] A. Kowluru, Biochem. Pharmacol. 81 (2011) 965–975.
[38] S. Yoshida, K. Ishizawa, N. Ayuzawa, K. Ueda, M. Takeuchi, W. Kawarazaki, T. Fujita, M. Nagase, Nephron Exp. Nephrol. 126 (2014) 16–24.

REFERENCES

1.   Ionescu-Tirgoviste C, Gagniuc PA, Gubceac E, Mardare L, Popescu I, Dima S, Militaru M. A 3D map of the islet routes throughout the healthy human pancreas. Sci Rep. 2015;5:14634. doi: 10.1038/srep14634. PubMed PMID: 26417671; PMCID: 4586491.

2.   Cabrera O, Berman DM, Kenyon NS, Ricordi C, Berggren PO, Caicedo A. The unique cytoarchitecture of human pancreatic islets has implications for islet cell function. Proc Natl Acad Sci U S A. 2006;103(7):2334-9. doi: 10.1073/pnas.0510790103. PubMed PMID: 16461897; PMCID: 1413730.

3.   Scharfmann R, Xiao X, Heimberg H, Mallet J, Ravassard P. Beta cells within single human islets originate from multiple progenitors. PLoS One. 2008;3(10):e3559. doi: 10.1371/journal.pone.0003559. PubMed PMID: 18958289; PMCID: 2571119.

4.   Weiss M, Steiner DF, Philipson LH. Insulin Biosynthesis, Secretion, Structure, and Structure-Activity Relationships. In: De Groot LJ, Beck-Peccoz P, Chrousos G, Dungan K, Grossman A, Hershman JM, Koch C, McLachlan R, New M, Rebar R, Singer F, Vinik A, Weickert MO, editors. Endotext. South Dartmouth (MA)2000.

5.   Chang L, Chiang SH, Saltiel AR. Insulin signaling and the regulation of glucose transport. Mol Med. 2004;10(7-12):65-71. doi: 10.2119/2005-00029.Saltiel. PubMed PMID: 16307172; PMCID: 1431367.

6.   Lee J, Pilch PF. The insulin receptor: structure, function, and signaling. Am J Physiol. 1994;266(2 Pt 1):C319-34. PubMed PMID: 8141246.

7.   Kanzaki M. Insulin receptor signals regulating GLUT4 translocation and actin dynamics. Endocr J. 2006;53(3):267-93. PubMed PMID: 16702775.

8.   Wang Z, Thurmond DC. Mechanisms of biphasic insulin-granule exocytosis - roles of the cytoskeleton, small GTPases and SNARE proteins. J Cell Sci. 2009;122(Pt 7):893-903. doi: 10.1242/jcs.034355. PubMed PMID: 19295123; PMCID: 2720925.

9.   von Herrath M, Sanda S, Herold K. Type 1 diabetes as a relapsing-remitting disease? Nat Rev Immunol. 2007;7(12):988-94. doi: 10.1038/nri2192. PubMed PMID: 17982429.

10.   Bensellam M, Laybutt DR, Jonas JC. The molecular mechanisms of pancreatic beta-cell glucotoxicity: recent findings and future research directions. Mol Cell Endocrinol. 2012;364(1-2):1-27. doi: 10.1016/j.mce.2012.08.003. PubMed PMID: 22885162.

11.   Skelly RH, Schuppin GT, Ishihara H, Oka Y, Rhodes CJ. Glucose-regulated translational control of proinsulin biosynthesis with that of the proinsulin endopeptidases PC2 and PC3 in the insulin-producing MIN6 cell line. Diabetes. 1996;45(1):37-43. PubMed PMID: 8522057.

12.   Guest PC, Bailyes EM, Hutton JC. Endoplasmic reticulum Ca2+ is important for the proteolytic processing and intracellular transport of proinsulin in the pancreatic beta-cell. Biochem J. 1997;323 (Pt 2):445-50. PubMed PMID: 9163336; PMCID: 1218339.

13.   Flamez D, Berger V, Kruhoffer M, Orntoft T, Pipeleers D, Schuit FC. Critical role for cataplerosis via citrate in glucose-regulated insulin release. Diabetes. 2002;51(7):2018-24. PubMed PMID: 12086928.

14.   Poitout V, Robertson RP. Glucolipotoxicity: fuel excess and beta-cell dysfunction. Endocr Rev. 2008;29(3):351-66. doi: 10.1210/er.2007-0023. PubMed PMID: 18048763; PMCID: 2528858.

15.   Unger RH, Grundy S. Hyperglycaemia as an inducer as well as a consequence of impaired islet cell function and insulin resistance: implications for the management of diabetes. Diabetologia. 1985;28(3):119-21. PubMed PMID: 3888754.

16.   Metz SA, Rabaglia ME, Pintar TJ. Selective inhibitors of GTP synthesis impede exocytotic insulin release from intact rat islets. J Biol Chem. 1992;267(18):12517-27. PubMed PMID: 1352288.

17.   Metz SA, Meredith M, Rabaglia ME, Kowluru A. Small elevations of glucose concentration redirect and amplify the synthesis of guanosine 5'-triphosphate in rat islets.

J Clin Invest. 1993;92(2):872-82. doi: 10.1172/JCI116662. PubMed PMID: 8349822;

PMCID: 294926.

18.   Kowluru A. Small G proteins in islet beta-cell function. Endocr Rev. 2010;31(1):52-78. doi:

10.1210/er.2009-0022. PubMed PMID: 19890090; PMCID: 2852207.

19.   Arora DK, Syed I, Machhadieh B, McKenna CE, Kowluru A. Rab-geranylgeranyl

transferase regulates glucose-stimulated insulin secretion from pancreatic beta cells.

Islets. 2012;4(5):354-8. doi: 10.4161/isl.22538. PubMed PMID: 23114750; PMCID:

3524143.

20.   Kowluru A, Kowluru RA. Protein prenylation in islet beta-cell function in health and

diabetes: Putting the pieces of the puzzle together. Biochem Pharmacol. 2015;98(3):363-

70. doi: 10.1016/j.bcp.2015.07.004. PubMed PMID: 26215874.

21.   Zhang FL, Casey PJ. Protein prenylation: molecular mechanisms and functional

consequences. Annu Rev Biochem. 1996;65:241-69. doi:

10.1146/annurev.bi.65.070196.001325. PubMed PMID: 8811180.

22.   Asahara S, Shibutani Y, Teruyama K, Inoue HY, Kawada Y, Etoh H, Matsuda T, Kimura-

Koyanagi M, Hashimoto N, Sakahara M, Fujimoto W, Takahashi H, Ueda S, Hosooka T,

Satoh T, Inoue H, Matsumoto M, Aiba A, Kasuga M, Kido Y. Ras-related C3 botulinum

toxin substrate 1 (RAC1) regulates glucose-stimulated insulin secretion via modulation of

F-actin. Diabetologia. 2013;56(5):1088-97. doi: 10.1007/s00125-013-2849-5. PubMed

PMID: 23412604; PMCID: 3622740.

23.   Kowluru A. Friendly, and not so friendly, roles of Rac1 in islet beta-cell function: lessons

learnt from pharmacological and molecular biological approaches. Biochem Pharmacol.

2011;81(8):965-75. doi: 10.1016/j.bcp.2011.01.013. PubMed PMID: 21300027; PMCID:

3073707.

24.   Veluthakal R, Madathilparambil SV, McDonald P, Olson LK, Kowluru A. Regulatory roles

for Tiam1, a guanine nucleotide exchange factor for Rac1, in glucose-stimulated insulin

secretion in pancreatic beta-cells. Biochem Pharmacol. 2009;77(1):101-13. doi: 10.1016/j.bcp.2008.09.021. PubMed PMID: 18930714; PMCID: 2605786.

25.   Veluthakal R, Tunduguru R, Arora DK, Sidarala V, Syeda K, Vlaar CP, Thurmond DC, Kowluru A. VAV2, a guanine nucleotide exchange factor for Rac1, regulates glucose-stimulated insulin secretion in pancreatic beta cells. Diabetologia. 2015;58(11):2573-81. doi: 10.1007/s00125-015-3707-4. PubMed PMID: 26224100; PMCID: 4591202.

26.   Gao Y, Dickerson JB, Guo F, Zheng J, Zheng Y. Rational design and characterization of a Rac GTPase-specific small molecule inhibitor. Proc Natl Acad Sci U S A. 2004;101(20):7618-23. doi: 10.1073/pnas.0307512101. PubMed PMID: 15128949; PMCID: 419655.

27.   Onesto C, Shutes A, Picard V, Schweighoffer F, Der CJ. Characterization of EHT 1864, a novel small molecule inhibitor of Rac family small GTPases. Methods Enzymol. 2008;439:111-29. doi: 10.1016/S0076-6879(07)00409-0. PubMed PMID: 18374160.

28.   Desire L, Bourdin J, Loiseau N, Peillon H, Picard V, De Oliveira C, Bachelot F, Leblond B, Taverne T, Beausoleil E, Lacombe S, Drouin D, Schweighoffer F. RAC1 inhibition targets amyloid precursor protein processing by gamma-secretase and decreases Abeta production in vitro and in vivo. J Biol Chem. 2005;280(45):37516-25. doi: 10.1074/jbc.M507913200. PubMed PMID: 16150730.

29.   Rosenblatt AE, Garcia MI, Lyons L, Xie Y, Maiorino C, Desire L, Slingerland J, Burnstein KL. Inhibition of the Rho GTPase, Rac1, decreases estrogen receptor levels and is a novel therapeutic strategy in breast cancer. Endocr Relat Cancer. 2011;18(2):207-19. doi: 10.1677/ERC-10-0049. PubMed PMID: 21118977; PMCID: 3644524.

30.   Martinez LA, Tejada-Simon MV. Pharmacological inactivation of the small GTPase Rac1 impairs long-term plasticity in the mouse hippocampus. Neuropharmacology. 2011;61(1-2):305-12. doi: 10.1016/j.neuropharm.2011.04.017. PubMed PMID: 21569781; PMCID: 3106418.

31.   Katz E, Sims AH, Sproul D, Caldwell H, Dixon MJ, Meehan RR, Harrison DJ. Targeting of Rac GTPases blocks the spread of intact human breast cancer. Oncotarget. 2012;3(6):608-19. doi: 10.18632/oncotarget.520. PubMed PMID: 22689141; PMCID: 3442288.

32.   Stefanini L, Boulaftali Y, Ouellette TD, Holinstat M, Desire L, Leblond B, Andre P, Conley PB, Bergmeier W. Rap1-Rac1 circuits potentiate platelet activation. Arterioscler Thromb Vasc Biol. 2012;32(2):434-41. doi: 10.1161/ATVBAHA.111.239194. PubMed PMID: 22075250; PMCID: 3262085.

33.   Nagase M, Fujita T. Role of Rac1-mineralocorticoid-receptor signalling in renal and cardiac disease. Nat Rev Nephrol. 2013;9(2):86-98. doi: 10.1038/nrneph.2012.282. PubMed PMID: 23296296.

34.   Veluthakal R, Kaur H, Goalstone M, Kowluru A. Dominant-negative alpha-subunit of farnesyl- and geranyltransferase inhibits glucose-stimulated, but not KCl-stimulated, insulin secretion in INS 832/13 cells. Diabetes. 2007;56(1):204-10. doi: 10.2337/db06-0668. PubMed PMID: 17192483.

35.   Newsholme P, Morgan D, Rebelato E, Oliveira-Emilio HC, Procopio J, Curi R, Carpinelli A. Insights into the critical role of NADPH oxidase(s) in the normal and dysregulated pancreatic beta cell. Diabetologia. 2009;52(12):2489-98. doi: 10.1007/s00125-009-1536-z. PubMed PMID: 19809798.

36.   Morgan D, Rebelato E, Abdulkader F, Graciano MF, Oliveira-Emilio HR, Hirata AE, Rocha MS, Bordin S, Curi R, Carpinelli AR. Association of NAD(P)H oxidase with glucose-induced insulin secretion by pancreatic beta-cells. Endocrinology. 2009;150(5):2197-201. doi: 10.1210/en.2008-1149. PubMed PMID: 19147679.

37.   Oliveira HR, Verlengia R, Carvalho CR, Britto LR, Curi R, Carpinelli AR. Pancreatic beta-cells express phagocyte-like NAD(P)H oxidase. Diabetes. 2003;52(6):1457-63. PubMed PMID: 12765957.

38.   Leloup C, Tourrel-Cuzin C, Magnan C, Karaca M, Castel J, Carneiro L, Colombani AL, Ktorza A, Casteilla L, Penicaud L. Mitochondrial reactive oxygen species are obligatory signals for glucose-induced insulin secretion. Diabetes. 2009;58(3):673-81. doi: 10.2337/db07-1056. PubMed PMID: 19073765; PMCID: 2646066.

39.   Pi J, Collins S. Reactive oxygen species and uncoupling protein 2 in pancreatic beta-cell function. Diabetes Obes Metab. 2010;12 Suppl 2:141-8. doi: 10.1111/j.1463-1326.2010.01269.x. PubMed PMID: 21029311.

40.   Morgan D, Oliveira-Emilio HR, Keane D, Hirata AE, Santos da Rocha M, Bordin S, Curi R, Newsholme P, Carpinelli AR. Glucose, palmitate and pro-inflammatory cytokines modulate production and activity of a phagocyte-like NADPH oxidase in rat pancreatic islets and a clonal beta cell line. Diabetologia. 2007;50(2):359-69. doi: 10.1007/s00125-006-0462-6. PubMed PMID: 17151863.

41.   Syed I, Kyathanahalli CN, Kowluru A. Phagocyte-like NADPH oxidase generates ROS in INS 832/13 cells and rat islets: role of protein prenylation. Am J Physiol Regul Integr Comp Physiol. 2011;300(3):R756-62. doi: 10.1152/ajpregu.00786.2010. PubMed PMID: 21228337; PMCID: 3064276.

42.   Giacco F, Brownlee M. Oxidative stress and diabetic complications. Circ Res. 2010;107(9):1058-70. doi: 10.1161/CIRCRESAHA.110.223545. PubMed PMID: 21030723; PMCID: 2996922.

43.   Maritim AC, Sanders RA, Watkins JB, 3rd. Diabetes, oxidative stress, and antioxidants: a review. J Biochem Mol Toxicol. 2003;17(1):24-38. doi: 10.1002/jbt.10058. PubMed PMID: 12616644.

44.   Spector A. Review: Oxidative stress and disease. J Ocul Pharmacol Ther. 2000;16(2):193-201. doi: 10.1089/jop.2000.16.193. PubMed PMID: 10803430.

45. Lenzen S, Drinkgern J, Tiedge M. Low antioxidant enzyme gene expression in pancreatic islets compared with various other mouse tissues. Free Radic Biol Med. 1996;20(3):463-6. PubMed PMID: 8720919.

46. Drews G, Krippeit-Drews P, Dufer M. Oxidative stress and beta-cell dysfunction. Pflugers Arch. 2010;460(4):703-18. doi: 10.1007/s00424-010-0862-9. PubMed PMID: 20652307.

47. Cnop M, Welsh N, Jonas JC, Jorns A, Lenzen S, Eizirik DL. Mechanisms of pancreatic beta-cell death in type 1 and type 2 diabetes: many differences, few similarities. Diabetes. 2005;54 Suppl 2:S97-107. PubMed PMID: 16306347.

48. Kowluru A, Kowluru RA. Phagocyte-like NADPH oxidase [Nox2] in cellular dysfunction in models of glucolipotoxicity and diabetes. Biochem Pharmacol. 2014;88(3):275-83. doi: 10.1016/j.bcp.2014.01.017. PubMed PMID: 24462914.

49. Syed I, Kyathanahalli CN, Jayaram B, Govind S, Rhodes CJ, Kowluru RA, Kowluru A. Increased phagocyte-like NADPH oxidase and ROS generation in type 2 diabetic ZDF rat and human islets: role of Rac1-JNK1/2 signaling pathway in mitochondrial dysregulation in the diabetic islet. Diabetes. 2011;60(11):2843-52. doi: 10.2337/db11-0809. PubMed PMID: 21911753; PMCID: 3198065.

50. Syed I, Jayaram B, Subasinghe W, Kowluru A. Tiam1/Rac1 signaling pathway mediates palmitate-induced, ceramide-sensitive generation of superoxides and lipid peroxides and the loss of mitochondrial membrane potential in pancreatic beta-cells. Biochem Pharmacol. 2010;80(6):874-83. doi: 10.1016/j.bcp.2010.05.006. PubMed PMID: 20493824; PMCID: 2919057.

51. Yuan H, Lu Y, Huang X, He Q, Man Y, Zhou Y, Wang S, Li J. Suppression of NADPH oxidase 2 substantially restores glucose-induced dysfunction of pancreatic NIT-1 cells. FEBS J. 2010;277(24):5061-71. doi: 10.1111/j.1742-4658.2010.07911.x. PubMed PMID: 21073655.

52. Subasinghe W, Syed I, Kowluru A. Phagocyte-like NADPH oxidase promotes cytokine-induced mitochondrial dysfunction in pancreatic beta-cells: evidence for regulation by Rac1. Am J Physiol Regul Integr Comp Physiol. 2011;300(1):R12-20. doi: 10.1152/ajpregu.00421.2010. PubMed PMID: 20943855; PMCID: 3023281.

53. Cargnello M, Roux PP. Activation and function of the MAPKs and their substrates, the MAPK-activated protein kinases. Microbiol Mol Biol Rev. 2011;75(1):50-83. doi: 10.1128/MMBR.00031-10. PubMed PMID: 21372320; PMCID: 3063353.

54. Pearson G, Robinson F, Beers Gibson T, Xu BE, Karandikar M, Berman K, Cobb MH. Mitogen-activated protein (MAP) kinase pathways: regulation and physiological functions. Endocr Rev. 2001;22(2):153-83. doi: 10.1210/edrv.22.2.0428. PubMed PMID: 11294822.

55. Kim EK, Choi EJ. Pathological roles of MAPK signaling pathways in human diseases. Biochim Biophys Acta. 2010;1802(4):396-405. doi: 10.1016/j.bbadis.2009.12.009. PubMed PMID: 20079433.

56. Coulombe P, Meloche S. Atypical mitogen-activated protein kinases: structure, regulation and functions. Biochim Biophys Acta. 2007;1773(8):1376-87. doi: 10.1016/j.bbamcr.2006.11.001. PubMed PMID: 17161475.

57. Dhillon AS, Hagan S, Rath O, Kolch W. MAP kinase signalling pathways in cancer. Oncogene. 2007;26(22):3279-90. doi: 10.1038/sj.onc.1210421. PubMed PMID: 17496922.

58. Weston CR, Davis RJ. The JNK signal transduction pathway. Curr Opin Genet Dev. 2002;12(1):14-21. PubMed PMID: 11790549.

59. Raman M, Chen W, Cobb MH. Differential regulation and properties of MAPKs. Oncogene. 2007;26(22):3100-12. doi: 10.1038/sj.onc.1210392. PubMed PMID: 17496909.

60. Leppa S, Bohmann D. Diverse functions of JNK signaling and c-Jun in stress response and apoptosis. Oncogene. 1999;18(45):6158-62. doi: 10.1038/sj.onc.1203173. PubMed PMID: 10557107.

61. Picco V, Pages G. Linking JNK Activity to the DNA Damage Response. Genes Cancer. 2013;4(9-10):360-8. doi: 10.1177/1947601913486347. PubMed PMID: 24349633; PMCID: 3863338.

62. Vallerie SN, Hotamisligil GS. The role of JNK proteins in metabolism. Sci Transl Med. 2010;2(60):60rv5. doi: 10.1126/scitranslmed.3001007. PubMed PMID: 21123811.

63. Dong C, Yang DD, Tournier C, Whitmarsh AJ, Xu J, Davis RJ, Flavell RA. JNK is required for effector T-cell function but not for T-cell activation. Nature. 2000;405(6782):91-4. doi: 10.1038/35011091. PubMed PMID: 10811224.

64. Ma AD, Metjian A, Bagrodia S, Taylor S, Abrams CS. Cytoskeletal reorganization by G protein-coupled receptors is dependent on phosphoinositide 3-kinase gamma, a Rac guanosine exchange factor, and Rac. Mol Cell Biol. 1998;18(8):4744-51. PubMed PMID: 9671484; PMCID: 109060.

65. Zarubin T, Han J. Activation and signaling of the p38 MAP kinase pathway. Cell Res. 2005;15(1):11-8. doi: 10.1038/sj.cr.7290257. PubMed PMID: 15686620.

66. Ambrosino C, Nebreda AR. Cell cycle regulation by p38 MAP kinases. Biol Cell. 2001;93(1-2):47-51. PubMed PMID: 11730321.

67. Thornton TM, Rincon M. Non-classical p38 map kinase functions: cell cycle checkpoints and survival. Int J Biol Sci. 2009;5(1):44-51. PubMed PMID: 19159010; PMCID: 2610339.

68. Cuenda A, Rousseau S. p38 MAP-kinases pathway regulation, function and role in human diseases. Biochim Biophys Acta. 2007;1773(8):1358-75. doi: 10.1016/j.bbamcr.2007.03.010. PubMed PMID: 17481747.

69. Huang H, Ryu J, Ha J, Chang EJ, Kim HJ, Kim HM, Kitamura T, Lee ZH, Kim HH. Osteoclast differentiation requires TAK1 and MKK6 for NFATc1 induction and NF-kappaB

transactivation by RANKL. Cell Death Differ. 2006;13(11):1879-91. doi: 10.1038/sj.cdd.4401882. PubMed PMID: 16498455.

70. Houde M, Laprise P, Jean D, Blais M, Asselin C, Rivard N. Intestinal epithelial cell differentiation involves activation of p38 mitogen-activated protein kinase that regulates the homeobox transcription factor CDX2. J Biol Chem. 2001;276(24):21885-94. doi: 10.1074/jbc.M100236200. PubMed PMID: 11283019.

71. Aouadi M, Laurent K, Prot M, Le Marchand-Brustel Y, Binetruy B, Bost F. Inhibition of p38MAPK increases adipogenesis from embryonic to adult stages. Diabetes. 2006;55(2):281-9. PubMed PMID: 16443758.

72. Bost F, Aouadi M, Caron L, Binetruy B. The role of MAPKs in adipocyte differentiation and obesity. Biochimie. 2005;87(1):51-6. doi: 10.1016/j.biochi.2004.10.018. PubMed PMID: 15733737.

73. Cappellini A, Tazzari PL, Mantovani I, Billi AM, Tassi C, Ricci F, Conte R, Martelli AM. Antiapoptotic role of p38 mitogen activated protein kinase in Jurkat T cells and normal human T lymphocytes treated with 8-methoxypsoralen and ultraviolet-A radiation. Apoptosis. 2005;10(1):141-52. doi: 10.1007/s10495-005-6069-4. PubMed PMID: 15711930.

74. Gutierrez-Uzquiza A, Arechederra M, Bragado P, Aguirre-Ghiso JA, Porras A. p38alpha mediates cell survival in response to oxidative stress via induction of antioxidant genes: effect on the p70S6K pathway. J Biol Chem. 2012;287(4):2632-42. doi: 10.1074/jbc.M111.323709. PubMed PMID: 22139847; PMCID: 3268422.

75. Sumara G, Formentini I, Collins S, Sumara I, Windak R, Bodenmiller B, Ramracheya R, Caille D, Jiang H, Platt KA, Meda P, Aebersold R, Rorsman P, Ricci R. Regulation of PKD by the MAPK p38delta in insulin secretion and glucose homeostasis. Cell. 2009;136(2):235-48. doi: 10.1016/j.cell.2008.11.018. PubMed PMID: 19135240; PMCID: 2638021.

76.   De Zutter GS, Davis RJ. Pro-apoptotic gene expression mediated by the p38 mitogen-

       activated protein kinase signal transduction pathway. Proc Natl Acad Sci U S A.

       2001;98(11):6168-73. doi: 10.1073/pnas.111027698. PubMed PMID: 11344273; PMCID:

       33440.

77.   Saurin AT, Martin JL, Heads RJ, Foley C, Mockridge JW, Wright MJ, Wang Y, Marber

       MS. The role of differential activation of p38-mitogen-activated protein kinase in

       preconditioned ventricular myocytes. FASEB J. 2000;14(14):2237-46. doi: 10.1096/fj.99-

       0671com. PubMed PMID: 11053245.

78.   Alsayed Y, Uddin S, Mahmud N, Lekmine F, Kalvakolanu DV, Minucci S, Bokoch G,

       Platanias LC. Activation of Rac1 and the p38 mitogen-activated protein kinase pathway in

       response to all-trans-retinoic acid. J Biol Chem. 2001;276(6):4012-9. doi:

       10.1074/jbc.M007431200. PubMed PMID: 11060298.

79.   Bulavin DV, Saito S, Hollander MC, Sakaguchi K, Anderson CW, Appella E, Fornace AJ,

       Jr. Phosphorylation of human p53 by p38 kinase coordinates N-terminal phosphorylation

       and apoptosis in response to UV radiation. EMBO J. 1999;18(23):6845-54. doi:

       10.1093/emboj/18.23.6845. PubMed PMID: 10581258; PMCID: 1171747.

80.   Meulmeester E, Jochemsen AG. p53: a guide to apoptosis. Curr Cancer Drug Targets.

       2008;8(2):87-97. PubMed PMID: 18336191.

81.   Batinac T, Gruber F, Lipozencic J, Zamolo-Koncar G, Stasic A, Brajac I. Protein p53--

       structure, function, and possible therapeutic implications. Acta Dermatovenerol Croat.

       2003;11(4):225-30. PubMed PMID: 14670223.

82.   Lane DP. Cancer. p53, guardian of the genome. Nature. 1992;358(6381):15-6. doi:

       10.1038/358015a0. PubMed PMID: 1614522.

83.   Vousden KH, Lu X. Live or let die: the cell's response to p53. Nat Rev Cancer.

       2002;2(8):594-604. doi: 10.1038/nrc864. PubMed PMID: 12154352.

84. Donehower LA, Harvey M, Slagle BL, McArthur MJ, Montgomery CA, Jr., Butel JS, Bradley A. Mice deficient for p53 are developmentally normal but susceptible to spontaneous tumours. Nature. 1992;356(6366):215-21. doi: 10.1038/356215a0. PubMed PMID: 1552940.

85. Dippold WG, Jay G, DeLeo AB, Khoury G, Old LJ. p53 transformation-related protein: detection by monoclonal antibody in mouse and human cells. Proc Natl Acad Sci U S A. 1981;78(3):1695-9. PubMed PMID: 6940183; PMCID: 319199.

86. Finlay CA, Hinds PW, Levine AJ. The p53 proto-oncogene can act as a suppressor of transformation. Cell. 1989;57(7):1083-93. PubMed PMID: 2525423.

87. Vogelstein B, Lane D, Levine AJ. Surfing the p53 network. Nature. 2000;408(6810):307-10. doi: 10.1038/35042675. PubMed PMID: 11099028.

88. Meek DW, Anderson CW. Posttranslational modification of p53: cooperative integrators of function. Cold Spring Harb Perspect Biol. 2009;1(6):a000950. doi: 10.1101/cshperspect.a000950. PubMed PMID: 20457558; PMCID: 2882125.

89. Bode AM, Dong Z. Post-translational modification of p53 in tumorigenesis. Nat Rev Cancer. 2004;4(10):793-805. doi: 10.1038/nrc1455. PubMed PMID: 15510160.

90. Moll UM, Petrenko O. The MDM2-p53 interaction. Mol Cancer Res. 2003;1(14):1001-8. PubMed PMID: 14707283.

91. Wang YH, Tsay YG, Tan BC, Lo WY, Lee SC. Identification and characterization of a novel p300-mediated p53 acetylation site, lysine 305. J Biol Chem. 2003;278(28):25568-76. doi: 10.1074/jbc.M212574200. PubMed PMID: 12724314.

92. Joerger AC, Fersht AR. The tumor suppressor p53: from structures to drug discovery. Cold Spring Harb Perspect Biol. 2010;2(6):a000919. doi: 10.1101/cshperspect.a000919. PubMed PMID: 20516128; PMCID: 2869527.

93. Kern SE, Kinzler KW, Bruskin A, Jarosz D, Friedman P, Prives C, Vogelstein B. Identification of p53 as a sequence-specific DNA-binding protein. Science. 1991;252(5013):1708-11. PubMed PMID: 2047879.

94. Chene P. The role of tetramerization in p53 function. Oncogene. 2001;20(21):2611-7. doi: 10.1038/sj.onc.1204373. PubMed PMID: 11420672.

95. Stommel JM, Marchenko ND, Jimenez GS, Moll UM, Hope TJ, Wahl GM. A leucine-rich nuclear export signal in the p53 tetramerization domain: regulation of subcellular localization and p53 activity by NES masking. EMBO J. 1999;18(6):1660-72. doi: 10.1093/emboj/18.6.1660. PubMed PMID: 10075936; PMCID: 1171253.

96. Kim H, Kim K, Choi J, Heo K, Baek HJ, Roeder RG, An W. p53 requires an intact C-terminal domain for DNA binding and transactivation. J Mol Biol. 2012;415(5):843-54. doi: 10.1016/j.jmb.2011.12.001. PubMed PMID: 22178617; PMCID: 3267882.

97. Ahn J, Prives C. The C-terminus of p53: the more you learn the less you know. Nat Struct Biol. 2001;8(9):730-2. doi: 10.1038/nsb0901-730. PubMed PMID: 11524665.

98. Liang SH, Clarke MF. The nuclear import of p53 is determined by the presence of a basic domain and its relative position to the nuclear localization signal. Oncogene. 1999;18(12):2163-6. doi: 10.1038/sj.onc.1202350. PubMed PMID: 10321742.

99. O'Brate A, Giannakakou P. The importance of p53 location: nuclear or cytoplasmic zip code? Drug Resist Updat. 2003;6(6):313-22. PubMed PMID: 14744495.

100. Oren M, Damalas A, Gottlieb T, Michael D, Taplick J, Leal JF, Maya R, Moas M, Seger R, Taya Y, Ben-Ze'Ev A. Regulation of p53: intricate loops and delicate balances. Ann N Y Acad Sci. 2002;973:374-83. PubMed PMID: 12485897.

101. Prives C, Hall PA. The p53 pathway. J Pathol. 1999;187(1):112-26. doi: 10.1002/(SICI)1096-9896(199901)187:1<112::AID-PATH250>3.0.CO;2-3. PubMed PMID: 10341712.

102. Barak Y, Juven T, Haffner R, Oren M. mdm2 expression is induced by wild type p53 activity. EMBO J. 1993;12(2):461-8. PubMed PMID: 8440237; PMCID: 413229.

103. Jones SN, Roe AE, Donehower LA, Bradley A. Rescue of embryonic lethality in Mdm2-deficient mice by absence of p53. Nature. 1995;378(6553):206-8. doi: 10.1038/378206a0. PubMed PMID: 7477327.

104. Kubbutat MH, Jones SN, Vousden KH. Regulation of p53 stability by Mdm2. Nature. 1997;387(6630):299-303. doi: 10.1038/387299a0. PubMed PMID: 9153396.

105. Haupt Y, Maya R, Kazaz A, Oren M. Mdm2 promotes the rapid degradation of p53. Nature. 1997;387(6630):296-9. doi: 10.1038/387296a0. PubMed PMID: 9153395.

106. Loughery J, Cox M, Smith LM, Meek DW. Critical role for p53-serine 15 phosphorylation in stimulating transactivation at p53-responsive promoters. Nucleic Acids Res. 2014;42(12):7666-80. doi: 10.1093/nar/gku501. PubMed PMID: 24928858; PMCID: 4081099.

107. Reed SM, Quelle DE. p53 Acetylation: Regulation and Consequences. Cancers (Basel). 2014;7(1):30-69. doi: 10.3390/cancers7010030. PubMed PMID: 25545885; PMCID: 4381250.

108. Riley T, Sontag E, Chen P, Levine A. Transcriptional control of human p53-regulated genes. Nat Rev Mol Cell Biol. 2008;9(5):402-12. doi: 10.1038/nrm2395. PubMed PMID: 18431400.

109. Mirza A, Wu Q, Wang L, McClanahan T, Bishop WR, Gheyas F, Ding W, Hutchins B, Hockenberry T, Kirschmeier P, Greene JR, Liu S. Global transcriptional program of p53 target genes during the process of apoptosis and cell cycle progression. Oncogene. 2003;22(23):3645-54. doi: 10.1038/sj.onc.1206477. PubMed PMID: 12789273.

110. He G, Siddik ZH, Huang Z, Wang R, Koomen J, Kobayashi R, Khokhar AR, Kuang J. Induction of p21 by p53 following DNA damage inhibits both Cdk4 and Cdk2 activities.

Oncogene. 2005;24(18):2929-43. doi: 10.1038/sj.onc.1208474. PubMed PMID: 15735718.

111.   Carrier F, Smith ML, Bae I, Kilpatrick KE, Lansing TJ, Chen CY, Engelstein M, Friend SH, Henner WD, Gilmer TM, et al. Characterization of human Gadd45, a p53-regulated protein. J Biol Chem. 1994;269(51):32672-7. PubMed PMID: 7798274.

112.   Muller M, Wilder S, Bannasch D, Israeli D, Lehlbach K, Li-Weber M, Friedman SL, Galle PR, Stremmel W, Oren M, Krammer PH. p53 activates the CD95 (APO-1/Fas) gene in response to DNA damage by anticancer drugs. J Exp Med. 1998;188(11):2033-45. PubMed PMID: 9841917; PMCID: 2212386.

113.   Nakano K, Vousden KH. PUMA, a novel proapoptotic gene, is induced by p53. Mol Cell. 2001;7(3):683-94. PubMed PMID: 11463392.

114.   Oda E, Ohki R, Murasawa H, Nemoto J, Shibue T, Yamashita T, Tokino T, Taniguchi T, Tanaka N. Noxa, a BH3-only member of the Bcl-2 family and candidate mediator of p53-induced apoptosis. Science. 2000;288(5468):1053-8. PubMed PMID: 10807576.

115.   Muller M, Strand S, Hug H, Heinemann EM, Walczak H, Hofmann WJ, Stremmel W, Krammer PH, Galle PR. Drug-induced apoptosis in hepatoma cells is mediated by the CD95 (APO-1/Fas) receptor/ligand system and involves activation of wild-type p53. J Clin Invest. 1997;99(3):403-13. doi: 10.1172/JCI119174. PubMed PMID: 9022073; PMCID: 507813.

116.   Bennett M, Macdonald K, Chan SW, Luzio JP, Simari R, Weissberg P. Cell surface trafficking of Fas: a rapid mechanism of p53-mediated apoptosis. Science. 1998;282(5387):290-3. PubMed PMID: 9765154.

117.   Wu GS, Burns TF, McDonald ER, 3rd, Meng RD, Kao G, Muschel R, Yen T, el-Deiry WS. Induction of the TRAIL receptor KILLER/DR5 in p53-dependent apoptosis but not growth arrest. Oncogene. 1999;18(47):6411-8. doi: 10.1038/sj.onc.1203025. PubMed PMID: 10597242.

118. Liu X, Yue P, Khuri FR, Sun SY. p53 upregulates death receptor 4 expression through an intronic p53 binding site. Cancer Res. 2004;64(15):5078-83. doi: 10.1158/0008-5472.CAN-04-1195. PubMed PMID: 15289308.

119. Khadija S, Veluthakal R, Sidarala V, Kowluru A. Glucotoxic and diabetic conditions induce caspase 6-mediated degradation of nuclear lamin A in human islets, rodent islets and INS-1 832/13 cells. Apoptosis. 2014;19(12):1691-701. doi: 10.1007/s10495-014-1038-4. PubMed PMID: 25292013; PMCID: 4225171.

120. Mohammed AM, Syeda K, Hadden T, Kowluru A. Upregulation of phagocyte-like NADPH oxidase by cytokines in pancreatic beta-cells: attenuation of oxidative and nitrosative stress by 2-bromopalmitate. Biochem Pharmacol. 2013;85(1):109-14. doi: 10.1016/j.bcp.2012.09.024. PubMed PMID: 23092759; PMCID: 3529999.

121. Flores-Lopez LA, Diaz-Flores M, Garcia-Macedo R, Avalos-Rodriguez A, Vergara-Onofre M, Cruz M, Contreras-Ramos A, Konigsberg M, Ortega-Camarillo C. High glucose induces mitochondrial p53 phosphorylation by p38 MAPK in pancreatic RINm5F cells. Mol Biol Rep. 2013;40(8):4947-58. doi: 10.1007/s11033-013-2595-2. PubMed PMID: 23657598.

122. Rey FE, Cifuentes ME, Kiarash A, Quinn MT, Pagano PJ. Novel competitive inhibitor of NAD(P)H oxidase assembly attenuates vascular O(2)(-) and systolic blood pressure in mice. Circ Res. 2001;89(5):408-14. PubMed PMID: 11532901.

123. Park L, Anrather J, Zhou P, Frys K, Pitstick R, Younkin S, Carlson GA, Iadecola C. NADPH-oxidase-derived reactive oxygen species mediate the cerebrovascular dysfunction induced by the amyloid beta peptide. J Neurosci. 2005;25(7):1769-77. doi: 10.1523/JNEUROSCI.5207-04.2005. PubMed PMID: 15716413.

124. Park L, Anrather J, Girouard H, Zhou P, Iadecola C. Nox2-derived reactive oxygen species mediate neurovascular dysregulation in the aging mouse brain. J Cereb Blood

Flow Metab. 2007;27(12):1908-18. doi: 10.1038/sj.jcbfm.9600491. PubMed PMID: 17429347.

125. Gupte RS, Floyd BC, Kozicky M, George S, Ungvari ZI, Neito V, Wolin MS, Gupte SA. Synergistic activation of glucose-6-phosphate dehydrogenase and NAD(P)H oxidase by Src kinase elevates superoxide in type 2 diabetic, Zucker fa/fa, rat liver. Free Radic Biol Med. 2009;47(3):219-28. doi: 10.1016/j.freeradbiomed.2009.01.028. PubMed PMID: 19230846; PMCID: 2700195.

126. Lee S, Paudel O, Jiang Y, Yang XR, Sham JS. CD38 mediates angiotensin II-induced intracellular Ca(2+) release in rat pulmonary arterial smooth muscle cells. Am J Respir Cell Mol Biol. 2015;52(3):332-41. doi: 10.1165/rcmb.2014-0141OC. PubMed PMID: 25078456; PMCID: 4370261.

127. Williams HC, Griendling KK. NADPH oxidase inhibitors: new antihypertensive agents? J Cardiovasc Pharmacol. 2007;50(1):9-16. doi: 10.1097/FJC.0b013e318063e820. PubMed PMID: 17666910.

128. Shutes A, Onesto C, Picard V, Leblond B, Schweighoffer F, Der CJ. Specificity and mechanism of action of EHT 1864, a novel small molecule inhibitor of Rac family small GTPases. J Biol Chem. 2007;282(49):35666-78. doi: 10.1074/jbc.M703571200. PubMed PMID: 17932039.

129. Babelova A, Jansen F, Sander K, Lohn M, Schafer L, Fork C, Ruetten H, Plettenburg O, Stark H, Daniel C, Amann K, Pavenstadt H, Jung O, Brandes RP. Activation of Rac-1 and RhoA contributes to podocyte injury in chronic kidney disease. PLoS One. 2013;8(11):e80328. doi: 10.1371/journal.pone.0080328. PubMed PMID: 24244677; PMCID: 3820652.

130. Wang Y, Kunit T, Ciotkowska A, Rutz B, Schreiber A, Strittmatter F, Waidelich R, Liu C, Stief CG, Gratzke C, Hennenberg M. Inhibition of prostate smooth muscle contraction and prostate stromal cell growth by the inhibitors of Rac, NSC23766 and EHT1864. Br J

Pharmacol. 2015;172(11):2905-17. doi: 10.1111/bph.13099. PubMed PMID: 25631101; PMCID: 4439884.

131.   Yoshida S, Ishizawa K, Ayuzawa N, Ueda K, Takeuchi M, Kawarazaki W, Fujita T, Nagase M. Local mineralocorticoid receptor activation and the role of Rac1 in obesity-related diabetic kidney disease. Nephron Exp Nephrol. 2014;126(1):16-24. doi: 10.1159/000358758. PubMed PMID: 24603367.

132.   Stanley AC, Wong CX, Micaroni M, Venturato J, Khromykh T, Stow JL, Lacy P. The Rho GTPase Rac1 is required for recycling endosome-mediated secretion of TNF in macrophages. Immunol Cell Biol. 2014;92(3):275-86. doi: 10.1038/icb.2013.90. PubMed PMID: 24343664.

133.   Navarro-Lerida I, Sanchez-Perales S, Calvo M, Rentero C, Zheng Y, Enrich C, Del Pozo MA. A palmitoylation switch mechanism regulates Rac1 function and membrane organization. EMBO J. 2012;31(3):534-51. doi: 10.1038/emboj.2011.446. PubMed PMID: 22157745; PMCID: 3273400.

134.   Lambert PF, Kashanchi F, Radonovich MF, Shiekhattar R, Brady JN. Phosphorylation of p53 serine 15 increases interaction with CBP. J Biol Chem. 1998;273(49):33048-53. PubMed PMID: 9830059.

135.   Sanchez-Prieto R, Rojas JM, Taya Y, Gutkind JS. A role for the p38 mitogen-acitvated protein kinase pathway in the transcriptional activation of p53 on genotoxic stress by chemotherapeutic agents. Cancer Res. 2000;60(9):2464-72. PubMed PMID: 10811125.

136.   Yoshida M, Shiojima I, Ikeda H, Komuro I. Chronic doxorubicin cardiotoxicity is mediated by oxidative DNA damage-ATM-p53-apoptosis pathway and attenuated by pitavastatin through the inhibition of Rac1 activity. J Mol Cell Cardiol. 2009;47(5):698-705. doi: 10.1016/j.yjmcc.2009.07.024. PubMed PMID: 19660469.

137.   Oleson BJ, Broniowska KA, Schreiber KH, Tarakanova VL, Corbett JA. Nitric oxide induces ataxia telangiectasia mutated (ATM) protein-dependent gammaH2AX protein

formation in pancreatic beta cells. J Biol Chem. 2014;289(16):11454-64. doi:
10.1074/jbc.M113.531228. PubMed PMID: 24610783; PMCID: 4036281.

138. Henneman L, Schneiders MS, Turkenburg M, Waterham HR. Compromized
geranylgeranylation of RhoA and Rac1 in mevalonate kinase deficiency. J Inherit Metab
Dis. 2010;33(5):625-32. doi: 10.1007/s10545-010-9173-8. PubMed PMID: 20814828;
PMCID: 2946549.

139. Marine JC. p53 stabilization: the importance of nuclear import. Cell Death Differ.
2010;17(2):191-2. doi: 10.1038/cdd.2009.183. PubMed PMID: 20062067.

140. Cardaci S, Filomeni G, Rotilio G, Ciriolo MR. p38(MAPK)/p53 signalling axis mediates
neuronal apoptosis in response to tetrahydrobiopterin-induced oxidative stress and
glucose uptake inhibition: implication for neurodegeneration. Biochem J.
2010;430(3):439-51. doi: 10.1042/BJ20100503. PubMed PMID: 20590525.

141. Mayr M, Hu Y, Hainaut H, Xu Q. Mechanical stress-induced DNA damage and rac-
p38MAPK signal pathways mediate p53-dependent apoptosis in vascular smooth muscle
cells. FASEB J. 2002;16(11):1423-5. doi: 10.1096/fj.02-0042fje. PubMed PMID:
12205035.

142. Cheng Q, Chen J. Mechanism of p53 stabilization by ATM after DNA damage. Cell Cycle.
2010;9(3):472-8. doi: 10.4161/cc.9.3.10556. PubMed PMID: 20081365; PMCID:
2977994.

143. Saito S, Goodarzi AA, Higashimoto Y, Noda Y, Lees-Miller SP, Appella E, Anderson CW.
ATM mediates phosphorylation at multiple p53 sites, including Ser(46), in response to
ionizing radiation. J Biol Chem. 2002;277(15):12491-4. doi: 10.1074/jbc.C200093200.
PubMed PMID: 11875057.

144. Bakkenist CJ, Kastan MB. DNA damage activates ATM through intermolecular
autophosphorylation and dimer dissociation. Nature. 2003;421(6922):499-506. doi:
10.1038/nature01368. PubMed PMID: 12556884.

145. Hickson I, Zhao Y, Richardson CJ, Green SJ, Martin NM, Orr AI, Reaper PM, Jackson SP, Curtin NJ, Smith GC. Identification and characterization of a novel and specific inhibitor of the ataxia-telangiectasia mutated kinase ATM. Cancer Res. 2004;64(24):9152-9. doi: 10.1158/0008-5472.CAN-04-2727. PubMed PMID: 15604286.

146. Mohammed AM, Kowluru A. Activation of apocynin-sensitive NADPH oxidase (Nox2) activity in INS-1 832/13 cells under glucotoxic conditions. Islets. 2013;5(3):129-31. doi: 10.4161/isl.25058. PubMed PMID: 23695780.

147. Shiota M, Printz RL. Diabetes in Zucker diabetic fatty rat. Methods Mol Biol. 2012;933:103-23. doi: 10.1007/978-1-62703-068-7_8. PubMed PMID: 22893404.

148. Harmon JS, Gleason CE, Tanaka Y, Poitout V, Robertson RP. Antecedent hyperglycemia, not hyperlipidemia, is associated with increased islet triacylglycerol content and decreased insulin gene mRNA level in Zucker diabetic fatty rats. Diabetes. 2001;50(11):2481-6. PubMed PMID: 11679425.

149. Syeda K, Mohammed AM, Arora DK, Kowluru A. Glucotoxic conditions induce endoplasmic reticulum stress to cause caspase 3 mediated lamin B degradation in pancreatic beta-cells: protection by nifedipine. Biochem Pharmacol. 2013;86(9):1338-46. doi: 10.1016/j.bcp.2013.08.023. PubMed PMID: 23994168; PMCID: 3832847.

150. Kowluru RA, Kowluru A, Veluthakal R, Mohammad G, Syed I, Santos JM, Mishra M. TIAM1-RAC1 signalling axis-mediated activation of NADPH oxidase-2 initiates mitochondrial damage in the development of diabetic retinopathy. Diabetologia. 2014;57(5):1047-56. doi: 10.1007/s00125-014-3194-z. PubMed PMID: 24554007.

151. Shen E, Li Y, Li Y, Shan L, Zhu H, Feng Q, Arnold JM, Peng T. Rac1 is required for cardiomyocyte apoptosis during hyperglycemia. Diabetes. 2009;58(10):2386-95. doi: 10.2337/db08-0617. PubMed PMID: 19592621; PMCID: 2750234.

152. Olukman M, Orhan CE, Celenk FG, Ulker S. Apocynin restores endothelial dysfunction in streptozotocin diabetic rats through regulation of nitric oxide synthase and NADPH

oxidase expressions. J Diabetes Complications. 2010;24(6):415-23. doi: 10.1016/j.jdiacomp.2010.02.001. PubMed PMID: 20226688.

153. Cifuentes-Pagano E, Saha J, Csanyi G, Ghouleh IA, Sahoo S, Rodriguez A, Wipf P, Pagano PJ, Skoda EM. Bridged tetrahydroisoquinolines as selective NADPH oxidase 2 (Nox2) inhibitors. Medchemcomm. 2013;4(7):1085-92. doi: 10.1039/C3MD00061C. PubMed PMID: 24466406; PMCID: 3897123.

154. Bedard K, Krause KH. The NOX family of ROS-generating NADPH oxidases: physiology and pathophysiology. Physiol Rev. 2007;87(1):245-313. doi: 10.1152/physrev.00044.2005. PubMed PMID: 17237347.

155. Liu Y, Collins C, Kiosses WB, Murray AM, Joshi M, Shepherd TR, Fuentes EJ, Tzima E. A novel pathway spatiotemporally activates Rac1 and redox signaling in response to fluid shear stress. J Cell Biol. 2013;201(6):863-73. doi: 10.1083/jcb.201207115. PubMed PMID: 23733346; PMCID: 3678169.

156. Montalvo-Ortiz BL, Castillo-Pichardo L, Hernandez E, Humphries-Bickley T, De la Mota-Peynado A, Cubano LA, Vlaar CP, Dharmawardhane S. Characterization of EHop-016, novel small molecule inhibitor of Rac GTPase. J Biol Chem. 2012;287(16):13228-38. doi: 10.1074/jbc.M111.334524. PubMed PMID: 22383527; PMCID: 3339933.

157. Karunakaran S, Saeed U, Mishra M, Valli RK, Joshi SD, Meka DP, Seth P, Ravindranath V. Selective activation of p38 mitogen-activated protein kinase in dopaminergic neurons of substantia nigra leads to nuclear translocation of p53 in 1-methyl-4-phenyl-1,2,3,6-tetrahydropyridine-treated mice. J Neurosci. 2008;28(47):12500-9. doi: 10.1523/JNEUROSCI.4511-08.2008. PubMed PMID: 19020042.

158. Hoshino A, Ariyoshi M, Okawa Y, Kaimoto S, Uchihashi M, Fukai K, Iwai-Kanai E, Ikeda K, Ueyama T, Ogata T, Matoba S. Inhibition of p53 preserves Parkin-mediated mitophagy and pancreatic beta-cell function in diabetes. Proc Natl Acad Sci U S A.

2014;111(8):3116-21. doi: 10.1073/pnas.1318951111. PubMed PMID: 24516131; PMCID: 3939874.

159. Nyblom HK, Bugliani M, Fung E, Boggi U, Zubarev R, Marchetti P, Bergsten P. Apoptotic, regenerative, and immune-related signaling in human islets from type 2 diabetes individuals. J Proteome Res. 2009;8(12):5650-6. doi: 10.1021/pr9006816. PubMed PMID: 19852514.

160. Davda D, El Azzouny MA, Tom CT, Hernandez JL, Majmudar JD, Kennedy RT, Martin BR. Profiling targets of the irreversible palmitoylation inhibitor 2-bromopalmitate. ACS Chem Biol. 2013;8(9):1912-7. doi: 10.1021/cb400380s. PubMed PMID: 23844586; PMCID: 3892994.

161. Merrell MA, Wakchoure S, Lehenkari PP, Harris KW, Selander KS. Inhibition of the mevalonate pathway and activation of p38 MAP kinase are independently regulated by nitrogen-containing bisphosphonates in breast cancer cells. Eur J Pharmacol. 2007;570(1-3):27-37. doi: 10.1016/j.ejphar.2007.05.075. PubMed PMID: 17640631.

ABSTRACT

MECHANISMS OF PANCREATIC BETA CELL DYSFUNCTION IN DIABETES

by

VAIBHAV SIDARALA

August 2016

Advisor: Dr. Anjaneyulu Kowluru

Major: Pharmaceutical Sciences

Degree: Doctor of Philosophy

Diabetes is a serious medical condition characterized by decreased insulin secretion from pancreatic β-cells and decreased insulin sensitivity in the peripheral tissues, resulting in elevated levels of blood glucose. According to the International Diabetes Federation, about 387 million cases have been reported worldwide in the year 2013 and it is estimated that about 500 million people would be affected by 2050. Type 2 diabetes, which accounts for about 90% of the total number of cases, is caused by decreased insulin sensitivity in the peripheral tissues and decreased glucose-stimulated insulin secretion from the pancreatic β-cells. The underlying mechanisms involved in β-cell dysfunction under hyperglycemic conditions are currently under investigation. Previous studies in our laboratory have implicated the role of Rac1-Nox2-induced oxidative stress in pancreatic β-cell dysfunction in models of impaired insulin secretion and T2DM. Studies in pancreatic islets derived from the ZDF rat and human diabetic donors have revealed increased activation of Rac1 and Nox2 subunits in these models. Further investigations have suggested the involvement of stress kinases in the activation of downstream apoptotic pathways, leading to β-cell death. Therefore, the primary objective of my dissertation project is to determine the role of Rac1-Nox2-derived oxidative stress in the activation of p38MAPK and p53 tumor suppressor, culminating in β-cell death under glucotoxic conditions.

122

Our studies have revealed that exposure of clonal β-cells (INS-1 832/13 cells) and rodent islets to glucotoxic conditions, results in the activation of p38MAPK and p53. We first, examined the regulatory role of Rac1-Nox2 holoenzyme in the activation of p38MAPK. We utilized pharmacological agents which target Rac1 and Nox2 function by various mechanisms and observed that inhibition of Rac1-Nox2 holoenzyme prevented HG-induced activation of p38MAPK. Since, it is well established that p38MAPK induces apoptosis via p53-dependent mechanisms, we next examined the regulation of p53 under these conditions. We observed that HG-induced p53 phosphorylation was significantly blocked in the presence of inhibitors of Rac1 [EHT1864] and p38MAPK [SB203580]. Additionally, co-provision of Simvastatin, a global inhibitor of protein prenylation, and GGTI-2147, an inhibitor of geranylgeranylation, blocked HG-induced p53 phosphorylation, indicating that Rac1 prenylation is requisite for these signaling events. Furthermore, using cell death detection assay, we observed that inhibition of Rac1 [EHT1864] prevented HG-induced β-cell death. In our next set of studies, we verified our in vitro findings in INS-1 832/13 cells and rodent islets using human islets and islets derived from the ZDF rat. We observed increased activation of p38MAPK-p53 signaling axis in these models, thereby demonstrating the role of Rac1-p38MAPK-p53 signaling pathway in β-cell apoptosis under glucotoxic stress. In conclusion, we were able to demonstrate that sustained activation of Rac1-Nox2 enzyme complex leads to excess ROS generation, and the resulting oxidative stress activates downstream p38MAPK-p53 signaling axis, which in turn, promotes activation of apoptotic genes, ultimately resulting in β-cell death. Our studies provide evidence that therapeutic intervention of this signaling pathway could be used as a tool for the prevention of β-cell dysfunction and the onset of type 2 diabetes.

AUTOBIOGRAPHICAL STATEMENT

Education

- PhD in pharmaceutical sciences, Eugene Applebaum College of Pharmacy and Health Sciences, Wayne State University, Detroit, MI, USA
- Bachelor's in Pharmacy, Al-Ameen College of Pharmacy, Rajiv Gandhi University Of Health Sciences, Bangalore, India

Awards

- 2016 George C. Fuller Endowed Scholarship, Wayne State University
- Graduate Research Assistantship 2015-2016

Publications

- NSC23766, a known inhibitor of Tiam1-Rac1 signaling module, prevents the onset of Type 1 diabetes in the NOD mouse model. Rajakrishnan Veluthakal, **Vaibhav Sidarala** and Anjaneyulu Kowluru. *Cell Physiol Biochem* 2016 [Accepted]

- VAV2, a guanine nucleotide exchange factor for Rac1, regulates glucose-stimulated insulin secretion in pancreatic beta cells. Veluthakal R, Tunduguru R, Arora DK, **Sidarala V**, Syeda K, Vlaar CP, Thurmond DC, Kowluru A. *Diabetologia* 2015; 58(11):2573-81. PMID: 26224100

- Phagocyte-like NADPH oxidase (Nox2) promotes activation of p38MAPK in pancreatic β-cells under glucotoxic conditions: Evidence for a requisite role of Ras-related C3 botulinum toxin substrate 1 (Rac1). **Sidarala V**, Veluthakal R, Syeda K, Vlaar C, Newsholme P, Kowluru A. *Biochemical Pharmacology* 2015; 95(4):301-10. PMID: 25881746

- EHT 1864, a small molecule inhibitor of Ras-related C3 botulinum toxin substrate 1 (Rac1), attenuates glucose-stimulated insulin secretion in pancreatic β-cells. **Sidarala V**, Veluthakal R, Syeda K, Kowluru A. *Cell Signalling* 2015; 27(6):1159-67. PMID: 25725286

- Glucotoxic and diabetic conditions induce caspase 6-mediated degradation of nuclear lamin A in human islets, rodent islets and INS-1 832/13 cells. Khadija S, Veluthakal R, **Sidarala V**, Kowluru A. *Apoptosis* 2014; 19(12):1691-701. PMID: 25292013